creative commons
COMMONS DEED

저작자표시-비영리-변경금지 2.0 대한민국

이용자는 아래의 조건을 따르는 경우에 한하여 자유롭게

- 이 저작물을 복제, 배포, 전송, 전시, 공연 및 방송할 수 있습니다.

다음과 같은 조건을 따라야 합니다:

저작자표시. 귀하는 원저작자를 표시하여야 합니다.

비영리. 귀하는 이 저작물을 영리 목적으로 이용할 수 없습니다.

변경금지. 귀하는 이 저작물을 개작, 변형 또는 가공할 수 없습니다.

- 귀하는, 이 저작물의 재이용이나 배포의 경우, 이 저작물에 적용된 이용허락조건을 명확하게 나타내어야 합니다.
- 저작권자로부터 별도의 허가를 받으면 이러한 조건들은 적용되지 않습니다.

저작권법에 따른 이용자의 권리는 위의 내용에 의하여 영향을 받지 않습니다.

이것은 이용허락규약(Legal Code)을 이해하기 쉽게 요약한 것입니다.

Disclaimer

dCollection

A DISSERTATION FOR THE DEGREE OF DOCTOR OF PHILOSOPHY

Cytogenetic Analysis for Genome Divergence and Compatibility in the Brassicaceae Family

배추과에서 유전체 다양성과 친화성 연구를 위한 세포유전학적 분석

FEBRUARY 2020

HYE RANG PARK

MAJOR IN HORTICULTURAL SCIENCE AND BIOTECHNOLOGY

DEPARTMENT OF PLANT SCIENCE

COLLEGE OF AGRICULTURE AND LIFE SCIENCES

THE GRADUATE SCHOOL OF SEOUL NATIONAL UNIVERSITY

Cytogenetic Analysis for Genome Divergence and Compatibility in the Brassicaceae Family

UNDER THE DIRECTION OF DR. JIN HOE HUH
SUBMITTED TO THE FACULTY OF THE GRADUATE SCHOOL OF
SEOUL NATIONAL UNIVERSITY

BY
HYE RANG PARK

MAJOR IN HORTICULTURAL SCIENCE AND BIOTECHNOLOGY
DEPARTMENT OF PLANT SCIENCE

FEBRUARY 2020

APPROVED AS A QUALIFIED DISSERTATION OF HYE RANG PARK
FOR THE DEGREE OF DOCTOR OF PHILOSOPHY
BY THE COMMITTEE MEMBERS

CHAIRMAN	**Byoung-Cheorl Kang, Ph.D.**
VICE-CHAIRMAN	**Jin Hoe Huh, Ph.D.**
MEMBER	**Doil Choi, Ph.D.**
MEMBER	**Tae-Jin Yang, Ph.D.**
MEMBER	**Hyun Hee Kim, Ph.D.**

Cytogenetic Analysis for Genome Divergence and Compatibility in the Brassicaceae Family

Hye Rang Park

Department of Plant Science, Seoul National University

ABSTRACT

The genera *Brassica* and *Raphanus* belong to the Brassicaceae family, which contain a variety of important crop species used as oilseed, condiment, or vegetables cultivated worldwide. These crops experienced polyploidization event, leading to speciation and morphotype diversification. Although polyploidization can give rise to genetic diversity, the resulting hybrids often suffer from genome instability and infertility. Notable among them are chromosomal defects, mainly caused by genome compatibility between distantly related genomes. To understand mechanism of chromosome stability during hybridization, cytogenetic analysis was

performed in x*Brassicoraphanus*, a rare case of stabilized intergeneric allotetraploid (2n = 4x = 48) derived from a cross between Chinese cabbage (*Brassica rapa*; 2n = 2x = 20) and radish (*Raphanus sativus*; 2n = 2x = 18). In chaper I, I investigated the formation, progression, and completion of several hallmark features of meiosis in x*Brassicoraphanus*. This study provided comparative understanding of meiosis in allodiploid and allotetraploid x*Brassicoraphanus* and showed that faithful chromosome behaviors throughout meiosis could contribute to genome stabilization in the allotetraploid. In chaper II, four cultivars of x*Brassicoraphanus* BB1, BB4, BB6, and BB50 with varying degrees of pollen viability and seed abortion were investigated. The relatively less stable line BB4 exhibited more abnormal chromosome behaviors and the formation of inviable pollens and micronuclei than BB 50. In chapter III, among diverse subspecies of *B. rapa*, turnip (*B. rapa* subsp. *rapa*) with a large bulbous taproot was used for investigation of phenotypic variations within the same species. I obtained a double haploid line of Ganghwa turnip, G14. In comparison with Chinese cabbage, transposable elements (TEs), particularly long terminal repeat (LTR) retrotransposons, were more enriched in turnip (G14), suggesting the effect of subspecies-specific TE divergence in huge phenotypic variations. Taken together, this study will provide insights into the effects of meiotic

behaviors and chromosome stability in the genome compatibility and divergence as well as TE-mediated morphological divergence within the same species in the Brassicaceae family.

Keywords: polyploidization, genome incompatibility, meiosis, micronuclei, transposable elements

Student number: 2012-30305

CONTENTS

LIST OF TABLES

LIST OF FIGURES

LIST OF ABBREVIATION

ANOVA	Analysis of variance
ASY1/3	ASYNAPTIC1/3
BA	6-benzylaminopurine
BAC	Bacterial Artificial Chromosome
BrASY1	*Brassica rapa* ASYNAPTIC1/3
BrHEI10	*Brassica rapa* HEI10
BrZYP1	*Brassica rapa* ZYP1
BSA	Bovine serum albumin
CAPS	Cleaved amplified polymorphic sequence
CF	*B. rapa* cv. Chiifu-401-42
COs	Crossovers
CTAB	Cetyltrimethylammonium bromide
DAPI	4', 6-diamidino-2-phenylindole
DIRS	Dictyostelium intermediate repeat sequence
DSB	Double strand break
EGTA	Ethylene glycol tetraacetic acid

ERV	Endogenous retroviruses
FACS	Fluorescence activated cell sorting
FISH	Fluorescence in situ hybridization
FITC	Fluorescein isothiocyanate
FSC	Forward scatter
GISH	Genomic in situ hybridization
HRP	Horseradish heroxidase
IBA	Indole-3-butyric acid
IgG	Immunoglobulin G
IgG-HRP	Immunoglobulin G- Horseradish peroxidase
INDELs	Insertions and deletions
ISH	In situ hybridization
LINE	Long interspersed nuclear element
LTR	Long terminal repeat
MLH1/3	MutL homolog 1/3
MSH4/5	MutS protein homolog 4/5
MTOCs	Microtubule-organizing centers
NAA	Naphthaleneacetic acid

NCO	Non cross-over
NLN-13	Nitsch and Nitsch medium with 13% sucrose
NMU	*N*-methyl-*N*-nitroso-urethane
PALM	Photoactivated Localization Microscopy
PBS	Phosphate-buffered saline
PE	Phycoerythrin
PEM	PIPES, EGTA, and MgSO4
PerCP	Peridin chlorophyll protein
Ph1	Pairing homeologous 1
PMC	Pollen mother cell
PMSF	Phenylmethylsulfonyl fluoride
PrBn	Paring regulator in *B. napus*
SCC3	Sister-chromatid cohesion protein 3
SD	Standard deviation
SEM	Scanning electron microscopy
SIM	Structured Illimination Microscopy
SINE	Short interspersed nuclear element
SMC1/3	Structural Maintenance Of Chromosomes 1/3

SNP	Single nucleotide polymorphism
SSC	Side scatter
SSR	Simple sequence repeat
STED	Stimulated emission depletion
STORM	Stochastic optical reconstruction microscopy
SYN1	Synapsin I
TE	Transposable element
WK	*R. sativus* cv. WK10039
Zip1	Zipper1
ZMM	Zip1, Zip2, Zip3, Zip4, Spo16, Msh4, Msh5 and Mer3
ZYP1	ZIPPER1

LITERATURE REVIEW

Polyploid in Brassicaceae

The Brassicaceae family consists of approximately 338 genera and total 3,709 species (Warwick et al., 2006). Among those, the Brassiceae tribe includes many important vegetable crops such as Chinese cabbage, big root radish, oilseed rapa, and turnip (Gómez-Campo and Prakash, 1999; Warwick, 2011). The crops in the tribe are highly diverged by their morphotypes, and different parts of the plant are preferentially consumed (Warwick et al., 2009; Schmidt and Bancroft, 2011). For example, Chinese cabbage and turnip are in same species, *Brassica rapa*. Chinese cabbage is a leafy vegetable whereas turnip is consumed as a root vegetable. The genomes of *Brassica* species share an additional whole genome triplication event from *Arabidopsis thaliana* lineage, which occurred approximately 13 to 17 million years ago (Yang et al., 1999; Town et al., 2006; Beilstein et al., 2010; Wang et al., 2011). As exemplified in Brassicaceae, whole genome duplication (WGD) or polyploidy happens ordinarily in the evolutionary history of many plants. Autopolyploid has multiple chromosome sets derived from a single taxon, such as potato (*Solanum tuberosum*) and banana (*Musa acuminata*). Allopolyploid has multiple chromosome sets

derived from two or more diverged taxa, such as wheat (*Triticum aestivum*), maize (*Zea mays* L.), cotton (*Gossypium hirsutum*), coffee (*Coffea arabica* or *canephora*), strawberry (*Fragaria x ananassa*), peanut (*Arachis hypogaea*) and many crops in Brassicaceae family (Comai, 2005; Leitch and Leitch, 2008; Renny-Byfield and Wendel, 2014). Polyploidization is often associated with interspecific or intergeneric hybridization, which results in the generation of new species and resources including crops listed above. Polyploidization after interspecific hybridization had been first described in the *Brassica* genus by U, Jang-choon (U, 1935). U showed how a new species could be synthesized by interspecific hybridization and polyploidization in his theory known as 'Synthesis of species' with U's triangle. It described the six economically important *Brassica* species, consisting of three diploids and three interspecific allotetraploids. Three diploids of the six widely cultivated species were *B. rapa* (AA genome, 2n = 2x = 20), *B. nigra* (BB genome, 2n = 2x = 16), and *B. oleracea* (CC genome, 2n = 2x = 18), while the other three species were allotetraploids resulting from interspecific hybridization between the diploids, *B. juncea* (AABB genomes, 2n = 4x = 36), *B. napus* (AACC genomes, 2n = 4x = 38), and *B. carinata* (BBCC genomes, 2n = 4x = 34) (U, 1935).

x*Brassicoraphanus*

Interspecific or intergeneric hybridization studies extensively performed in the Brassiceae tribe. There have been continuous reports about the productions of intergeneric hybridization in the Brassiceae tribe. x*Brassicoraphanus*, an intergeneric hybrid between *Brassica* and *Raphanus*, was first reported in the early 1800s (Sageret, 1826). In many trials for producing x*Brassicoraphanus*, most cases were constrained to develop infertile progenies (Karpechenko, 1927; McNaughton, 1979; Dolstra, 1982). There are only a few examples of successful development of fertile plants. A newly synthesized allopolyploid, x*Brassicoraphanus* attained high fertility and uniformity through mutagenesis in microspore culture for accelerated genetic stabilization as a new leafy vegetable crop. The several lines of x*Brassicoraphanus* BB1, BB4, BB5, BB6, and BB50 have a different fertility levels (Lee et al., 1989; 2002; 2011; 2017). Whether the mutagenesis in microspore culture contributed genetic stabilization has not yet been studied. The lines with different level of fertility can be used to investigate how the BB1 overcomes hybrid incompatibility and restores the fertility.

Genetic stabilization of polyploids

Polyploidization is accompanied with genome restructuring and passed through genome instability (Comai et al., 2000; Ramsey and Schemske, 2002; Comai, 2005). Transcriptomic and genomic disorders have been considered as 'shocks' which can be resulted in genetic instability. New synthesized hybrids have been expected to represent intermediate patterns of gene expression among between their parents (Soltis and Soltis, 2009). However, in the early synthesized generations, genomes are known to undergo genomic shock (McClintock, 1984; Jackson and Chen, 2010) and transcriptomic shock (Chelaifa et al., 2010). McClintock first proposed 'genomic shock' in allopolyploidization, homeologous translocation, transposable elements (TEs) activation can be arisen to produce huge range of genetic diversification along with genetic instability. Genome reorganization through retrotransposon activation has been observed in the cases of *Aegilops* (Senerchia et al., 2015). Transcriptomic shock causes instantaneous and saltational changes of gene expression between parental copies in new hybrids (Hegarty et al., 2006; Buggs et al., 2011). Next generation sequencing (NGS) based transcriptome analysis revealed transcriptomic changes in allopolyploid compared with its parents. Large amount of transcripts showed non-additive expressions after hybridization

and it was described as transcriptomic shock compared with genomic shock. Different levels of non-additive gene expression have been observed in various organisms including *Senecio*, wheat, and rice (Hegarty et al., 2006; Zhang et al., 2016; Wu et al., 2016).

Meiosis and genetic stabilization

Newly synthesized hybrids often show genetic instability which is observed as seed abortion. It was hard to gain high fertility in allopolyploid breeding (Prakash et al. 2009). In many cases, they failed to produce fertile pollen or egg cell. Thus, gametogenesis has been attended to understand the mechanism of genetic stabilization of allopolyploid. An organism in which cells contain more than two pairs of related chromosomes (homologous and/or homoeologous) has failed to produce gamete evenly during meiosis. The aberrant bivalent between homoeologous chromosomes formed in meiosis of allopolyploid. Multiple or illegitimate chiasmatic associations would result in aneuploidy and partial fertility because of homologous chromosome missegregation (Cifuentes et al., 2010; Hollister, 2015). The aberrant pairing configurations such as two homoeologous bivalents or a quadrivalent may result in homoeologous segregating to the same daughter nuclei in the first meiotic division (Szadkowski et al., 2010). The aberrant

meiosis was observed in the first generation of the synthesized *B. napus* lines (Cifuentes et al., 2010; Szadkowski et al., 2010; Xiong et al., 2011). Monosomic-trisomic plants were generated as a frequency of about 5% in which loss or gain A1 and / or C1 the two homoeologous A1 and C1 chromosomes between *B. rapa* and *B. oleracea* (Cheng et al., 2014).

Importance of prophase I in genetic stabilization

Meiosis is a particular process that ensures to generate four haploid gametes in sexual eukaryotes. Nucleus is reduced by homologous chromosomes segregation during the first meiotic division and nucleus is equated by sister chromatids segregation during the second cell division (Roeder, 1997). Each meiotic division divides at prophase, metaphase, anaphase, and telophase. The first stage, prophase I, is the longest and comprises five substages (i.e. leptotene, zygotene, pachytene, diplotene, and diakinesis) depending on changes in chromosome morphology. The cytological studies of meiotic chromosomes from yeast to Arabidopsis and other plant species were visualized through the extant advanced genetic and cytological approaches (Jones et al., 2003; Mézard et al., 2007; Pawlowski et al., 2013). These cytologically defined stages have been integrated with the identification and functional characterization of meiotic genes in model

organisms such as budding yeast (*Saccharomyces cerevisiae*) (Roeder, 1997; Zickler and Kleckner, 1998) and *A. thaliana* (Osman et al., 2011; Sanchez-Moran and Armstrong, 2014) and crops such as barley, maize, rice, and wheat (Mézard et al., 2007; Grandont et al., 2013; Mercier et al., 2015). The synthesized polyploids often raised large changes in gene expression patterns by genome doubling and shifted in epigenetic regulation of transposable elements with problems of mitosis and meiosis (Comai, 2005; Hollister, 2015; Grusz et al., 2017). Many synthesized polyploids exhibit meiotic irregularities (Comai, 2005; Cifuentes et al., 2010; Szadkowski et al., 2010). Allopolyploids commonly prevent multivalent formation by enforcing preferential pairing between homologs rather than less similar homoeologs (Sears, 1976; Jenczewski et al., 2003; Grandont et al., 2014). Reports showed aberrations in meiotic chromosome pairing by cytological studies in polyploids and hybrids of domesticated crops (Sears, 1976; Jenczewski et al., 2003; Grandont et al., 2014). However, allopolyploids of some domesticated crops had genetic loci known to control preferential pairing. The most crucial studies are on *Pairing homeologous 1* (*Ph1*) in allohexaploid bread wheat *Triticum aestivum* (Sears, 1976) and *Paring regulator* in *B. napus* (*PrBn*) (Jenczewski et al., 2003; Grandont et al., 2014). Eber and colleagues (1994) examined that sterile *B. napus* and

hybrids from a cross between *B*. *adpressa* and *R*. *raphanustrum*, which exhibited prevalent multivalents associations, and they speculated about homoeologous recombination.

Genetic components of meiosis

Meiosis is strictly controlled by genetic components. Studies of the related genes suggest that fertility restoration in polyploidy should be accompanied with proper functions of these genes. The components of cohesion complex (SYN1, SMC1/3 and SCC3) were loaded as foci in the two homologous chromosomes. The axial components (ASY1/3) begin to develop and DNA double strand break (DSB) repair complexes containing SPO11 appears in G2 phase. The axial components (ASY1/3) make linear structures along the sister chromatids. The recombination nodules including the recombinases (RAD51 and DMC1) initiate DNA base homology search to invade the nonsister homologous duplex, single-end invasion promoting interhomolog recombination in leptotene. The homologous chromosome initiates chromosome synapsis in zygotene and synapses completely into synaptonemal complexes (SCs), as a proteinaceous structure in pachytene. The SC includes a central element and two axial elements (ASY1/3) having tripartite structure that extends the clink in the chromosome axis

transversing filament protein (ZYP1) in pachytene. This proteinaceous structure starts up from zygotene to pachytene of prophase I, indispensably lines up homologous chromosome axis. The initiation of recombination starts synapsis, while the completion of synapsis contributes to the maturation of recombination intermediates into meiotic crossovers (COs). SC launches to break down and to condense chromosomes in diplotene. The homologous chromosomes remain to represent at chiasmata, cytological sites of COs. The double holliday junction was resolved into a CO separating homologs (Sanchez-Moran and Armstrong, 2014). In metaphase I, the micro spindles correctly attach to their centromeres. These spindles pull apart homologous chromosomes which remain tethering chiasmata in metaphase I. It is essential for correct chromosome orientation at least a single obligation of COs at metaphase I, and then homolog chromosomes may segregate evenly at anaphase I. Sister chromatids subsequently are separated with half the number of chromosomes during meiosis II (Grandont et al., 2013; Sanchez-Moran and Armstrong, 2014; Mercier et al., 2015; Bomblies et al., 2016). During meiosis, DSB repair in homologous templates initiates inter-homolog recombination molecules and matures these recombinations to cross over sites (Girard et al., 2015; Seguela-Arnaud et al., 2015). AtASY1 appears as foci on the chromosomes at the

beginning of G2. In late G2, AtASY1 starts appearing as a linear signal closely associated with the chromosome axis. In Arabidposis, AtASY1 protein, Hop1 in yeast is an important component of this meiotic chromosome axis. When AtASY1 is absent, chromosome pairing and synapsis are interrupted. Eventually, the formation of chiasmata is extremely reduced (Caryl et al., 2000). Also, meiotic events were represented by time-course in an *asy1* mutant of Arabidopsis that AtASY1 and AtDMC1 are significant for homologous recombination machinery (Sanchez-Moran et al., 2007). Another axial element, AtASY3 (Red1: in budding yeast), combines with AtASY1 (Ferdous et al., 2012). When the *ATZYP1A/B* (*Hop1* in yeast, *Zip1* in budding yeast, and *ZEP1* in rice) genes are inactivated, multivalents and bivalents are induced into non-homologous chromosomes. Therefore, the role of AtZYP1 in recombination between homologous and non-homologous chromosomes ensures meiotic chromosome recombination fidelity. AtZYP1 proteins are required to restrain the formation of synaptonemal complex and crossovers, between homologous chromosomes through immunolocalization (Higgins et al., 2005; Mézard et al., 2007). The synapsis of homologous chromosomes causes the initiation of recombination though the completion of synapsis at pachytene. Some recombination intermediates into meiotic crossovers

(COs). There are two kinds of COs in *S. cerevisiae* and plants. Class I COs are interference-sensitive and their formation is composed to ZMM proteins (SHOC1, ZIP4, MSH4/5, MER3, MLH1/3, HEI10 and PTD) (Mercier et al., 2015; Gonzalo et al., 2019). Class II COs are interference insensitive and cause to randomly distributed COs and repair as non-reciprocal exchanges between homologous chromosomes, termed non cross-overs (NCOs), composing to Mus81 proteins in *S. cerevisiae* and plants (Berchowitz et al., 2007; Higgins et al., 2008). The recombination molecules are designated in prophase I and accumulate in HEI10 at DSB sites. HEI10 containing an E3 ligase is required for formation of class I COs. AtHEI10 is necessary for normal CO levels and Class I COs. Also the AtHEI10 protein forms foci on meiotic chromosomes from leptotene to diakinesis (Chelysheva et al., 2012; Wang et al., 2012) (Figure 1).

Recent progress in cytogenetics

In twenty-five years ago, the first meiotic stages of Arabidopsis were observed using DAPI staining and fluorescence microscopy (Ross et al., 1996). Fluorescence *in situ* hybridization (FISH) and genomic *in situ* hybridization (GISH) have made huge contributions to understanding of chromosome structure within the last 160 years (Chester et al., 2000). The

entire chromosome painting with BACs using classic ISH strategies have been applied for detecting translocations and rearrangements and enabled to predict ancestral karyotypes in Brassicaceae (Mandáková and Lysak, 2008). Classic cytological studies by chromatin staining show the chromosomal diversity in species. Such cytotaxonomical approaches enabled to observe karyotypic alternations in chromosome number and morphology (Guerra, 2008). The overviews of chromosome behavior in mitosis and meiosis were also visualized through this method (Chester et. al., 2000). Time-course meiotic analysis in a pollen mother cell provided information on the duration of meiotic stages and essential molecular events which were visualized with immunolocalization of meiotic proteins (Sanchez-Moran et al., 2007). Immunocytology using antibodies of key meiotic components determines the location of meiotic proteins on the chromosomes during meiosis (Armstrong et al., 2003; Armstrong et al., 2013; Grandont et al., 2014; Gu et al., 2017). Advances in microscopy technologies are the other contributor for the progress of cytogenetics. The super-resolution microscopy, also called optical nanoscopy, overcomes restriction conventional microscopies and connects the resolution gaps between light and electron microscopy. This state-of-the-art technology super-resolution microscopy, such as Structured Illimination Microscopy (SIM),

Photoactivated Localization Microscopy (PALM), Stochastic Optical Reconstruction Microscopy (STORM), and Stimulated Emission Depletion (STED) microscopy offer opportunities for observing molecular structures, interactions and functions in plant cell (Schermelleh at al., 2010; Schubert, 2017) and can be applied in the study of meiosis in plants (Wang et al., 2012; Probst, 2018).

Concluding remarks

Recently, reference genomes of Brassicaceae crops have been published for *B. rapa* (Wang et al., 2011), *B. oleracea* (Liu et al., 2014), *B. napus* (Chalhoub et al., 2014), *B. jucea* (Yang et al., 2016), and *R. sativus* (Kitashiba et al., 2014; Jeong et al., 2016). Progresses in genomic and cytogenetic technologies have been accomplished last decades. Studies about meiosis components performed with forward and reverse genetics in Arabidopsis can be efficiently applied in those Brassicaceae crops with the technical advances. It will be possible to understand the molecular mechanisms of polyploid formation and genetic stability establishment especially in the Brassiceae tribe.

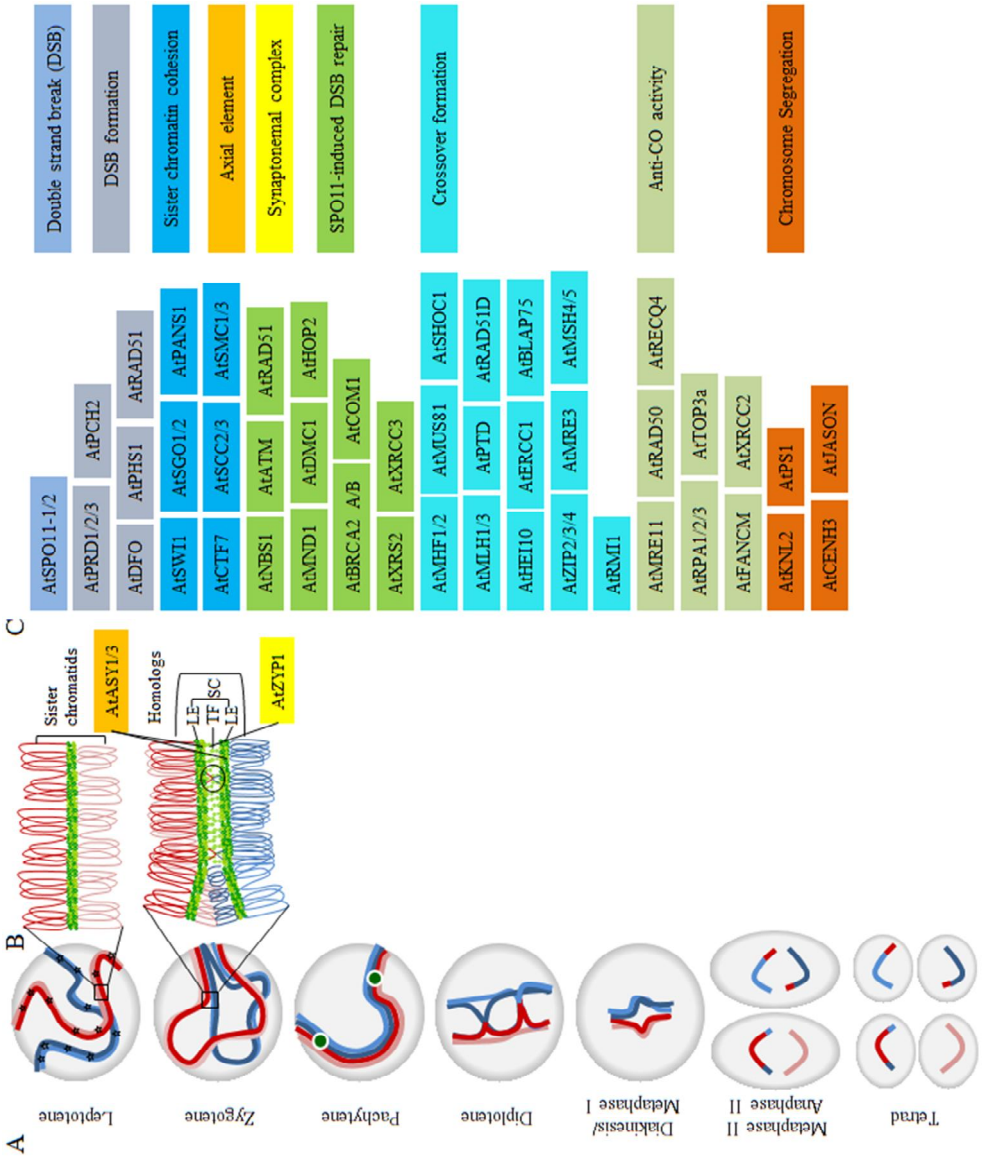

Figure 1. Schematic representation of meiotic protein of Arabidopsis. (A) The process of meiosis with homologous chromosomes in pollen mother cells is illustrated (marked as red and blue). Double strand breaks (DSBs: asterisks) at leptotene and crossovers (COs: green circles) at pachytene. (B) Sister chromatids are illustrated (dark and light red and blue) in loops anchored on chromosome axes (light and dark green circles). Homologous chromosomes consist of transverse filaments (TF) between homologous

axes and lateral elements (LE) at zygotene. The synaptonemal complex (SC) is formed between homologous chromosomes at this stage. (C) Arabidopsis meiotic genes are represented on different colors of their role in the meiotic process.

REFERENCES

Armstrong, S.J. and Jones, G.H. (2003). Meiotic cytology and chromosome behaviour in wild-type *Arabidopsis thaliana*. J. Exp. Bot. **54,** 1-10.

Armstrong, S.J. and Osman, K. (2013). Immunolocalization of meiotic proteins in *Arabidopsis thaliana*: method 2. Methods Mol. Biol. **990,** 103-107.

Beilstein, M.A., Nagalingum, N.S., Clements, M.D., Manchester, S.R., and Mathews, S. (2010). Dated molecular phylogenies indicate a Miocene origin for *Arabidopsis thaliana*. Proc. Natl. Acad. Sci. U.S.A. **107,** 18724-18728.

Berchowitz, L.E., Francis, K.E., Bey, A.L., and Copenhaver, G.P. (2007). The role of *AtMUS81* in interference-insensitive crossovers in *A. thaliana*. PLoS Genet. **3,** e132.

Bomblies, K., Jones, G., Franklin, C., Zickler, D., and Kleckner, N. (2016). The challenge of evolving stable polyploidy: could an increase in "crossover interference distance" play a central role? Chromosoma **125,** 287-300.

Buggs, R.J., Zhang, L., Miles, N., Tate, J.A., Gao, L., Wei, W., Schnable, P.S., Barbazuk, W.B., Soltis, P.S., and Soltis, D.E. (2011). Transcriptomic shock generates evolutionary novelty in a newly formed, natural allopolyploid plant. Curr. Biol. **21,** 551-556.

Caryl, A.P., Armstrong, S.J., Jones, G.H., and Franklin, F.C.H. (2000). A homologue of the yeast *HOP1* gene is inactivated in the *Arabidopsis* meiotic mutant *asy1*. Chromosoma **109,** 62-71.

Chester, M., Leitch, A. R., Soltis, P. S., and Soltis, D. E. (2010) Review of the application of modern cytogenetic methods (FISH/GISH) to the study of reticulation (polyploidy/hybridisation). Genes. **1,** 166–192.

Chalhoub, B., Denoeud, F., Liu, S., Parkin, I.A., Tang, H., Wang, X., Chiquet, J., Belcram, H., Tong, C., Samans, B., Correa, M., Da Silva, C., Just, J., Falentin, C., Koh, C.S., Le Clainche, I., Bernard, M., Bento, P., Noel, B., Labadie, K., Alberti, A., Charles, M., Arnaud, D., Guo, H., Daviaud, C., Alamery, S., Jabbari, K., Zhao, M., Edger, P.P. et al. (2014). Early allopolyploid evolution in the post-Neolithic *Brassica napus* oilseed genome. Science **345,** 950-953.

Chelaifa, H., Monnier, A., and Ainouche, M. (2010). Transcriptomic changes following recent natural hybridization and allopolyploidy in the salt marsh species *Spartina* x *townsendii* and *Spartina anglica* (Poaceae). New Phytol. **186,** 161-174.

Chelysheva, L., Vezon, D., Chambon, A., Gendrot, G., Pereira, L., Lemhemdi, A., Vrielynck, N., Le Guin, S., Novatchkova, M., and Grelon, M. (2012). The *Arabidopsis* HEI10 is a new ZMM protein related to Zip3. PLoS Genet. **8,** e1002799.

Cheng, F., Wu, J., and Wang, X. (2014). Genome triplication drove the diversification of *Brassica* plants. Hortic. Res. **1,** 14024.

Cifuentes, M., Eber, F., Lucas, M.O., Lode, M., Chevre, A.M., and Jenczewski, E. (2010). Repeated polyploidy drove different levels of crossover suppression between homoeologous chromosomes in *Brassica napus* allohaploids. Plant Cell **22,** 2265-2276.

Comai, L. (2000). Genetic and epigenetic interactions in allopolyploid plants. Plant Mol. Biol. **43,** 387-399.

Comai, L. (2005). The advantages and disadvantages of being polyploid. Nat. Rev. Genet. **6,** 836-846.

Dolstra, O. (1982). Synthesis and fertility of x*Brassicoraphanus* and ways of transferring *Raphanus* characters to *Brassica*. Agric. Res. Rep. **917,** 1-90.

Eber, F., Chevre, A.M., Baranger, A., Vallee, P., Tanguy, X., and Renard, M. (1994). Spontaneous hybridization between a male-sterile oilseed rape and two weeds. Theor. Appl. Genet. **88,** 362-368.

Ferdous, M., Higgins, J.D., Osman, K., Lambing, C., Roitinger, E., Mechtler, K., Armstrong, S.J., Perry, R., Pradillo, M., Cunado, N., and Franklin, F.C. (2012). Inter-homolog crossing-over and synapsis in *Arabidopsis* meiosis are dependent on the chromosome axis protein AtASY3. PLoS Genet. **8,** e1002507.

Girard, C., Chelysheva, L., Choinard, S., Froger, N., Macaisne, N., Lehmemdi, A., Mazel, J., Crismani, W., Mercier, R. (2015). AAA-ATPase FIDGETIN-LIKE 1 and helicase FANCM antagonize meiotic crossovers by distinct mechanisms. PLoS Genet. **11,** e1005369.

Gómez-Campo, C. and Prakash, S. (1999). Origin and domestication. In Developments in plant genetics and breeding (Amsterdam, Netherlands: Elsevier), pp. 33-58.

Gonzalo A., Lucas M. O., Charpentier C., Sandmann G., Lloyd A. Jenczewski E. (2019). Reducing MSH4 copy number prevents meiotic crossovers between non-homologous chromosomes in *Brassica napus*. Nat. Commun. **10,** 2354.

Grandont, L., Jenczewski, E., and Lloyd, A. (2013). Meiosis and its deviations in polyploid plants. Cytogenet. Genome Res. 1**40,** 171-

184.

Grandont, L., Cunado, N., Coriton, O., Huteau, V., Eber, F., Chevre, A.M., Grelon, M., Chelysheva, L., and Jenczewski, E. (2014). Homoeologous chromosome sorting and progression of meiotic recombination in *Brassica napus*: ploidy does matter! Plant Cell **26,** 1448-1463.

Grusz, A.L., Sigel, E.M, and Witherup, C. (2017). Homoeologous chromosome pairing across the eukaryote phylogeny. Mol. Phylogenet. Evol.**117,** 83-94.

Gu, L., Walters, J.R., and Knipple, D.C. (2017). Conserved patterns of sex chromosome dosage compensation in the Lepidoptera (WZ/ZZ): insights from a moth neo-Z chromosome. Genome Biol. Evol. **9,** 802-816.

Guerra, M. (2008). Chromosome numbers in plant cytotaxonomy: concepts and implications. Cytogenet. Genome Res. **120,** 339-350.

Hegarty, M.J., Barker, G.L., Wilson, I.D., Abbott, R.J., Edwards, K.J., and Hiscock, S.J. (2006). Transcriptome shock after interspecific hybridization in *Senecio* is ameliorated by genome duplication. Curr. Biol. **16,** 1652-1659.

Higgins, J.D., Sanchez-Moran, E., Armstrong, S.J., Jones, G.H., and Franklin, F.C. (2005). The *Arabidopsis* synaptonemal complex protein ZYP1 is required for chromosome synapsis and normal fidelity of crossing over. Genes Dev. **19,** 2488-2500.

Higgins, J.D., Buckling, E.F., Franklin, F.C.H., and Jones, G.H. (2008). Expression and functional analysis of *AtMUS81* in *Arabidopsis* meiosis reveals a role in the second pathway of crossing-over. Plant J. **54,** 152-162.

Hollister, J.D. (2015). Polyploidy: adaptation to the genomic environment. New Phytol. **205,** 1034-1039.

Jackson, S. and Chen, Z.J. (2010). Genomic and expression plasticity of polyploidy. Curr. Opin. Plant Biol. **13,** 153-159.

Jenczewski, E., Eber, F., Grimaud, A., Huet, S., Lucas, M.O., Monod, H., and Chevre, A.M. (2003). *PrBn*, a major gene controlling homeologous pairing in oilseed rape (*Brassica napus*) haploids. Genetics **164,** 645-653.

Jeong, Y.M., Kim , N., Ahn, B.O., Oh, M., Chung, W.H., Chung, H., Jeong, S., Lim, K.B., Hwang, Y.J., Ki, G.B., Baek, S., Choi, S.B., Hyung, D.J., Lee, S.W., Sohn, S.H., Kwon, S.J., Jin, M., Seol, Y.J., Chae, W.B., Choi, K.J., Park, B.S., and Yu, H.J. (2016). Elucidating the triplicated ancestral genome structure of radish based on chromosome-level comparison with the *Brassica* genomes. Theor. Appl. Genet. **129,** 1357-1372.

Jones, G.H., Armstrong, S.J., Caryl, A.P., and Franklin, F.C. (2003). Meiotic chromosome synapsis and recombination in *Arabidopsis thaliana*; an integration of cytological and molecular approaches. Chromosome Res. **11,** 205-215.

Karpechenko, G.D. (1924). Hybrids of ♀*Raphanus sativus* L. × ♂*Brassica oleacea* L. J. Genet. **14,** 375-396.

Kitashiba, H., Li, F., Hirakawa, H., Kawanabe, T., Zou, Z., Hasegawa, Y., Tonosaki, K., Shirasawa, S., Fukushima, A., Yokoi, S., Takahata, Y., Kakizaki, T., Ishida, M., Okamoto, S., Sakamoto, K., Shirasawa, K., Tabata, S., and Nishio, T. (2014). Draft sequences of the radish (*Raphanus sativus* L.) genome. DNA Res. **21,** 481-490.

Lee, S.S., Woo, J.G., and Shin, H.H. (1989). Obtaining intergeneric hybrid plant between *Brassica campestris* and *Raphanus sativus* through young ovule culture. Korean J. Breed. **21,** 52-57.

Lee, S.S., Choi, W.J., and Woo, J.G. (2002). Development of a new vegetable crop in x*Brassicoraphanus* by hybridization of *Brassica campestris* and *Raphanus sativus*. J. Korean Soc. Hort. Sci. **43,** 693-698.

Lee, S.S., Lee, S.A., Yang, J., and Kim, J. (2011). Developing stable progenies of x*Brassicoraphanus*, an intergeneric allopolyploid between *Brassica rapa* and *Raphanus sativus*, through induced mutation using microspore culture. Theor. Appl. Genet. **122,** 885-891.

Lee, S.S., Hwang, B.H., Kim, T.Y., Yang, J., Han, N. R., Kim, J., Kim, H. H., Belandres, H. R. (2017). Developing stable cultivar through microspore mutagenesis in x*Brassicoraphanus koranhort*, inter-generic allopolyploid between *Brassica rapa* and *Raphanus sativus*. Am. J. Plant Sci. **8,** 1345-1356.

Leitch, A.R. and Leitch, I.J. (2008). Genomic plasticity and the diversity of polyploid plants. Science **320,** 481-483.

Liu, S., Liu, Y., Yang, X., Tong, C., Edwards, D., Parkin, I.A., Zhao, M., Ma, J., Yu, J., Huang, S., Wang, X., Wang, J., Lu, K., Fang, Z., Bancroft, I., Yang, T.J., Hu, Q., Wang, X., Yue, Z., Li, H., Yang, L., Wu, J., Zhou, Q., Wang, W., King, G.J., Pires, J.C., Lu, C., Wu, Z., Sampath, P., Wang, Z., Guo, H., Pan, S., Yang, L., Min, J., Zhang, D., Jin, D., Li, W., Belcram, H., Tu, J., Guan, M., Qi, C., Du, D., Li, J., Jiang, L., Batley, J., Sharpe, A.G., Park, B.S., Ruperao, P., Cheng, F. et al. (2014). The *Brassica oleracea* genome

reveals the asymmetrical evolution of polyploid genomes. Nat. Commun. **5,** 3930.

Mandáková, T. and Lysak, M.A. (2008). Chromosomal phylogeny and karyotype evolution in x=7 crucifer species (Brassicaceae). Plant Cell **20,** 2559–2570.

McClintock, B. (1984). The significance of responses of the genome to challenge. Science **226,** 792-801.

McNaughton, I.H. (1979). The current position and problems in the breeding of *Raphanobrassica* (radicole) as a forage crop. In: Proceedings of the 4th Eucarpia-confererence Breed Cruciferous crops, pp 22–28.

Mercier, R., Mezard, C., Jenczewski, E., Macaisne, N., and Grelon, M. (2015). The molecular biology of meiosis in plants. Annu. Rev. Plant Biol. **66,** 297-327.

Mezard, C., Vignard, J., Drouaud, J., and Mercier, R. (2007). The road to crossovers: plants have their say. Trends Genet. **23,** 91-99.

Osman, K., Higgins, J.D., Sanchez-Moran, E., Armstrong, S.J., and Franklin, F.C. (2011). Pathways to meiotic recombination in *Arabidopsis thaliana*. New Phytol. **190,** 523-544.

Pawlowski, W.P., Grelon, M., and Armstrong, S.J. (2013). Plant meiosis. (New York, NY: Spinger).

Prakash, S., Bhat, S.R., Quiros, C.F., Kirti, P.B., and Chopra, V.L. (2009). *Brassica* and its close allies: cytogenetics and evolution. Plant Breed. Rev. **31,** 21-187.

Probst, A.V. (2018). A compendium of methods to analyze the spatial organization of plant chromatin. Methods Mol. Biol. **1675,** 397-418.

Ramsey, J. and Schemske, D.W. (2002). Neopolyploidy in flowering

plants. Annu. Rev. Ecol. Syst. **33,** 589-639.

Renny-Byfield, S., and Wendel, J.F. (2014). Doubling down on genomes: polyploidy and crop plants. Am. J. Bot. **101,** 1711-1725.

Roeder, G.S. (1997). Meiotic chromosomes: it takes two to tango. Genes Dev. **11,** 2600-2621.

Ross, K.J., Fransz, P., and Jones, G.H. (1996). A light microscopic atlas of meiosis in *Arabidopsis thaliana*. Chromosome Res. **4,** 507-516.

Sageret, M. (1826). Considerations surla production des variants et des varieties en general, et sur celled de la famille de Cucurbitacee s en particulier. Ann. Sci. Nat. **8,** 94-314.

Sanchez-Moran, E., Santos, J.L., Jones, G.H., and Franklin, F.C.H. (2007). ASY1 mediates AtDMC1-dependent interhomolog recombination during meiosis in *Arabidopsis*. Genes Dev. **21,** 2220-2233.

Sanchez-Moran, E. and Armstrong, S.J. (2014). Meiotic chromosome synapsis and recombination in *Arabidopsis thaliana*: new ways of integrating cytological and molecular approaches. Chromosome Res. **22,** 179-190.

Schermelleh, L., Heintzmann, R., and Leonhardt, H. (2010). A guide to super-resolution fluorescence microscopy. J. Cell Biol. **190,** 165-175.

Schubert, V. (2017). Super-resolution microscopy-applications in plant cell research. Front. Plant Sci. **8,** 531.

Sears, E.R. (1976). Genetic control of chromosome pairing in wheat. Annu. Rev. Genet. **10,** 31–51.

Séguéla-Arnaud, M., Crismani, W., Larcheveque, C., Mazel, J., Froger, N., Choinard, S., Lemhemdi, A., Macaisne, N., Van Leene, J., Gevaert, K., De Jaeger, G., Chelysheva L., and Mercier, R.

(2015). Multiple mechanisms limit meiotic crossovers: TOP3α and two BLM homologs antagonize crossovers in parallel to FANCM. Proc. Natl. Acad. Sci. U. S. A. **112,** 4713-4718.

Senerchia, N., Felber, F., and Parisod, C. (2015). Genome reorganization in F1 hybrids uncovers the role of retrotransposons in reproductive isolation. Proc. Royal Soc. B **282,** 20142874.

Soltis, P. S. and Soltis, D.E. (2009). The role of hybridization in plant speciation. **60,** 561-588.

Szadkowski, E., Eber, F., Huteau, V., Lode, M., Huneau, C., Belcram, H., Coriton, O., Manzanares-Dauleux, M.J., Delourme, R., King, G.J., Chalhoub, B., Jenczewski, E., and Chevre, A.M. (2010). The first meiosis of resynthesized *Brassica napus*, a genome blender. New Phytol. **186,** 102-112.

Town, C.D., Cheung, F., Maiti, R., Crabtree, J., Haas, B.J., Wortman, J.R., Hine, E.E., Althoff, R., Arbogast, T.S., Tallon, L.J., Vigouroux, M., Trick, M., and Bancroft, I. (2006). Comparative genomics of *Brassica oleracea* and *Arabidopsis thaliana* reveal gene loss, fragmentation, and dispersal after polyploidy. Plant Cell **18,** 1348-1359.

U, N. (1935). Genome analysis in *Brassica* with special reference to the experimental formation of *B. napus* and peculiar mode of fertilization. Jpn. J. Bot. **7,** 389-452.

Wang, K., Wang, M., Tang, D., Shen, Y., Miao, C., Hu, Q., Lu, T., Cheng, Z. (2012). The role of rice HEI10 in the formation of meiotic crossovers. PLoS Genet. **8,** e1002809.

Wang, X., Wang, H., Wang, J., Sun, R., Wu, J., Liu, S., Bai, Y., Mun, J.H., Bancroft, I., Cheng, F., Huang, S., Li, X., Hua, W., Wang, J.,

Wang, X., Freeling, M., Pires, J.C., Paterson, A.H., Chalhoub, B., Wang, B., Hayward, A., Sharpe, A.G., Park, B.S., Weisshaar, B., Liu, B., Li, B., Liu, B., Tong, C., Song, C., Duran, C., Peng, C., Geng, C., Koh, C., Lin, C., Edwards, D., Mu, D., Shen, D., Soumpourou, E., Li, F., Fraser, F., Conant, G., Lassalle, G., King, G.J., Bonnema, G., Tang, H., Wang, H., Belcram, H. et al. (2011). The genome of the mesopolyploid crop species *Brassica rapa*. Nat. Genet. **43,** 1035-1039.

Wang, K., Wang, M., Tang, D., Shen, Y., Miao, C., Hu, Q., Lu, T., and Cheng, Z. (2012). The role of rice HEI10 in the formation of meiotic crossovers. PLoS Genet. **8,** e1002809.

Warwick, S.I., Francis, A., and Al-Shehbaz, I.A. (2006). Brassicaceae: species checklist and database on CD-Rom. Plant. Syst. Evol. **259,** 249-258.

Warwick, S.I., Francis, A., and Gugel, R.K. (2009). Guide to wild germplasm of *Brassica* and allied crops (tribe Brassiceae, Brassicaceae). 3rd Edition. Agric Agri-food Res Branch Publ, Ottawa,ON, Canada. Contribution No. 991475 and pdf files at http://www.brassica.info.

Warwick, S.I. (2011). Brassicaceae in agriculture. In genetics and genomics of the Brassicaceae (New York, NY: Springer), pp. 33-65.

Wu, Y., Sun, Y., Wang, X., Lin, X., Sun, S., Shen, K., Wang, J., Jiang, T., Zhong, S., Xu, C., and Liu, B. (2016). Transcriptome shock in an interspecific F1 triploid hybrid of *Oryza* revealed by RNA sequencing. J. Integr. Plant Biol. **58,** 150-164.

Xiong, Z., Gaeta, R.T., and Pires, J.C. (2011). Homoeologous shuffling and chromosome compensation maintain genome balance in

resynthesized allopolyploid *Brassica napus*. Proc. Natl. Acad. Sci. U. S. A. **108,** 7908-7913.

Yang, J., Liu, D.,Wang, X., Ji, C., Cheng, F. (2016) The genome sequence of allopolyploid *Brassica juncea* and analysis of differential homoeolog gene expression influencing selection. Nat. Genet. **48,** 1225-1232.

Yang, Y.W., Lai, K.N., Tai, P.Y., and Li, W.H. (1999). Rates of nucleotide substitution in angiosperm mitochondrial DNA sequences and dates of divergence between *Brassica* and other angiosperm lineages. J. Mol. Evol. **48,** 597-604.

Zhang, D., Pan, Q., Tan, C., Zhu, B., Ge, X., Shao, Y., and Li, Z. (2016). Genome-wide gene expressions respond differently to A-subgenome origins in *Brassica napus* synthetic hybrids and natural allotetraploid. Front. Plant Sci. **7,** 1508.

Zickler, D. and Kleckner, N. (1998). The leptotene-zygotene transition of meiosis. Annu. Rev. Genet. **32,** 619-697.

CHAPTER 1

Meiotic chromosome stability and suppression of crossover between non-homologous chromosomes in x*Brassicoraphanus*, an intergeneric allotetraploid derived from a cross between *Brassica rapa* and *Raphanus sativus*

ABSTRACT

Hybridization and polyploidization are major driving forces in plant evolution. Allopolyploids can be occasionally formed from a cross between distantly related species but often suffer from chromosome instability and infertility. x*Brassicoraphanus* is an intergeneric allotetraploid (AARR; 2n = 4x = 38) derived from a cross between *Brassica rapa* (AA; 2n = 2x = 20) and *Raphanus sativus* (RR; 2n = 2x = 18). x*Brassicoraphanus* is fertile and genetically stable, while retaining complete sets of both *B. rapa* and *R. sativus* chromosomes. Precise control of meiotic recombination is essential for the production of balanced gametes, and crossovers (COs) must occur exclusively between homologous chromosomes. Many interspecific hybrids have problems with meiotic division at early generations, in which interactions between non-homologous chromosomes often bring about aneuploidy and unbalanced gamete formation. I analyzed meiotic chromosome behaviors in pollen mother cells (PMCs) of allotetraploid and allodiploid F1 individuals of newly synthesized x*Brassicoraphanus*. Allotetraploid x*Brassicoraphanus* PMCs showed a normal diploid-like meiotic behavior. By contrast, allodiploid x*Brassicoraphanus* PMCs

displayed abnormal segregation of chromosomes mainly due to the absence of homologous pairs. Notably, during early stages of meiosis I many of allodiploid x*Brassicoraphanus* chromosomes behave independently with few interactions between *B. rapa* and *R. sativus* chromosomes, forming many univalent chromosomes before segregation. Chromosomes were randomly assorted at later stages of meiosis, and tetrads with unequal numbers of chromosomes were formed at completion of meiosis. Coimmunolocalization of ASY1, HEI10, and ZYP1 proteins mediating chromosomal synapsis, meiotic recombination, and synaptonemal complex (SC) revealed that COs and SC normally occurred in allotetraploid x*Brassicoraphanus*, whereas a smaller number of recombination foci and synaptonemal complex were formed in allodiploid x*Brassicoraphanus*. These findings suggest that structural dissimilarity between *B. rapa* and *R. sativus* chromosomes prevents non-homologous interactions between the parental chromosomes in x*Brassicoraphanus*, allowing normal diploid-like meiosis. This study also suggests that CO suppression and a failure of SC formation between non-homologous chromosomes are required for correct meiotic progression in newly synthesized allopolyploids, which is important for the formation of viable gametes and reproductive success in the hybrid progeny.

INTRODUCTION

Hybridization and polyploidization are major driving forces in plant evolution (Van de Peer et al., 2017). More than 80% of extant plants are regarded as polyploids that have undergone whole-genome duplication (WGD) in their evolutionary path (Ramsey and Schemske, 2002; Otto et al., 2007). Polyploids can be divided into two classes: ones that undergo WGD (autopolyploids) and the other resulting from hybridization between different species followed by chromosome doubling (allopolyploids). Allopolyploids can be occasionally formed from a cross between distantly related species, for instance, between the individuals that belong to different species or even different genera. Interspecific hybridization and allopolyploidization are likely to contribute to the emergence of many important crop plants such as oilseed rape (*Brassica napus*), cotton (*Gossypium hirsutum*), tobacco (*Nicotiana tabacum*), wheat (*Triticum aestivum*), sugarcane (*Saccharum officinarum*), and coffee (*Coffea arabica*) (Renny-Byfield and Wendel, 2014). However, many studies report that most synthetic allopolyploids exhibited genetic instability and sterility, the latter of which is mainly caused by meiotic abnormalities during sexual gamete

formation (Madlung et al., 2005; Mestiri et al., 2010; Szadkowski et al., 2010 and 2011).

Meiosis is the process by which the number of chromosomes in a diploid cell is reduced by half producing haploid gametes that are capable of sexual reproduction. Meiosis is divided into two stages, meiosis I and II, each of which comprises prophase, metaphase, anaphase and telophase. In particular, during meiotic prophase I, the homologous chromosomes pair with each other forming a synapsis, and undergo genetic recombination. Formation of synapsis and a crossover (CO) between homologous chromosomes are essential for subsequent chromosome segregation, producing four haploid gametic cells during meiosis II. Errors in meiosis often cause aneuploidy and uneven segregation of chromosomes leading to the failure of functional gamete formation. Such meiotic failure is one of the main causes of sterility observed in many synthetic hybrids, which is manifest as a post-zygotic barrier that prevents hybridization between different species (Dion-Cote and Barbarsh, 2017).

In early generations of synthetic hybrids non-homologous chromosome pairing, multivalent formation, and chromosome rearrangement are frequently observed, and exert a detrimental effect on the survival of allopolyploid plants (Bomblies et al., 2016; Wendel et al., 2018). Thus,

meiosis is critical to the success of sexual reproduction ensuring correct segregation of chromosomes into balanced gametes. During homologous chromosomes are synapsed, the synaptonemal complex (SC) is formed at the interface between the chromosomes along the axis. ASYNAPTIC1 (ASY1) and ZIPPER1 (ZYP1) are the axial and lateral elements of meiotic chromosomes, respectively, both of which are loaded onto chromatids upon synapsis formation (Armstrong et al., 2002; Higgins et al., 2005). HUMAN ENHANCER OF INVASION 10 (HEI10) is a component of ZMM complex (ZIP4, MSH4/5, MER3, MLH1/3) that mediates a meiotic crossover (Chelysheva et al., 2012; Mercier et al., 2015; Gonzalo et al., 2019). The coordinated action of these proteins is crucial for the establishment and progression of synapsis formation and recombination, and abnormal meiosis often results from the lack of proper configuration of these chromatin components.

The Brassicaceae family contains a number of vegetable crops such as broccoli, cabbage, cauliflower, oilseed rape, turnip and radish. Several *Brassica* species are famous for interspecific hybridization to produce allotetraploid plants. For instance, three diploid species *B. rapa* (AA), *B. nigra* (BB), and *B. oleracea* (CC) can be crossed to each other producing allotetraploid species *B. napus* (AACC), *B. juncea* (AABB) and *B. carinata*

(BBCC). Such interspecific cross combinations are epitomized by the model of 'U's Triangle' (U, 1935). In the Brassicaceae family, hybridization between different species can be expanded to the intergeneric level. Since 1826 when intergeneric hybridization between *Brassica* and *Raphanus* was first reported (Prakash et al., 2009), the allotetraploid plants have been sporadically generated but failed to survive due to genetic instability and sterility (Karpechenko, 1924; McNaughton, 1979; Dolstra, 1982). The recently developed x*Brassicoraphanus* (AARR; 2n = 4x = 38) is also synthesized from a cross between *B. rapa* (AA; 2n = 2x = 20) and *Raphanus sativus* (RR; 2n = 2x = 18). Unlike other synthetic allopolyploid plants, x*Brassicoraphanus* displays great fertility and genetic uniformity over successive generations (Lee et al., 2011).

In this study, I investigated meiotic chromosome behaviors in pollen mother cells (PMCs) of newly synthesized allodiploid (AR) and allotetraploid (AARR) x*Brassicoraphanus* plants. These observations revealed fairly independent assortment of A and R chromosomes during meiosis in x*Brassicoraphanus* without substantial non-homologous interactions. This intrinsically prevents chromatid exchanges between the two parental chromosomes, which would otherwise lead to aneuploidy or chromosome rearrangements often observed in many interspecific hybrids.

MATERIALS AND METHODS

Plant materials and growth condition

Seeds of *B. rapa* cv. Chiifu-401-42, *R. sativus* cv. WK10039, and x*Brassicoraphanus* cv. BB1 were sown on 1× Murashige and Skoog (MS) medium (Duchefa, The Netherlands) in a growth chamber under 16 h of fluorescent light at 20 ± 10 μmol m^{-2} s^{-1}, at 24°C for two weeks. The seedlings were vernalized in the 4°C cold chamber for 4 weeks with 16 h of light and 8 h of dark. The plants were transferred to pots in the greenhouse with the same light condition.

Production of synthetic allodiploid and allotetraploid x*Brassicoraphanus*

Synthetic allodiploid x*Brassicoraphanus* were produced by crossing *B. rapa* as a seed parent with *R. sativus* as a pollen donor. Thirty-day-old immature hybrid seeds were cultured on MS medium (Duchefa, Netherlands) supplemented with 2% sucrose (w/v) and 0.8% plant agar (w/v). The seeds were vernalized and transferred to the above-described conditions. The newly synthesized allodiploid x*Brassicoraphanus* individuals were

subjected to chromosome doubling with 0.3% colchicine treatment for two days. Flow cytometry was used to verify the ploidy level (Pfosser et al., 1995).

Flow cytometric analysis

Leaves of the colchicine treated plants were subjected to ploidy analysis. Chinese cabbage, *B. rapa* cv. Chiifu (2n = 2x =20), was used as a diploid control. Approximately 20 mg of leaves were used for each sample, which were finely chopped with a clean razor blade in 1 mL of ice-cold Tris-$MgCl_2$ buffer (0.2 M Tris, 4 mM $MgCl_2$, 0.5% Triton X-100, pH 7.5) in a glass petri dish on ice (Pfosser et al. 1995). Nuclei from the cells was stained in 50 μg L^{-1} of propidium iodide with 50 μg L^{-1} of RNase, filtered through a 40-μm cell strainer, and kept on ice. Flow cytometry was performed with a medium flow rate in a FACS Canto II flow cytometer (BD Biosciences, USA), and data were analyzed with BD FACSDiva software (BD Biosciences, USA). An FL2 detector was used to measure fluorescence, and phycoerythrin (PE), peridin chlorophyll protein (PerCP), forward scatter (FSC), and side scatter (SSC) parameters were used for analysis according to the manufacturer's protocol.

Immunofluorescence of α-tubulin

For detection of α-tubulin, the method of Wang et al. (2010) was adopted with modifications. The anthers were freshly collected and fixed in 4% paraformaldehyde (v/v) in PEM buffer (50mM Pipes, 5mM EGTA, 2mM $MgSO_4$, pH6.9) for 50 min. The anthers were rinsed in PEM buffer three times for 5 min each and dipped in 10% dimethylsulfoxide for 15 min and then extracted with 1% Triton X-100 for 45 min. The anthers were then rinsed, respectively, in PEM buffer and PBS buffer (137 mM NaCl, 2.7 mM KCl, 7 mM Na_2HPO_4, 1.5 mM KH_2PO_4, pH 7.3) again three times for 5 min. The treated anthers were squeezed in SuperFrost Plus™ Adhesion (Thermo Scientific, USA). The pollen mother cells were incubated with a mouse monoclonal antibody against α-tubulin (Invitrogen, USA) diluted 1:100 in PBS buffer for 2 h at 37°C in a moist chamber. The slides were washed three times for 5 min each with the PBS buffer, and were incubated in a FITC- conjugated anti-mouse IgG (F0257, Sigma, USA) diluted 1:50 in PBS buffer for 2 h at 37°C in a dark chamber. The slides were washed three times again with PBS buffer, and were mounted with 4', 6-diamidino-2-phenylindole (DAPI) in Vectashield antifade Mounting Medium (Vector Laboratories, USA). The prepared slides were imaged using a Leica

confocal microscope SP8X controlled by Leica LAS X (Leica Microsystem, Germany).

Genomic *in situ* hybridization (GISH) analysis

Slide preparation

The Inflorescence were fixed in the Carnoy's solution (ethanol : glacial acetic acid, 3 : 1 v/v) for 24 h and stored at -20°C in 70% ethanol until use. The fixed inflorescences were rinsed in distilled water and checked for meiosis stage by 3% aceto-orcein staining. When optimal meiosis stages were confirmed, the slide preparation was followed by enzyme treatments of the inflorescences. Anthers were thoroughly washed with distilled water and digested in the enzyme mixture including 2% Cellulase R-10 (Duchefa Biochemie, The Netherlands), 1% Macerozyme R-10 (Duchefa Biochemie, The Netherlands), 1% Pectinase (Sigma-Aldrich, USA), and 0.5% Pectolyase Y23 (Sigma-Aldrich, USA) in 150 mM citrate buffer (pH 4.5) to degrade the cell walls at 37 °C for 60~90 min (Kwon and Kim, 2009; Belandres et al., 2015). Treated anthers on the SuperFrost Plus™ Adhesion glass slide (Thermo Fisher, USA) were squashed in 60% acetic acid on a slide warmer and air dried.

Probe preparation

Genomic DNA was extracted and purified from young leaves of *B. rapa* cv. Chiifu-401-42 and *R. sativus* cv. WK10039 using the CTAB extraction method. The genomic DNA was fragmented by sonication and the lengths of the probes DNA fragments were determined by agarose-gel electrophoresis within the range of 200-500 bp. The fragmented genomic DNA of *B. rapa* Chiifu-401-42 was labelled with digoxigenin-11-dUTP (Roche, Germany) and *R. sativus* cv. WK10039 was labelled with biotin-16-dUTP (Roche, Germany) by nick translation and used as probes, after which were stored at -20°C until use.

Hybridization

For analysis of GISH, the method of Kwon et al. (2009) was adopted with modifications. Slides were pretreated with RNase A (RBC, Taiwan) buffer (1mg·mL^{-1} RNase A in 2x SSC) at 37°C for 90 min. The slides were washed 3 times for 3 min each with 2x SSC (Biosesang, Korea). The slides were dehydrated in ethanol series (70, 95, and 100%, 5 min each at room temperature (RT)) and air-dried. The slides were subsequently denatured with 70% deionized formamide (Amresco, USA) in 2x SSC for 10 min at 70°C, dehydrated in ethanol series (70, 95, and 100% , 5 min each -20°C)

and air-dried at dark. A hybridization mixture that consisted of 50% deionized formamide, 10% dextran sulfate, 2x SSC, 15 ng labeled DNA in sterile distilled water was prepared and applied to 40 μL per slide. The GISH mixture was denatured at 94°C and cooled on ice for 10 min, then mounted on slides and placed in a humid incubator at 37°C overnight. The next day, the slides were washed sequentially in 2x SSC for 5 min, 50% deionized formamide in 2x SSC for 5 min, 2x SSC for 5 min, and finally 4x SSC for 5 min at RT. For blocking, the slides were treated with 5% goat serum (Vector Laboratories, USA) in 4x SSCT (0.1% Tween-20 in 4x SSC) for 5 min at 37°C. In first detection, dig- and biotin- labelled probes were detected with anti-dig rhodamine (Roche, Germany) and biotin-anti-avidin (Roche, Germany) in 1% BSA (Amresco, USA) in 4x SSCT for 1 h at 37°C. Then the slides were washed in 4x SSCT 3 times for 10 min each at 37°C. For blocking, the slides were treated with 5% BSA in 4x SSCT for 5 min at 37°C. For the second detection, dig- and biotin- labelled probes were detected with avidin-FITC (Vector Laboratories, USA) and anti-sheep Texas red (Vector Laboratories, USA) in 1% BSA in 4x SSCT for 1 h at 37°C. The slides were then washed in 4x SSCT 3 times for 10 min each at 37°C. The slides were dehydrated in ethanol series (70, 95, and 100%, 5 min each at RT) and air-dried at dark. Forty microliters of DAPI in Vectashield

reagent (Vector Laboratories, USA) was used to counterstain the chromosomes and the slides were covered with glass coverslips.

RNA extraction and cDNA synthesis

Total RNA was extracted from fresh young flowering buds using an RNAprep Pure Kit (Qiagen, Germany), and the first-strand cDNA was synthesized from 1 μg of total RNA using the PrimeScript ^{TM} RT Master Mix (Perfect Real Time, TaKaRa, Japan) according to the manufacturer's instructions. The synthesized cDNA was diluted to a final concentration of 20 ng μL^{-1} with nuclease free water.

Immunolocalization of proteins

Protein Expression

The coding regions of *ASY1*, *HEI10*, and *ZYP1* genes were amplified from cDNA of *B. rapa* bud with primers listed in Table I-1. The fragments of *BrASY*1 (708 bp), *BrHEI*10 (906 bp), and *BrZYP*1 (1332 bp) were inserted into pET-28a vector (Novagen, USA) with appropriate restriction enzyme digestion (Table I-2). The resulting constructs were transformed into *Escherichia coli* Rosetta2 (DE3) strains (Novagen, USA). Transformants were grown at 30°C in 1 L of LB medium in the presence of

50 μg mL^{-1} of kanamycin and 50 μg mL^{-1} of chloramphenicol until the OD_{600} reached to 0.4. Protein expression was induced with 1mM of isopropyl b-D-thiogalactopyranoside (IPTG) at 16°C for 16 h. Cells were harvested by centrifugation at 6,500 rpm for 15 min at 4°C, and the pellet was resuspended in 100 mL of ice-cold column buffer (50 mM Tris-HCl, pH 7.4, 100 mM NaCl, 10% glycerol, 0.1 mM dithiothreitol, 0.1 mM PMSF). Cells were lysed by sonication for 5 min in ice (output power, 4; duty cycle, 50%; Branson Sonifer 250, Branson, USA). The lysate was subjected to centrifugation at 9,000 rpm for 25 min at 4°C. Inclusion bodies were collected by centrifugation and dissolved in 4 M urea buffer. And the soluble lysate was purified by a 5-mL HisTrap FF column (GE Health care, USA) with a linear gradient of ice-cold column buffer (50 mM Tris-HCl, pH 7.4, 100 mM NaCl, 10% glycerol, 0.1 mM dithiothreitol, 250 mM imidazole). Protein concentration was estimated using the Coomassie Brilliant Blue R 250 dye-binding method (Bradford, 1976).

Production of antibody

The purified BrASY1, BrHEI10, and BrZYP1proteins were used to produce polyclonal antibodies from rabbit and rat by Youngin Frontier (Korea).

Western blotting

The antibodies were tested for their specificity by western blotting. The ASY1, HEI10, and ZYP1 proteins lysates were separated by electrophoresis on 10% SDS-polyacrylamide gel. The gel was blotted onto a Hybond C membrane (GE Healthcare, USA). The membrane was blocked with TBST (20 mM Tris-HCl pH 7.4, 137 mM NaCl, 0.1% Tween-20) containing 5% BSA for 1 h at room temperature and then incubated with primary antibody solution (anti-ASY1 form rabbit, anti-ZYP1 from rabbit and rat, and anti-HEI10 from rabbit) for 1 h at room temperature. After three times washing with TBST, the membrane was incubated with horseradish heroxidase (HRP)-conjugated secondary antibodies (goat anti-rabbit IgG-HRP (1:10000, SC-2004, Santa Cruz, USA) and goat anti-rat IgG HRP-linked antibody (1:1000, 7077S, Cell Signaling, USA) for 1 h at room temperature. The signals were detected with SuperSignal West Pico Chemiluminescent Substrate (Thermo Scientific, USA) and exposed using a Fusion FX7 imaging system (Vilber Lourmat, France).

Antibody slide pretreatment

A modified version of the method described by Chelysheva et al. (2013) was used to prepare chromosome spreads. The floral buds were fixed in an

aceto-ethanol (1:3 v/v) solution at 4°C until use. The fixed inflorescences were rinsed in distilled water and checked for the meiosis stage by 3% aceto-orcein staining. The selected inflorescences were enzyme treated as described above. Twenty microliters of 60% acetic acid were added to the suspension of the selected anthers. The slides were placed on the slide warmer for 2 min at 45°C and added with 20 µL of 60% acetic acid on the slide and placed on it for 5 min at 45°C. The slides were treated with fresh cold aceto-ethanol (1:3, v/v) solution and dried in hood. The slides were put in Helllendahl jar with 10 mM citrate buffer pH 6 and then microwave for 45 sec at 850 W. The slides were transferred to PBST in a glass Hellendahl jar and incubated for 5 min at RT.

Immunolabelling

The primary antibodies (anti-ASY1 form rabbit, anti-HEI10 from rabbit anti-ZYP1 from rabbit and rat, and) were diluted to 1:250 in PBST-BSA and used 50 µL of the antibody working solution per slide, covered with 24x60 mm piece of parafilm. The slides were incubated at 4°C for 39~48 h in a moist chamber. The slides were washed in PBST for 15 min, 3 times at RT. The secondary antibodies (Goat anti-rabbit IgG H&L, Alexa Fluor 488 and Donkey anti-rat IgG H&L, Alexa Fluor 594) were mixed in PBST- BSA at a

dilution of 1:500. 50 μL of the antibody working solution per slide put and glasscover was covered with 24x60mm pieces of parafilm and incubated at 37°C for 1 h in a dark moist chamber. The slides were washed in PBST for 10 min 3 times at RT. Forty microliters of DAPI in Vectashield reagent (Vector Laboratories, USA) was mounted to counterstain the chromosomes and covered with a glass coverslip. Several meiotic stages stained with DAPI in Vectashield were imaged using an Axioskop2 microscope equipped with an Axiocam 506 color CCD camera (Zeiss, Germany). Images were processed using Adobe Photoshop CS6 (Adobe Systems Incorporated, USA).

Table I-1. List of oligonucleotides for cDNA cloning.

Genes	Forward (5' to 3')	Reverse (5' to 3')
ASY1	CCACGGAGCGAATTCAACT TTGTG	TCAATTAGCCTGAAATTTCTG GCGC
HEI10	ATGAGGTGCAACGCCTGTT GG	TTACGTGAACAGTTGCGGGC G
ZYP1b	GCAAAGCAGGCAATTGAAA AACTAGAGTCTGAAGC	GGTTGAGAGAGC CTT CTG AAA ACA GAT CTC C

Table I-2. List of oligonucleotides for cloning of antigen expression.

Primer name	Sequence (5' to 3')
ASY1_BamHI_F	ggatccCCACGGAGCGAATTCAACTTTGTG
ASY1_XhoI_R	GGctcgagCTCAATTAGCCTGAGATTTCTGG
HEI10_EcoRI_F	TTAAgaattcATGAGGTGCAACGCCTGTTGGAGGG
HEI10_XhoI_R	TTAActcgagGAACAGTTGCGGGCGAGAACG
ZYP1_BamHI_F	ggatccGAATTAGAAGCATTGTCTGAAAATCTGAGG
ZYP1_EcoRI_R	CgaattcCCCTAAGAGCCTTCTGAAAACAGATCTCC

Restriction enzyme sites are added for cloning into protein expression vector which are underlined.

RESULTS

Representative meiotic behavior as reference in *B. rapa* and *R. sativus*

Before investigating chromosomal behaviors of the synthetic allodiploid and allotetraploid, the parents, *B. rapa* cv. Chiifu-401-42 and *R. sativus* cv. WK10039, were observed as the controls which have not been reported yet. The chromosomal behaviors of meiosis in *B. rapa* and *R. sativus* were considered with DAPI staining (Figs. I-1 and I-2). At leptotene, meiotic chromosomes were initiated to condense (Figs. I-1A and I-2A). The alignments of homologous chromosomes initiated to form a synaptonemal complex at zygotene stage (Figs.I-1B and I-2B). At pachytene, all chromosomes were exactly aligned with one another, indicating that homologous chromosomes were fully synapsed (Figs. I-1C and I-2C). The synaptonemal complex disappeared and chromosomes were condensed distinctly to separate at diakinesis (Figs. I-1D and I-2D). Then bivalents of homologous chromosomes appeared. At metaphase I, ten and nine bivalents in *B. rapa* and *R. sativus*, respectively, were placed at metaphase plate (Figs. I-1E and I-2E). The homologous chromosomes were separated in ten chromosomes of *B. rapa* and nine chromosomes of *R. sativus* at telophase I (Figs. I-1F and I-2F). At telophase II (Figs. I-1G and I-2G), second meiotic

division resulted in four balanced gametes of ten chromosomes of *B. rapa* and nine chromosomes of *R. sativus* and led to equal tetrad formation in all cells observed (*n* =33 and 41 observed cells, respectively) (Figs. I-1H and I-2H). As described above, the parental lines did show no observable disorders throughout the meiosis and provided suitable chromosome behavior for further comparisons.

Impaired meiotic behavior in synthetic allodiploids x*Brassicoraphanus*

Since many synthetic allopolyploid plants display chromosomal aberrations typically caused by abnormal meiosis, I monitored meiotic chromosome behaviors in allodiploid x*Brassicoraphanus*. Meiotic chromosome behaviors in allodiploid x*Brassicoraphanus* were similar to those of the parents at early stages. However, single chromosomes without chromosome pairing were conspicuous, implying rare synapsis formation at pachytene (*n*=59 PMCs; Fig. I-3A), At diakinesis, bivalents were detected at low frequency and univalents were more frequently observed in allodiploid x*Brassicoraphanus* (Fig. I-3B). At metaphase I, the univalent chromosomes that failed to form chiasmata between non-homologous A and R chromosomes were observed (Fig. I-3C). Subsequently, meiotic chromosomes were unequally segregated, and in a rare occasion,

chromosome bridges appeared at telophase I (Fig. I-3D). In tetrad, unbalanced gametes were formed at the end of meiosis (Fig. I-3E).

Diploid-like meiotic behavior in synthetic allotetraploids x*Brassicoraphanus*

At pachytene, all chromosomes were closely juxtaposed, indicating complete synapsis between homologous chromosomes (Fig. I-4A). The SC disappeared and chromosomes were condensed into bivalents at diakinesis (Fig. I-4B). At metaphase I, all bivalents were aligned at the metaphase plate (Fig. I-4C). The homologous chromosomes were evenly separated at telophase I (Fig. I-4D). Finally, four balanced gametes were produced after the second meiotic division in all PMCs (n = 25; Fig. I-4E). These observations indicate that meiosis occurs normally in synthetic allotetraploid x*Brassicoraphanus* while ensuring faithful chromosome segregation after hybridization between *B. rapa* and *R. sativus*.

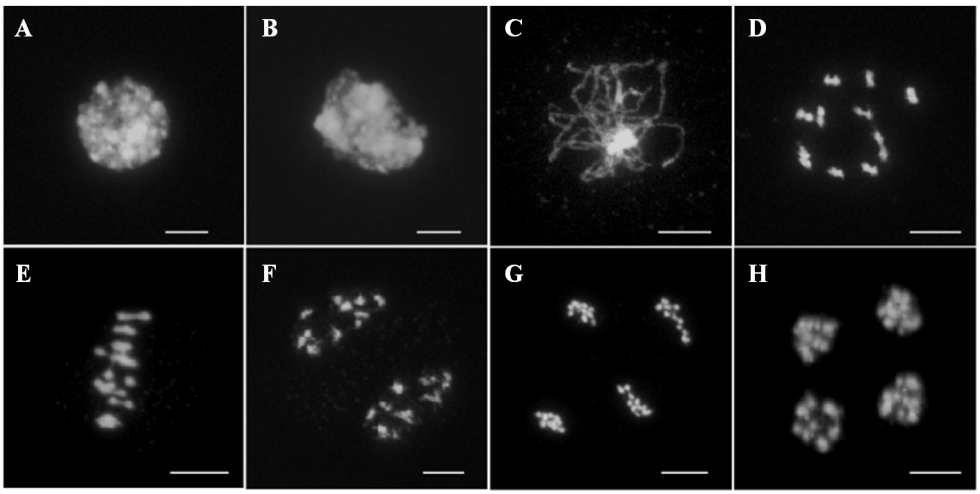

Figure I-1. Chromosome behavior during meiosis in PMCs of *B. rapa*. Leptotene (A), zygotene (B) pachytene (C), diakinesis (D): metaphase I (E), telophase I (F), telophase II (G), and tetrad (H). Scale bars = 10 μm.

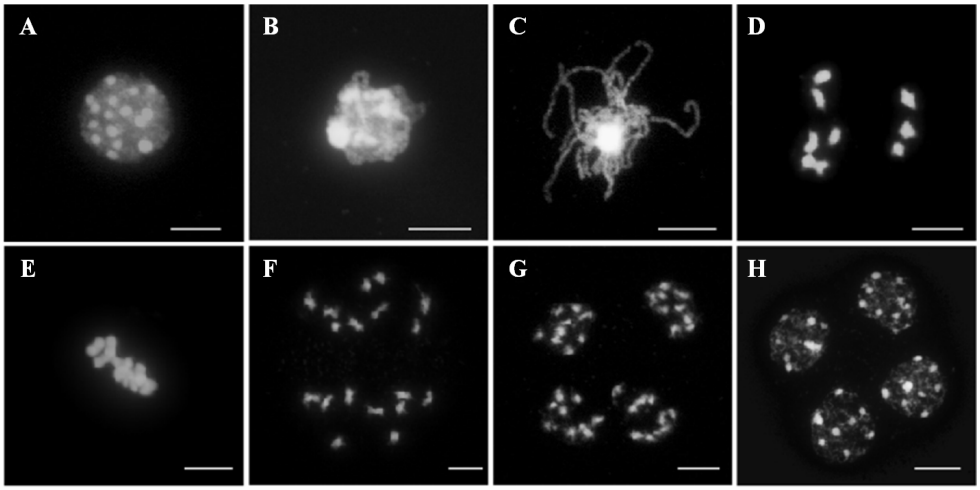

Figure I-2. Chromosome behavior during meiosis in PMCs of *R. sativus*. Leptotene (A), zygotene (B), pachytene (C), diakinesis(D), metaphase I (E), telophase I (F), telophase II (G), and tetrad (H). Scale bars = 10 μm.

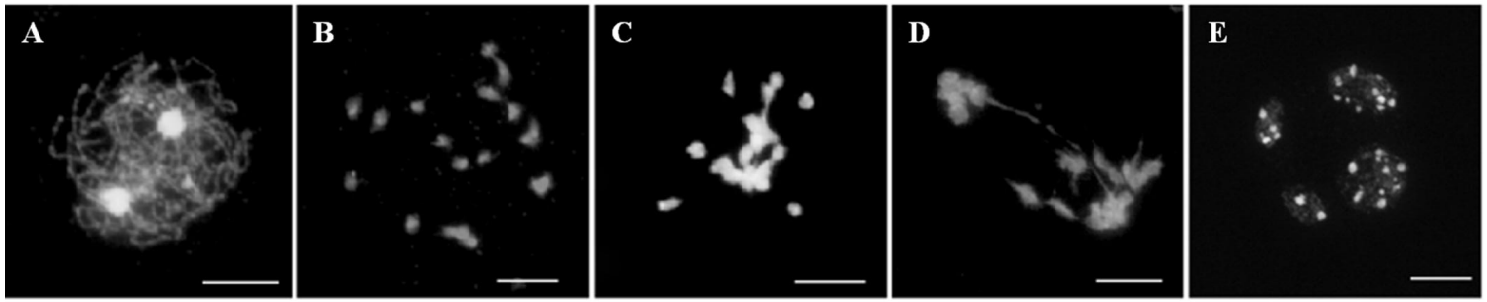

Figure I-3. Chromosome behavior during meiosis in PMCs of synthetic allodiploid x*Brassiconaphanus*. Pachytene (A), diakinesis(B), metaphase I (C), telophase I (D), and tetrad (E). Scale bars = 10 μm.

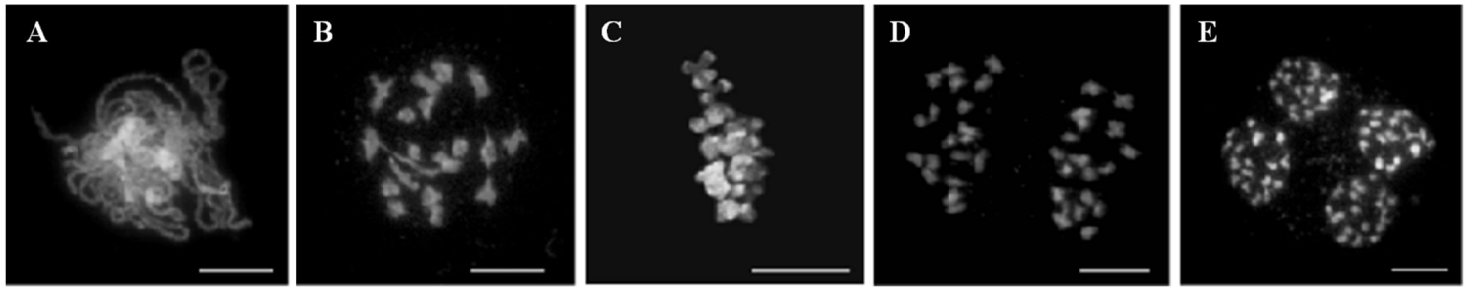

Figure I-4. Chromosome behavior during meiosis in PMCs of synthetic allotetraploid x*Brassiconaphanus*. Pachytene (A), diakinesis(B), metaphase I (C), telophase I (D), and tetrad (E).

Few non-homologous chromosome associations at meiosis of synthetic allodiploid x*Brassicoraphanus*

Non-homologous chromosome pairing often induces meiotic chromosome aberrations in many resynthesized allopolyploids (Madlung et al., 2005; Mestiri et al., 2010; Szadkowski et al., 2010 and 2011). To investigate non-homologous interactions between A and R chromosomes in x*Brassicoraphanus*, GISH analysis was performed during meiosis. In PMCs of allodiploid x*Brassicoraphanus*, ten chromosomes of *B. rapa* and nine chromosomes of *R. sativus* were present, but they mis-segregated at later stage of meiosis (Fig. I-5). At diakinesis, 0.36 A-A and 0.56 R-R autosyndetic bivalents on average were observed, whereas 1.16 A-R allosyndetic bivalents were present (Table I-3). Also, 4.63 A and 3.80 R univalents on average were observed at diakinesis in allodiploid x*Brassicoraphanus* (Table I-3). These observations indicate that non-homologous pairing is less prominent than unpaired univalents in allodiploid x*Brassicoraphanus*, albeit only 5.5% of PMCs (n = 55) contained 19 univalents without chromosome pairing (Fig. I-5A and E). At metaphase I, the univalent chromosomes failed to form chiasmata between non-homologous A and R chromosomes were often present (Fig. I-5B and F). At telophase I, chromosome bridges were often observed in allodiploid

x*Brassicoraphanus* PMCs (Fig. I-5C and G). At telophase II, A and R chromosomes were randomly segregated to each microspore (Fig. I-5H). A low frequency of A and R associations suggests that a considerably low level of meiotic recombination likely occur in allodiploid x*Brassicoraphanus*. This also suggests that non-homologous interactions between A and R chromosomes are not preferred during synapsis formation at early stages of meiosis.

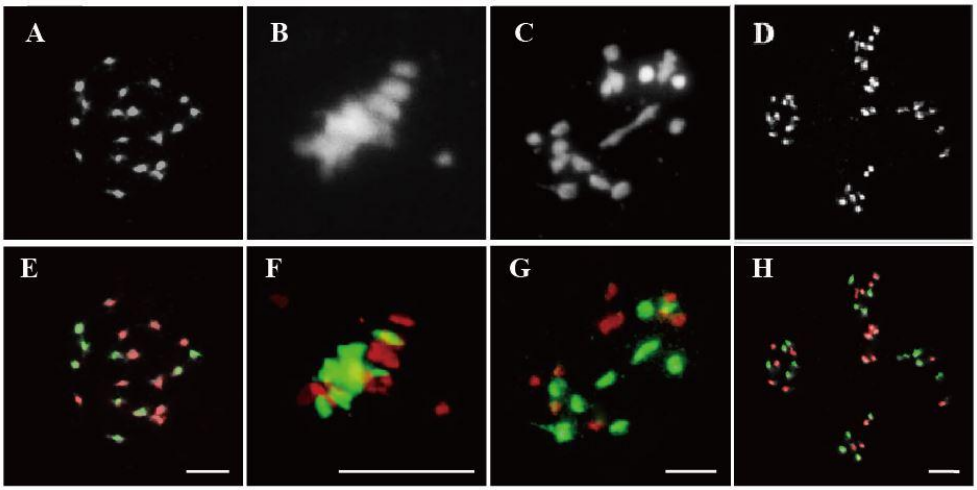

Figure I-5. Chromosome identification of x*Brassicoraphanus* by GISH analysis in PMCs of synthetic allodiploid x*Brassicoraphanus*. Distribution of A and R chromosomes were observed with DAPI staining (A, B, C, and D) and genome *in situ* hybridization (GISH) analysis (E, F, G, and H) in PMCs. The homoeologous pairings between A and R chromosomes were rarely detected in allodiploid x*Brassicoraphanus*. The A and R chromosomes are stained in red and green, respectively. Scale bars = 10 μm.

Table I-3. Chromosome associations in PMCs of allodiploids at diakinesis as revealed by GISH

Lines	Total PMCs	I			II				III	≥ IV
		I^A	I^R	Total	II^{AA}	II^{RR}	II^{AR}	Total		
#20	38	5.18 (0-9)	3.96 (2-7)	9.14 (2-15)	0.39 (0-2)	0.57 (0-1)	1.25 (0-4)	2.21 (0-5)	0.71 (0-2)	0.61 (0-2)
#30	16	4.05 (2-7)	3.15 (0-5)	7.20 (2-12)	0.40 (0-2)	0.60 (0-2)	1.50 (0-5)	2.50 (0-7)	0.95 (0-3)	0.85 (0-2)
#43	24	4.67 (0-10)	4.28 (1-9)	8.94 (2-19)	0.28 (0-2)	0.50 (0-2)	0.72 (0-2)	1.50 (0-4)	0.78 (0-3)	0.89 (0-2)
Average		4.63 ±0.57	3.80 ±0.58	8.43 ±1.07	0.36 ±0.07	0.56 ±0.05	1.16 ±0.4	2.07 ±0.52	0.81 ±0.12	0.78 ±0.15

I, univalent; II, bivalent; III, trivalent; ≥ IV, more than quardrivalent.
I^A and I^R indicate univalent belonging to the A and R genomes, respectively.
II^{AA} and II^{RR} indicate autosyndetic bivalents and II^{AR} indicates allosyndetic bivalents formed between A and R chromosomes

No homoeologous chromosome associations at meiosis of synthetic allotetraploid x*Brassicoraphanus*

Twenty chromosomes of *B. rapa* and 18 chromosomes of *R. sativus* existed in synthetic allotetraploid x*Brassicoraphanus* at diakinesis (Fig.I-6). At diakinesis and metaphase I, 19 bivalents were present in an autosyndetic (A-A or R-R) form, probably with ten A-A bivalents and nine R-R bivalents in allotetraploid x*Brassicoraphanus* (Fig.I-6A, B, E and F). At telophase I, chromosomes were correctly segregated, and ten A chromosomes and nine R chromosomes were evenly distributed at each pole in allotetraploid x*Brassicoraphanus* (Fig.I-6C and G). At telophase II, chromosomes were evenly segregated to tetrads with ten A and nine R haploid chromosomes, respectively (Fig.I-6D and H). A-R chromosome associations were unnoticeable during the entire course of meiosis in allotetraploid x*Brassicoraphanus*. These observations suggest the absence of non-homologous pairing between A and R chromosomes, which would prevent chromosome rearrangement and aneuploidy in allotetraploid x*Brassicoraphanus.*

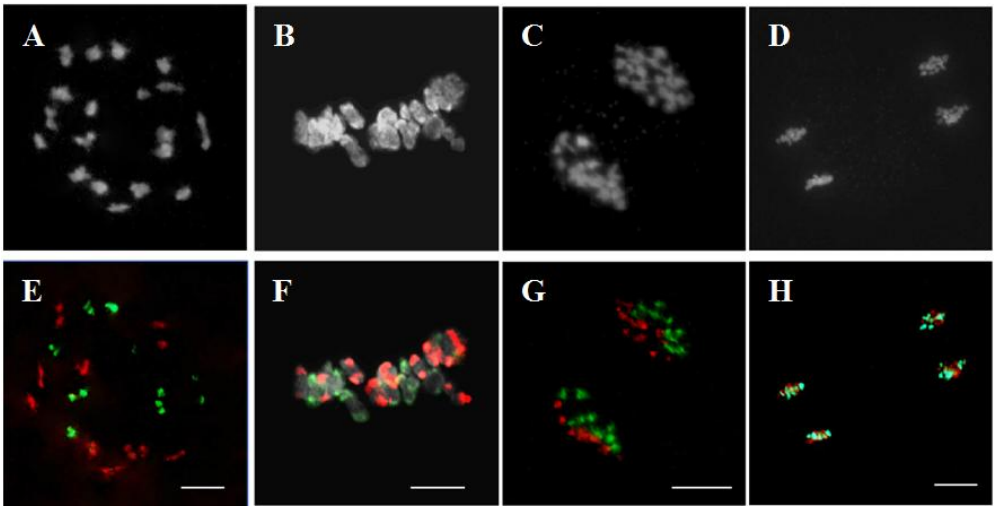

Figure I-6. Chromosome identification of x*Brassicoraphanus* by GISH analysis in PMCs of synthetic allotetraploid x*Brassicoraphanus*. Distribution of A and R chromosomes were observed with DAPI staining (A, B, C, and D) and genome *in situ* hybridization (GISH) analysis (E, F, G, and H) in PMCs. The A and R chromosomes are stained in red and green, respectively. Scale bars = 10 μm.

Few non-homologous interactions in x*Brassicoraphanus*

Interspecific hybridization often involves homoeologous exchanges during meiosis that eventually cause non-homologous recombination (Grandont et al., 2014; Szadkowski et al., 2011; Szadkowski et al., 2010; Xiong et al., 2011). To investigate homoeologous interactions between A and R chromosomes, the synapsis formation at meiotic prophase I was examined by coimmunolocalization of ASYNAPTIC1 (ASY1) and ZIPPER1 (ZYP1). ASY1 is the axial/lateral element of meiotic chromosomes, loaded onto chromatids before synapsis (Armstrong et al., 2002), and ZYP1 is the central element of the synaptonemal complex (SC), present in synapsed chromosomes (Higgins et al., 2005). ASY1 was correctly loaded on chromatids along the entire axis of pachytene chromosomes of *B. rapa*, *R. sativus*, x*Brassicoraphanus* cv. BB1, synthetic allodiploid (AR) and allotetraploid (AARR) x*Brassicoraphanus* (Fig. I-7). Notably, ZYP1 was co-localized with ASY1 at all euploid pachytene chromosomes (*B. rapa*, *R. sativus*, x*Brassicoraphanus* cv. BB1, allotetraploid) but very loosely associated with those of x*Brassicoraphanus* (AR) (Fig. I-7D). This observation is contrasting to the previous study that showed the association of ZYP1 with SC formed between non-homologous chromosomes in synthetic allodiploid *B. napus* (Grandont et al., 2014).

These findings suggest that *B. rapa* and *R. sativus* chromosomes share little homology, and thus, homoeologous interactions are prevented during meiosis while minimizing non-homologous exchanges that often lead to aneuploidy and/or chromosome reshuffling. This also supports this observation that both *B. rapa* and *R. sativus* genomes exist in entirety without losses in allotetraploid x*Brassicoraphanus* upon hybridization (Fig. I-6) presumably due to parental genome divergence.

Suppression of crossovers in synthetic allodiploid x*Brassicoraphanus*

Formation of COs and SC was investigated by coimmunolocalization of HEI10 and ZYP1 at pachytene of *B. rapa*, *R. sativus*, and synthetic allodiploid and allotetraploid x*Brassicoraphanus* (Fig. I-8). It is known that HEI10 is essential for transition of early recombination intermediates into final class I COs, which represent the actual sites where strand exchanges and recombination take place (Chelysheva et al., 2012; Gonzalo et al., 2019). To examine intensity and frequency of COs, HEI10 foci were examined in *B. rapa*, *R. sativus*, and synthetic allodiploid and allotetraploid x*Brassicoraphanus* (Fig. I-8 and 9). The average number of HEI10 foci at pachytene was 17.54 in *B. rapa* (n = 51 PMCs) and 17.33 in *R. sativus* (n = 18 PMCs) (Fig. I-10). In BB1, 30.92 foci on average were

observed (*n* = 13 PMCs), suggesting that an increase in number of COs was attributed to the doubled chromosome number by allopolyploidization. In synthetic allotetraploid x*Brassicoraphanus*, 19.74 HEI10 foci were observed on average (*n* = 79 PMCs) (Fig. I-10). Interestingly, only 4.38 HEI10 foci on average were detected in allodiploid x*Brassicoraphanus* (*n* = 34 PMCs) (Fig. I-10), and the HEI10 foci were less conspicuous compared to the parental species and allotetraploid x*Brassicoraphanus* (Fig. I-10). It is reported that the formations of large and bright HEI10 foci occur only in properly synapsed regions (Chelysheva et al., 2012; Grandont et al., 2014), and these observations suggest that a faint HEI10 signal and few ZYP1 formation are attributed to unstable synapsis between chromosomes in allodiploid x*Brassicoraphanus*. Also, non-homologous recombination is unlikely to occur in x*Brassicoraphanus* owing to few interactions between A and R chromosomes.

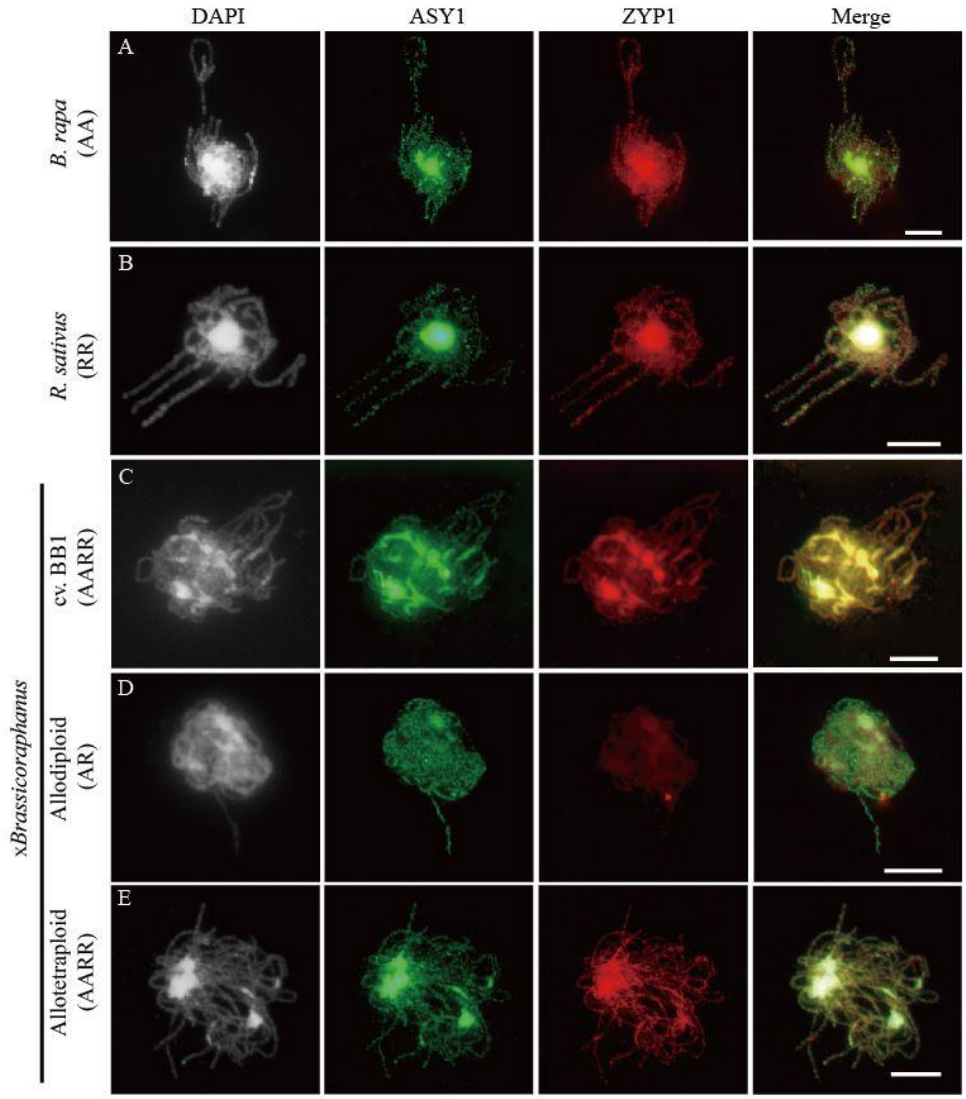

Figure I-7. Coimmunolocalization of ASY1 and ZYP1 at pachytene in *B. rapa* (A), *R. sativus* (B), x*Brassicoraphanus* cv. BB1 (C), and synthetic allodiploids (D) and allotetraploid x*Brassicoraphanus* (E). Few ZYP1 were detected in allodiploid x*Brassicoraphanus*. Chromosomes were labeled with DAPI (white), ASY1 (green), and ZYP1 (red) antibodies. The overlay of three signals is shown (merge). Scale bars = 10 μm.

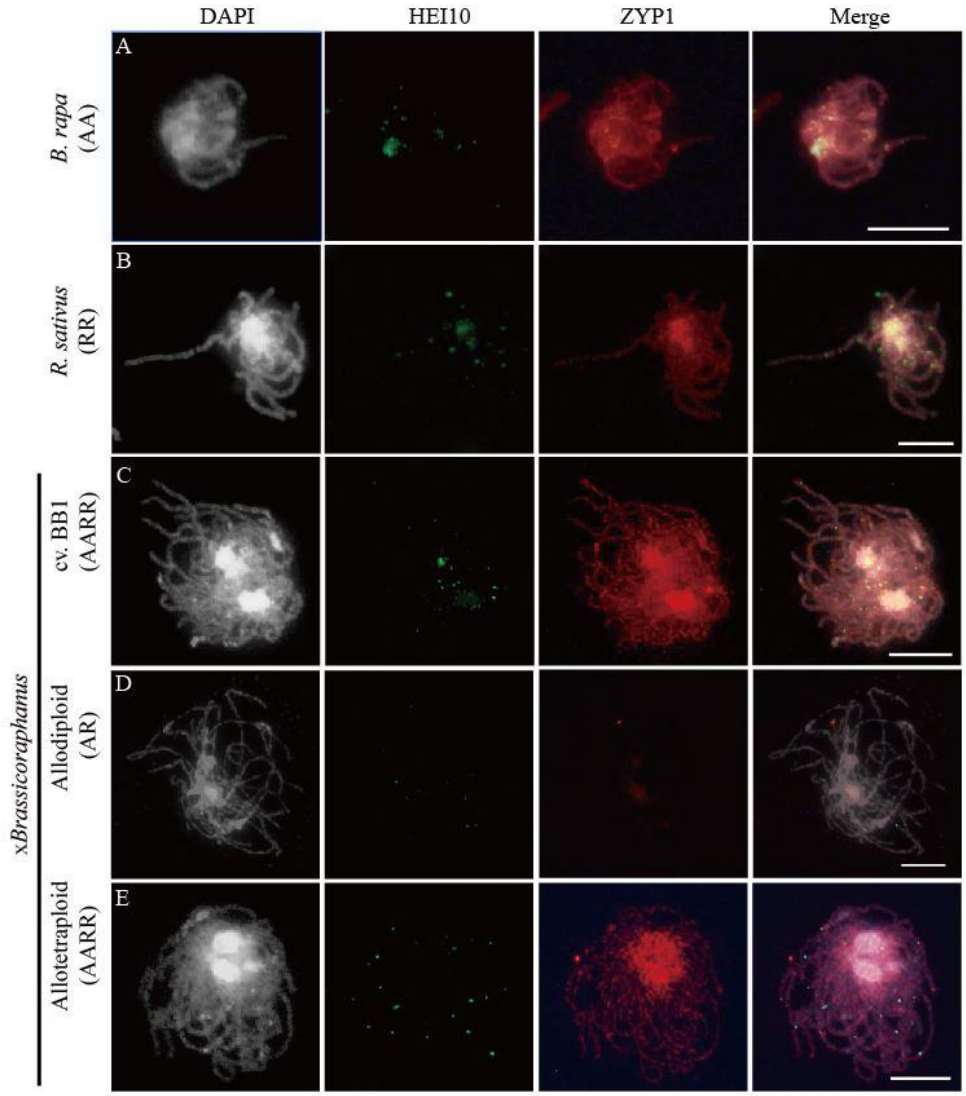

Figure I-8. Coimmunolocalization of HEI10 and ZYP1 at pachytene in *B. rapa* (A), *R. sativus* (B), x*Brassicoraphanus* cv. BB1 (C), and synthetic allodiploids (D) and allotetraploid x*Brassicoraphanus* (E). Few HEI10 foci and ZYP1 were detected in allodiploid x*Brassicoraphanus*. Chromosomes were labeled with DAPI (white), HEI10 (green), and ZYP1 (red) antibodies. The overlay of three signals is shown (merge). Scale bars = 10 μm.

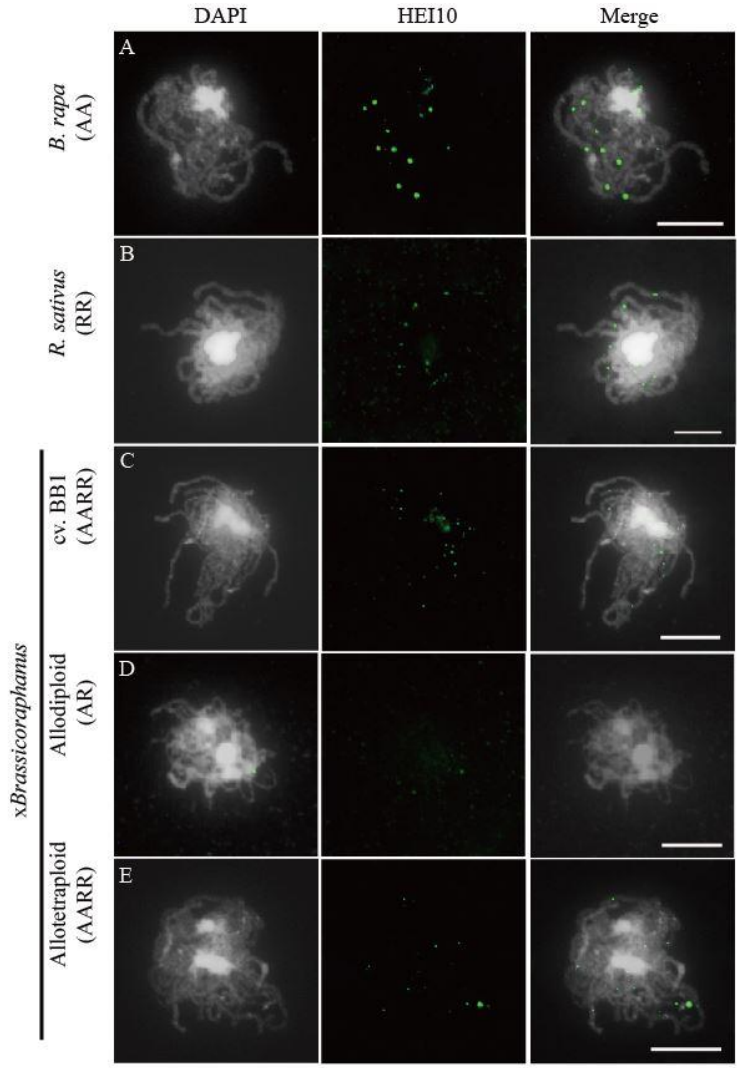

Figure I-9. Immunolocalization of HEI10 at pachytene. HEI10 foci were observed in PMCs of *B. rapa* (A), *R. sativus* (B), x*Brassicoraphanus* cv. BB1 (C), and synthetic allodiploids (D) and allotetraploid x*Brassicoraphanus* (E). Few HEI10 foci were detected in allodiploid x*Brassicoraphanus*. Chromosomes were labeled with DAPI (white) and HEI10 antibodies (green). The overlay of two signals is shown (merge). Scale bars = 10 μm.

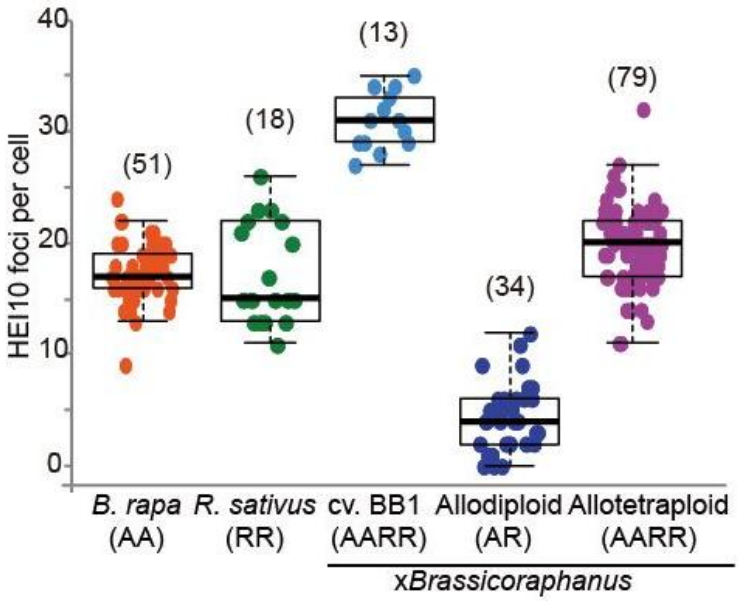

Figure I-10. The number of HEI10 foci per PMC at pachytene. The parental species showed similar number of HEI10 foci (17.54 ± 3.48 in *B. rapa* and 17.33 ± 4.51 in *R. sativus*). x*Brassicoraphanus* cv. BB1 represented twice number of HEI10 foci than parental species (30.92 ± 2.53) and slightly low number of foci were observed in synthetic allotetraploid x*Brassicoraphanus* (19.74 ± 3.52). In allodiploid x*Brassicoraphanus*, only few foci were detected (4.38 ± 2.97). The numbers of observed PMCs were represented in parenthesis.

Microtubule distribution and chromosome behaviors in *B. rapa and* x*Brassicoraphanus*

Microtubules are important for the formation of meiotic spindles to support correct segregations of chromosomes. Microtubule dynamics was investigated in *B. rapa*, x*Brassicoraphanus* cv. BB1, and allodiploid and allotetraploid x*Brassicoraphanus* through immunostaining of α-tubulin at different stages of meiosis (Figs. I-11 to I-14). Microtubules were initiated in the nuclear envelope at leptotene in *B. rapa*, BB1, and allodiploid and allotetraploid x*Brassicoraphanus* (Fig. I-11A, 12A, 13A, and 14A). The microtubules were lined into the perinuclear at pachytene (Fig. I-11B, 12B, and 14B). At diakinesis, the microtubules were present on the chromosomes (Fig. I-13B and 14C). The microtubules were arranged into the spindle structure and attached to kinetochores in bivalents at prometaphase I (Fig. I-11C, 12C, 13C, and 14D). At metaphase I, microtubules were arranged into the spindle structure and attached to kinetochores, engaging a typical bipolar fusiform configuration at the metaphase plate (Fig. I-11D, 12D, 13D, and 14E). At anaphase I, microtubules pushed chromosomes toward the opposite poles (Fig. I-11E, 12E and 13E). Notably, some chromosomes of allodiploid x*Brassicoraphanus* were not attached to meiotic spindles (Fig.I-14F). Then interzonal microtubules appeared at the equator forming the phragmoplast.

At metaphase II, two bipolar spindles formed from the opposite poles (Fig. I-11F). At telophase I, the chromosomes configurations were divided in cell between microtubules (Fig. I-12F). Chromosomes were further equally segregated with microtubules to bipolar attachment at anaphase II (Fig. I-11G). At prophase II, microtubules were initiated in the nuclear envelope (Fig. I-12G). At telophase II, the microtubules were appearing between four segregated chromosomes in preparation for cytokinesis (Fig. I-11H, 12H, and 14G). At completion of meiosis, microtubules dissolved and dispersed in the cytoplasm in tetrads (Fig. I-11I, 12I, 13F and 14H). These observations indicate that microtubules behave normally in x*Brassicoraphanus* PMCs.

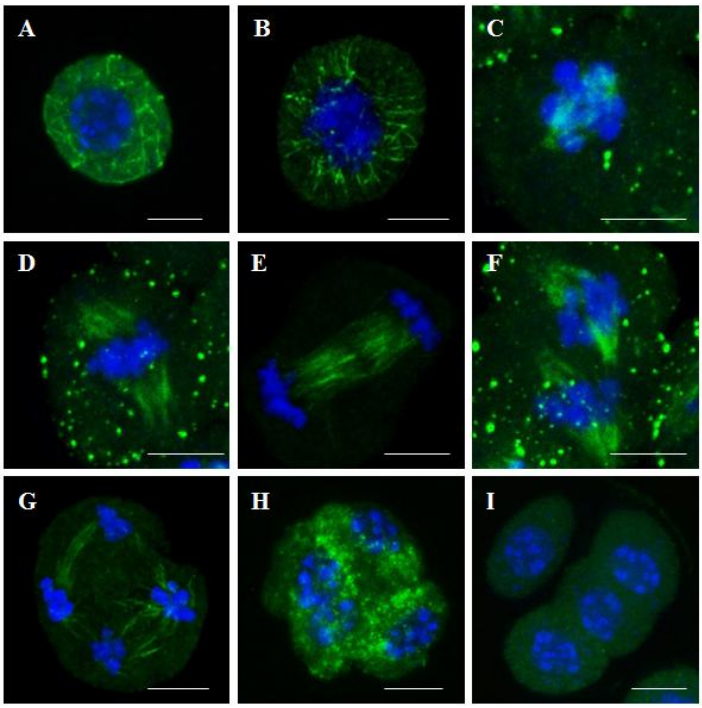

Figure 1-11. Microtubule distribution during meiosis in *B. rapa*. Leptotene (A), pachytene (B), prometaphase I (C), metaphase I (D), anaphase I (E), metaphase II (F), anaphase II (G), telophase II (H), and tetrad (I). Microtubules and chromosomes were in green and blue, respectively. Scale bars = 5 μm.

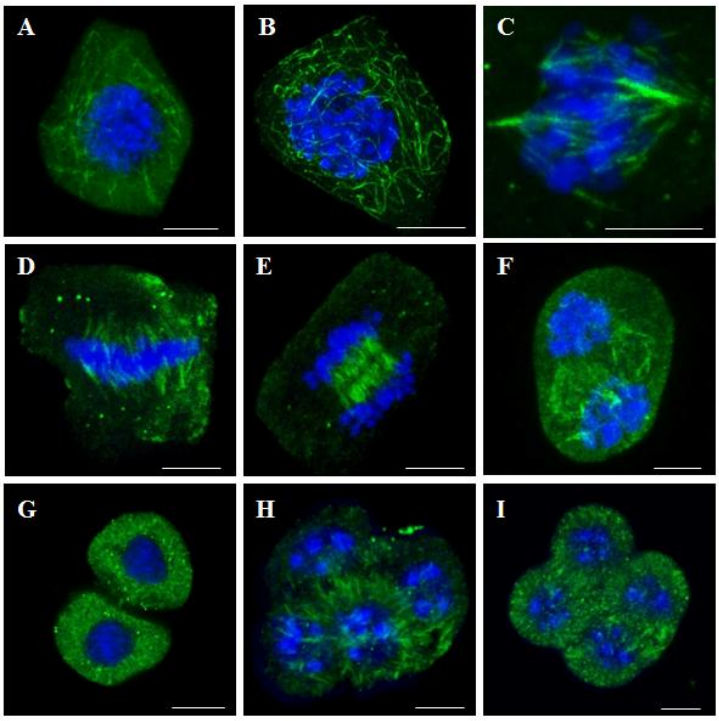

Figure I-12. Microtubule distribution during meiosis in x*Brassicoraphanus* cv. BB1. Leptotene (A), pachytene (B), prometaphase I (C), metaphase I (D), anaphase I (E), telophase I (F), prophase II (G), telophase II (H), and tetrad (I). Microtubules and chromosomes were in green and blue, respectively. Scale bars = 5 μm.

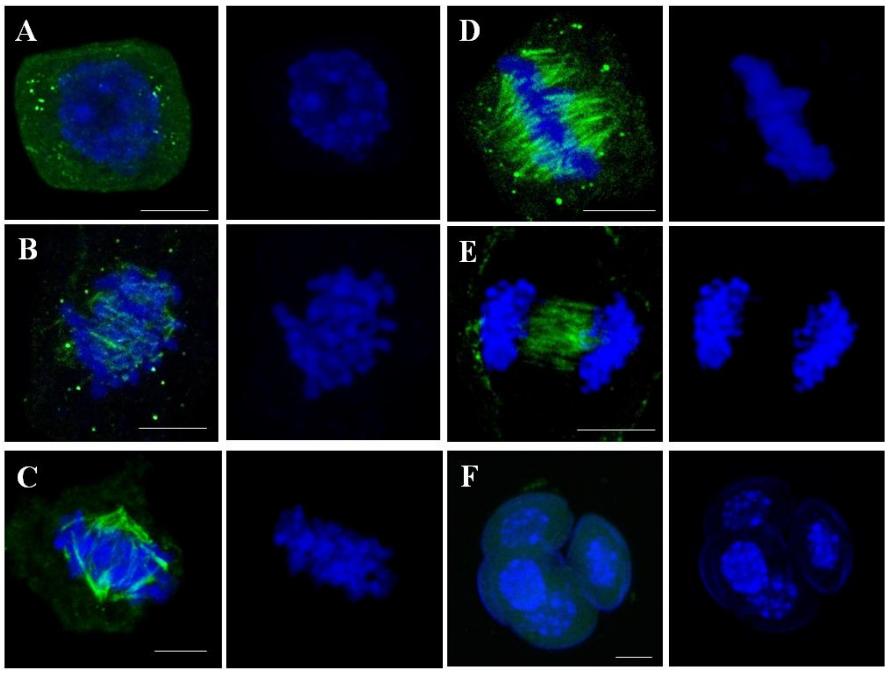

Figure I-13. Microtubule distribution during meiosis in synthetic allotetraploid x*Brassicoraphanus*. Leptotene (A), diakinesis (B), prometaphase I (C), metaphase I (D), anaphase I (E), and tetrad (F). Microtubules and chromosomes were in green and blue, respectively. Scale bars = 5 μm.

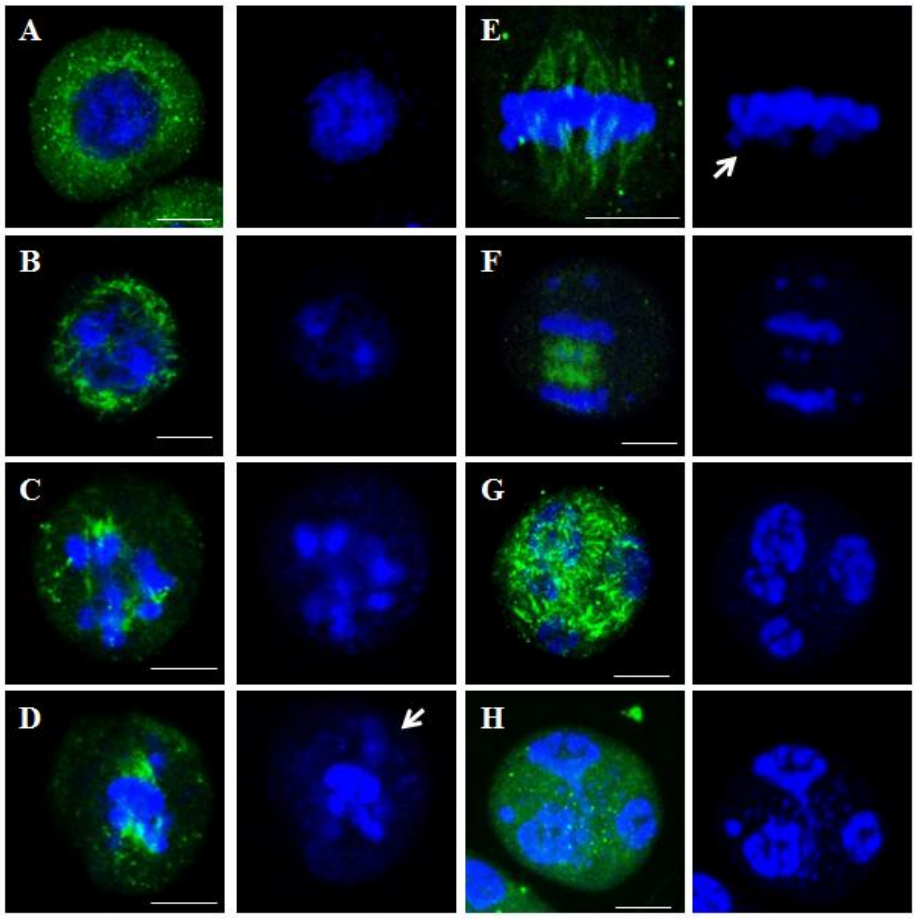

Figure I-14. Microtubule distribution during meiosis in synthetic allodiploid x*Brassicoraphanus*. Microtubule distribution during meiosis. Microtubule and chromosome behaviors were observed in PMCs of synthetic allodiploid. Leptotene (A), pachytene (B), diakinesis (C), prometaphase I (D), metaphase I (E), anaphase I (F), telophase (G), and tetrad (H). Microtubules and chromosomes were in green and blue, respectively. Scale bars = 5 μm.

DISCUSSION

Hybridization barriers exist in nature to prevent a gene flow between different species. In particular, the post-zygotic barrier that occurs after fertilization often results in hybrid inviability and sterility, the latter of which is generally associated with a failure in meiosis. Normal meiosis requires the formation of COs between homologous chromosome pairs, and when they are abolished or formed between multiple and/or non-homologous chromosomes, the chromosomes segregate abnormally, resulting in unbalanced gamete formation and reduced fertility (Martinez-Perez and Colaiacovo, 2009).

x*Brassicoraphanus* has a full complement of both parental chromosomes. Unlike many other resynthesized allopolyploids, x*Brassicoraphanus* did not show aneuploidy or apparent chromosome rearrangements, suggesting that COs and SC between non-homologous chromosomes rarely occur during meiosis. Indeed, the number of parental chromosome interactions per PMC in synthetic allodiploid x*Brassicoraphanus* (Table 1-3) is significantly lower than that of allodiploid

B. napus (1.16 vs. 3.45) (Cui et al., 2012). In addition, 55.64% and 88.9% of allodiploid chromosomes of x*Brassicoraphanus* and *B. napus* (Szadkowski et al., 2011), respectively, participated in the formation of bivalents or multivalents at early stages of meiotic prophase I (Table 1-3). We also showed that meiosis in allotetraploid x*Brassicoraphanus* proceeds normally like a diploid cell, albeit A-R chromosome interactions are sporadically observed in allodiploid x*Brassicoraphanus*. This suggests that during meiotic prophase I the chromosome pairing preferentially occurs between the homologous chromosomes of the same progenitor, although non-homologous interactions are also possible when there is no authentic homologous counterpart.

At early stages of meiotic prophase I, homologous chromosomes are aligned in juxtaposition and SCs are formed at the interface between them along the axis, where ASY1, HEI10, and ZYP1 proteins systematically participate in the formation of SC and COs to exchange chromatids. In resynthesized *B. napus*, synapsis is frequently formed between A and C chromosomes (C from *B. oleracea*) via similar segments carried by different chromosomes, and non-homologous recombination results in aneuploidy and interchromosomal rearrangement (Gaeta et al., 2007; Xiong et al., 2011). Such homoeologous regions are still remnant in *B. rapa* and *B. oleracea*

genomes although they have diverged several million years ago. For example, A1/C1, A2/C2, and the long arm of A5 and short arm of C4 chromosomes share high homology each other (Parkin et al., 2005). To note, allodiploid x*Brassicoraphanus* formed a smaller number of COs (4.38 between A and R; Fig. 1-10) than allodiploid *B. napus* (20.3 between A and C; Grandont et al., 2014). This strongly suggests that interactions between A and R chromosomes are intrinsically inhibited in x*Brassicoraphanus* probably due to a scarcity of homologous regions required for synapsis and recombination.

Recent study proposed that the genera *Brassica* and *Raphanus* are paraphyletic with a close relationship each other (Jeong et al., 2016). It is hypothesized that hexaploid progenitor chromosomes were rearranged into nine chromosomes in *R. sativus*, while undergoing differential subgenome fractionation and massive chromosome rearrangement (Jeong et al., 2016). Therefore, *B. rapa* and *R. sativus* genomes have gradually lost the similarity in genome structure after speciation and become divergent enough to inhibit A-R chromosome interactions. Such structural differences may allow independent assortment of A and R chromosomes during meiosis, which is conceivably beneficial to the acquisition of meiotic stability in x*Brassicoraphanus*.

REFERENCES

Armstrong, S.J., Caryl, A.P., Jones, G.H., and Franklin, F.C. (2002). Asy1, a protein required for meiotic chromosome synapsis, localizes to axis-associated chromatin in *Arabidopsis* and *Brassica*. J. Cell Sci. **115,** 3645-3655.

Bomblies, K., Jones, G., Franklin, C., Zickler, D., and Kleckner, N. (2016). The challenge of evolving stable polyploidy: could an increase in "crossover interference distance" play a central role? Chromosoma **125,** 287-300.

Bradford, M.M. (1976). A rapid and sensitive method for the quantification of microgram quantities of protein utilizing the principle of protein–dye binding. Anal. Biochem. **72,** 248-254.

Chelysheva, L.A., Grandont, L., and Grelon, M. (2013). Immunolocalization of meiotic proteins in Brassicaceae: method 1. Methods Mol. Biol. **990,** 93-101.

Chelysheva, L.A., Vezon, D., Chambon, A., Gendrot, G., Pereira, L., Lemhemdi, A., Vrielynck, N., Le Guin, S., Novatchkova, M., and Grelon, M. (2012). The *Arabidopsis* HEI10 is a new ZMM protein related to Zip3. PLoS Genet. **8,** e1002799.

Cui, C., Ge, X., Gautam, M., Kang, L., and Li, Z. (2012). Cytoplasmic and genomic effects on meiotic pairing in *Brassica* hybrids and allotetraploids from pair crosses of three cultivated diploids. Genetics **191,** 725-738.

Dion-Cote, A.M., and Barbash, D.A. (2017). Beyond speciation genes: an

overview of genome stability in evolution and speciation. Curr. Opin. Genet. Dev. **47,** 17-23.

Dolstra, O. (1982). Synthesis and fertility of x*Brassicoraphanus* and ways of transferring *Raphanus* characters to *Brassica*. Agric. Res. Rep. **917,** 1-90.

Gaeta, R.T., Pires, J.C., Iniguez-Luy, F., Leon, E., and Osborn, T.C. (2007). Genomic changes in resynthesized *Brassica napus* and their effect on gene expression and phenotype. Plant Cell **19,** 3403-3417.

Gonzalo, A., Lucas, M.O., Charpentier, C., Sandmann, G., Lloyd, A., and Jenczewski, E. (2019). Reducing MSH4 copy number prevents meiotic crossovers between non-homologous chromosomes in *Brassica napus*. Nat. Commun. **10,** 2354.

Grandont, L., Cuñado, N., Coriton, O., Huteau, V., Eber, F., Chevre, A.M., Grelon, M., Chelysheva, L., and Jenczewski, E. (2014). Homoeologous chromosome sorting and progression of meiotic recombination in *Brassica napus*: ploidy does matter! Plant Cell **26,** 1448-1463.

Higgins, J.D., Sanchez-Moran, E., Armstrong, S.J., Jones, G.H., and Franklin, F.C. (2005). The *Arabidopsis* synaptonemal complex protein ZYP1 is required for chromosome synapsis and normal fidelity of crossing over. Genes. Dev. **19,** 2488-2500.

Jeong, Y.M., Kim, N., Ahn, B.O., Oh, M., Chung, W.H., Chung, H., et al. (2016). Elucidating the triplicated ancestral genome structure of radish based on chromosome-level comparison with the *Brassica* genomes. Theor. Appl. Genet. **129,** 1357-1372.

Karpechenko, G.D. (1924). Hybrids of ♀*Raphanus sativus* L. × ♂*Brassica oleacea* L. J. Genet. **14,** 375-396.

Kwon, J.K. and Kim, B.D. (2009). Localization of 5S and 25S rRNA genes on somatic and meiotic chromosomes in *Capsicum* species of chili pepper. Mol. Cells **27,** 205-209.

Lee, S.S., Lee, S.A., Yang, J., and Kim, J. (2011). Developing stable progenies of x*Brassicoraphanus*, an intergeneric allopolyploid between *Brassica rapa* and *Raphanus sativus*, through induced mutation using microspore culture. Theor. Appl. Genet. **122,** 885-891.

Madlung, A., Tyagi, A.P., Watson, B., Jiang, H., Kagochi, T., Doerge, R.W., et al. (2005). Genomic changes in synthetic Arabidopsis polyploids. Plant J. **41,** 221-230.

Martinez-Perez, E., and Colaiacovo, M.P. (2009). Distribution of meiotic recombination events: talking to your neighbors. Curr. Opin. Genet. Dev. **19,** 105-112.

McNaughton, I.H. (1979) The current position and problems in the breeding of *Raphanobrassica* (radicole) as a forage crop. In: Proceedings of the 4th Eucarpia-confererence Breed Cruciferous crops, pp 22–28.

Mercier, R., Mezard, C., Jenczewski, E., Macaisne, N., and Grelon, M. (2015). The molecular biology of meiosis in plants. Annu. Rev. Plant Biol. **66,** 297-327.

Mestiri, I., Chague, V., Tanguy, A.M., Huneau, C., Huteau, V., Belcram, H., et al. (2010). Newly synthesized wheat allohexaploids display progenitor-dependent meiotic stability and aneuploidy but structural genomic additivity. New Phytol. **186,** 86-101.

Otto, S.P. (2007). The evolutionary consequences of polyploidy. Cell **131,** 452-462.

Parkin, I.A., Gulden, S.M., Sharpe, A.G., Lukens, L., Trick, M., Osborn, T.C., et al. (2005). Segmental structure of the *Brassica napus* genome based on comparative analysis with *Arabidopsis thaliana*. Genetics **171,** 765-781.

Pfosser, M., Amon, A., Lelley, T., and Heberlebors, E. (1995). Evaluation of sensitivity of flow-cytometry in detecting aneuploidy in wheat using disomic and ditelosomic wheat-rye addition lines. Cytometry **21,** 387-393.

Prakash, S., Bhat, S.R., Quiros, C.F., Kirti, P.B., and Chopra, V.L. (2009). *Brassica* and its close allies: cytogenetics and evolution. Plant Breed. Rev. **31,** 21-187.

Ramsey, J. and Schemske, D.W. (2002). Neopolyploidy in flowering plants. Annu. Rev. Ecol. Syst. **33,** 589-639.

Renny-Byfield, S., and Wendel, J.F. (2014). Doubling down on genomes: polyploidy and crop plants. Am. J. Bot. **101,** 1711-1725.

Szadkowski, E., Eber, F., Huteau, V., Lode, M., Coriton, O., Jenczewski, E., and Chevre, A.M. (2011). Polyploid formation pathways have an impact on genetic rearrangements in resynthesized *Brassica napus*. New Phytol. **191,** 884-894.

Szadkowski, E., Eber, F., Huteau, V., Lode, M., Huneau, C., Belcram, H., Coriton, O., Manzanares-Dauleux, M.J., Delourme, R., King, G.J., Chalhoub, B., Jenczewski, E., and Chevre, A.M. (2010). The first meiosis of resynthesized *Brassica napus*, a genome blender. New Phytol. **186,** 102-112.

U, N. (1935). Genome analysis in *Brassica* with special reference to the experimental formation of *B. napus* and peculiar mode of fertilization. Jpn. J. Bot. **7,** 389-452.

Van de Peer, Y., Mizrachi, E., and Marchal, K. (2017). The evolutionary significance of polyploidy. Nat. Rev. Genet. **18,** 411-424.

Wang, J., Kang, X.Y., and Zhu, Q. (2010). Variation in pollen formation and its cytological mechanism in an allotriploid white poplar. Tree Genet. Genomes **6,** 281-290.

Wendel, J.F., Lisch, D., Hu, G., and Mason, A.S. (2018). The long and short of doubling down: polyploidy, epigenetics, and the temporal dynamics of genome fractionation. Curr. Opin. Genet. Dev. **49,** 1-7.

Xiong, Z., Gaeta, R.T., and Pires, J.C. (2011). Homoeologous shuffling and chromosome compensation maintain genome balance in resynthesized allopolyploid *Brassica napus*. Proc. Natl. Acad. Sci. U. S. A. **108,** 7908-7913.

CHAPTER II

Formation of micronucleus and aborted pollen in x*Brassicoraphanus*, an intergeneric allotetraploid between *Brassica rapa* and *Raphanus sativus*

ABSTRACT

Interspecific or intergeneric hybridization can give rise to genetic diversity, but the resulting hybrids often suffer from diverse genetic and developmental defects. Notable among them are chromosomal instability and infertility, mainly caused by genome incompatibility between distantly related genomes. x*Brassicoraphanus* is a synthetic allotetraploid (2n = 4x = 38) derived from an intergeneric cross between Chinese cabbage (*Brassica rapa*; 2n = 20) and radish (*Raphanus sativus*; 2n = 18). Four lines of x*Brassicoraphanus* BB1, BB4, BB6, and BB50 were all descended from a genetically fixed individual, but display varying degrees of phenotypic diversity and pollen viability. For instance, the BB1 cultivar is the most stable in terms of phenotypic and genetic uniformity, whereas BB4 is relatively less stable with a high frequency of inviable pollen formation. Microscopic analysis revealed that more than half of BB4 pollens aborted with irregular morphology, while producing significantly large numbers of polyads during microsporogenesis, approximately 6.98% of which contained micronuclei. I also observed mispairing and abnormal segregation of meiotic chromosomes during microsporogenesis in BB4. It was

suggested that chromosome instability is persistent in the genome of hybrid offspring, accompanied with the formation of micronuclei and aborted pollen. Therefore, the disparate genomes in the hybrid species continuously require a subsequent stabilization process after hybridization, presumably involving gradual genome reconstruction and/or epigenetic changes to produce stable and fertile successive generations.

INTRODUCTION

Successful speciation through allopolyploidization should accompany with adaptation through recovering diploid-like meiosis. During adaptation, allopolyploid genome are highly revised, rearranged, and even eliminated (Comai, 2005; Hollister, 2015). The genome structure in paleopolyploids involved reduction in chromosome number, chromosome fusions, and various types of chromosomal rearrangements (Lagercrantz, 1998; Wendel, 2000). Several studies have demonstrated that genetic changes caused by homoeologous chromosome rearrangement are common in newly resynthesized *B. napus* allotetraploids (Song et al., 1995; Gaeta et al., 2007). The chromosomal reshuffling was introduced in newly created polyploid species in Brassicaceae (Szadkowski et al., 2010; Szadkowski et al., 2011; Xiong et al., 2011). However, some synthetic allotetraploids have high fertility, even with the high frequencies of aneuploidy and chromosome abnormalities in the early generations of *B. napus* (Xiong et al., 2011).

BB1, a cultivar of x*Brassicoraphanus*, was reported to be genetically stabilized for breeding a new leafy crop with trials to improve fertility (Lee et al., 1989). BB1 has siblings, BB4, BB6, and BB50, which are commonly

generated from OV115C generated during the breeding process. These x*Brassicoraphanus* lines having different fertility were made through the following process. They were first generated from an intergeneric hybridization between *B. rapa* cv. 'Jeonseung' (2n = 2x = 20) and *R. sativus* cv. 'Taebaek' (2n = 2x = 18). The first generation was obtained through ovule culture, followed by colchicine treatment (Lee et al., 1989; 2002; 2011; 2017). The siblings were generated from microspore culture of OV115C and maintained by self-pollination. BB4 and BB6 had low seed fertility, as other intergeneric hybrids (Dolstra, 1982; Lange et al., 1989). BB1 and BB50 showed improved fertility in successive generations which were treated with mutagen *N*-methyl-*N*-nitroso-urethane (NMU) during microspore culture (Fig. II-1). To verify chromosome complement and chromosome configuration, fluorescence *in situ* hybridization (FISH) karyotype analysis of another x*Brassicoraphanus* line BB5 (Belandres et al, 2015) and the karyotype and the genome *in situ* hybridization (GISH) of BB1 were conducted (Lim et al., 2012). However, how genetic stabilization was achieved in x*Brassicoraphanus* has not been studied. Since such examples restored fertility in short generations, it demonstrates that the hybridization barrier between *Brassica* and *Raphanus* can be overcome through unknown mechanism.

In this study, I confirmed fertility levels of x*Brassicoraphanus* lines by seed yield, pollen shape and viability. I further observed meiotic behaviors of x*Brassicoraphanus* lines with GISH to investigate relationship between chromosome behaviors in meiosis and fertility restoration in the recently stabilized allotetraploid.

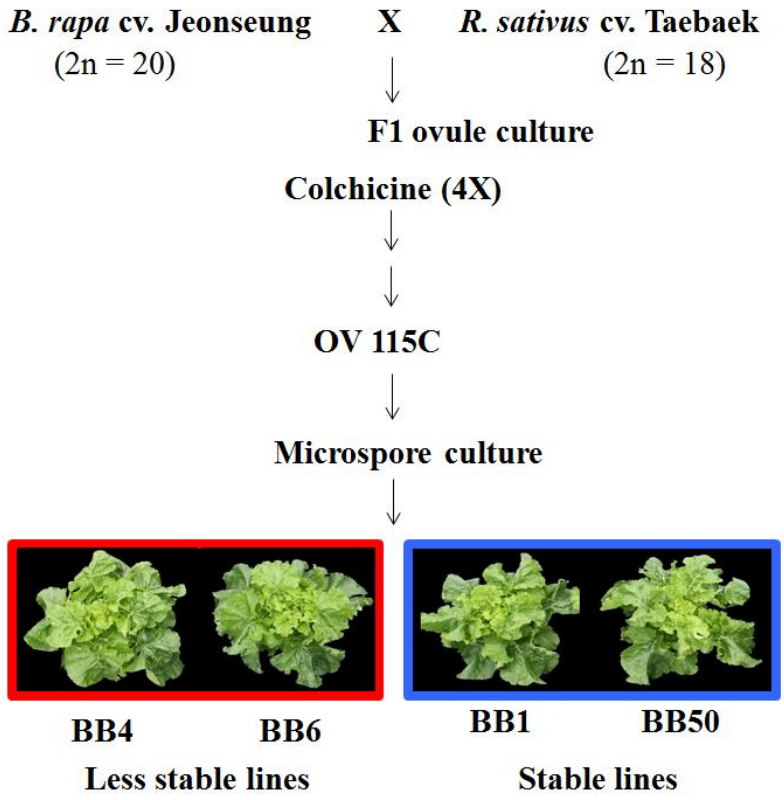

Figure II-1. Generation of x*Brassicoraphanus* lines.

MATERIALS AND METHODS

Plant materials and growth condition

Seeds of x*Brassicoraphanus cultivars* 'BB1', 'BB4', 'BB6', and 'BB50', the parents *B. rapa* cv. 'Chiifu-401-42', and *R. sativus* cv. 'WK10039' were sterilized in 50% hypochlorite solution with 0.1% triton X-100 for 90 sec, followed by 10 times washes with sterile distilled water. The seeds were plated on Murashige and Skoog (MS) medium (Duchefa, Haarlem, The Netherlands) supplemented with 2% sucrose (w/v) and 0.8% plant agar (w/v, Murashige and Skoog, 1962). The plates with seeds were placed at 24°C incubator with 16 h of light and 8 h of dark for 2 weeks. Then, plants were vernalized at 4°C incubator with 16 h of light and 8 h of dark for 4 weeks. Plants were transferred to soil in pots and placed in the green house with the same light condition.

Open-pollination experiment for seed yield with x*Brassicoraphanus* lines

After vernalization, the plants were transferred to a greenhouse and grown at 25°C under the same light condition. The plants were also grown

in the greenhouse of Seoul National University in Seoul, South Korea, from September 2016 to March 2017.

Alexander staining

Viabilities of pollen grains and tetrads were determined by Alexander staining according to published protocols (Peterson et al., 2010).

Scanning electron microscopy

For SEM evaluation, properly dried pollen of each cultivar was dusted on aluminum stubs with the thermosensitive glue. The sample on each stub was sputter-coated with 30 mÅ thick of a gold layer for 200 sec with 20 mA using a Sputter Coater (Leica, Austria). Pollen grains were observed using field emission scanning electron microscope (Supra, Carl Zeiss, Germany).

Genomic *in situ* hybridization (GISH) analysis

Slide preparation

The floral buds were fixed in the aceto-ethanol (1:3 v/v) solution for 24 h and stored at -20°C in 70% ethanol until use. The fixed inflorescences were rinsed in distilled water and checked for meiosis stage by 3% aceto-orcein staining. When optimal meiosis stages were confirmed, the slide

preparation was followed by enzyme treatments of the inflorescences. Anthers were thoroughly washed with distilled water and digested in the enzyme mixture including 2% Cellulase R-10 (Duchefa Biochemie, The Netherlands), 1% Macerozyme R-10 (Duchefa Biochemie, The Netherlands), 1% Pectinase (Sigma-Aldrich, USA), and 0.5% Pectolyase Y23 (Sigma-Aldrich, USA) in 150 mM citrate buffer (pH 4.5) to degrade the cell walls at 37 °C for 60~90 min (Kwon and Kim, 2009; Belandres et al., 2015). Treated anthers on the SuperFrost Plus™ Adhesion glass slide (Thermo Fisher, USA) were squashed in 60% acetic acid on a slide warmer and air dried.

Probe preparation

Total genomic DNA was extracted and purified from young leaves of *B. rapa* cv. 'Chiifu-401-42' and *R. sativus* cv. 'WK10039' using the CTAB extraction method. The genomic DNA was fragmented by sonication and the lengths of the probes DNA fragments were determined by agarose-gel electrophoresis within the range of 200-500 bp. The fragmented genomic DNA of *B. rapa* Chiifu-401-42 was labelled with digoxigenin-11-dUTP (Roche, Germany) and *R. sativus* cv. WK10039 was labelled with biotin-16-

dUTP (Roche, Germany) by nick translation and used as probes, after which were stored at -20°C until use.

Hybridization

For analysis of GISH, the method of Kwon and Kim (2009) was adopted with modifications. Slides were pretreated with RNase A (RBC, Taiwan) buffer (1mg·mL^{-1} RNase A in 2x SSC) at 37°C for 90 min. The slides were washed 3 times for 3 min each with 2x SSC (Biosesang, Korea). The slides were dehydrated in 70, 95, and 100% ethanol series for 5 min each at room temperature (RT) and air-dried. The slides were subsequently denatured with 70% deionized formamide (Amresco, OH, USA) in 2x SSC for 10 min at 70°C, dehydrated in ethanol series (70, 95, and 100% , 5 min each -20°C) and air-dried at dark. A hybridization mixture that consisted of 50% deionized formamide, 10% dextran sulfate, 2x SSC, 15 ng labeled DNA in sterile distilled water was prepared and applied to 40 μL per slide. The GISH mixture was denatured at 94°C and cooled on ice for 10 min, then mounted on slides and placed in a humid incubator at 37°C overnight. The next day, the slides were washed sequentially in 2x SSC for 5 min, 50% deionized formamide in 2x SSC for 5 min, 2x SSC for 5 min, and finally 4x SSC for 5 min at RT. For blocking, the slides were treated with 5% goat

serum (Vector Laboratories, CA, USA) in 4x SSCT (0.1% Tween-20 in 4x SSC) for 5 min at 37°C. In first detection, dig- and biotin- labelled probes were detected with anti-dig rhodamine (Roche, Germany) and biotin-anti-avidin (Roche, Germany) in 1% BSA (Amresco, USA) in 4x SSCT for 1 h at 37°C. Then the slides were washed in 4x SSCT 3 times for 10 min each at 37°C. For blocking, the slides were treated with 5% BSA in 4x SSCT for 5 min at 37°C. For the second detection, dig- and biotin- labelled probes were detected with avidin-FITC (Vector Laboratories, CA, USA) and anti-sheep Texas red (Vector Laboratories, USA) in 1% BSA in 4x SSCT for 1 h at 37°C. The slides were then washed in 4x SSCT 3 times for 10 min each at 37°C. The slides were dehydrated in 70, 95, and 100% ethanol series for 5 min each at (RT) and air-dried at dark. For staining, 40 µL DAPI in Vectashield (Vector Laboratories, USA) reagent was used to counterstain the chromosomes and the slides were covered with glass coverslips. Several meiotic stages stained with DAPI in Vectashield were imaged using an Axioskop2 microscope equipped with an Axiocam 506 color CCD camera (Zeiss, Germany). Images were processed using Adobe Photoshop CS6 (Adobe Systems Incorporated, USA).

RESULTS

Open-pollination experiment in x*Brassicoraphanus* lines

The x*Brassicoraphanus* lines were originated from a single plant and have different levels of fertility restoration. The x*Brassicoraphanus* lines were open-pollinationed in the glasshouse and their fertility was experimented by counting normal and aborted seed number. Average normal seed numbers silique were 5.2 in BB4, 3.2 in BB6, 2.8 in BB1, and 4.9 in BB50, respectively. However, average aborted seed numbers per silique were 4.7, 2.8, 1.8 and 1.1 in BB4, BB6, BB1, and BB50, respectively (Fig. II-2). It suggested that averages aborted seed number per silique was higher in BB4 and BB6 than those of BB1 and BB50. Frequency of normal seeds per silique was 52.5% in BB4, 52.4% in BB6, 60.4% in BB1, and 80% in BB50 (Fig. II-3). This suggested that BB50 is the most stable in fertility, whereas BB4 is relative less stable with a high frequency of aborted seed formation. Fertility was not fully recovered even in stable lines, BB1 and BB50. BB4 and BB50 were selected for further analysis.

Variable shapes and viability of pollen grains in x*Brassicoraphanus* lines

To confirm fertility of male gametophyte, normal pollen shape and viability were examined. Pollen shapes were observed in scanning electron microscope (SEM) and pollen viability was determined by Alexander staining in BB4 (Table II-1, Figs. II-4A and II-4B) and BB50 (Figs. II-4C and II-4D). The frequency of abnormal pollen was 65.74% in BB4, 69.47% in BB6, 58.80% in BB1, 29.84% in BB50 (Table III-1). The pollen grains had variable shapes (Fig. II-4A) and pollen viability had less 50% in BB4 (Fig. II-4B). The pollen grains had homogenous shapes (Fig. II-4C) and pollen viability had more than 50% in BB50 (Fig. II-4D).

Micronuclei and tetrad in x*Brassicoraphanus* lines

To investigate correlation of pollen viability and tetrad formation, normal tetrads were observed by Alexander staining with invariably four microspores (Figs. II-5A and II-5C). However, 6.98% of polyads (Fig. II-5B; Table II-2) with micronucleus (black arrow) were observed in BB4 compared to BB50 (Fig. II-5D). This suggests that BB4 is a relatively less stable line with high frequencies of inviable pollen formation than BB50.

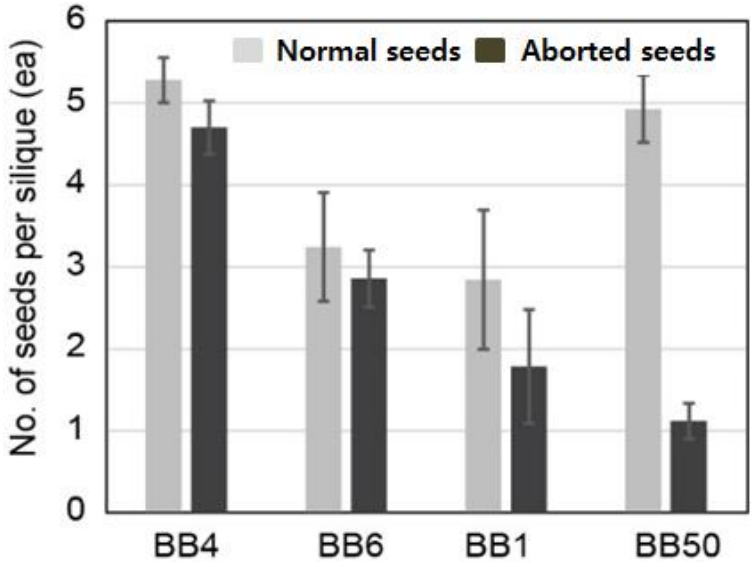

Figure II-2. Variable seeds viability in x*Brassicoraphanus* lines. Number of seeds per silique and following open pollination with x*Brassicoraphanus* lines. The straight lines refer to mean values

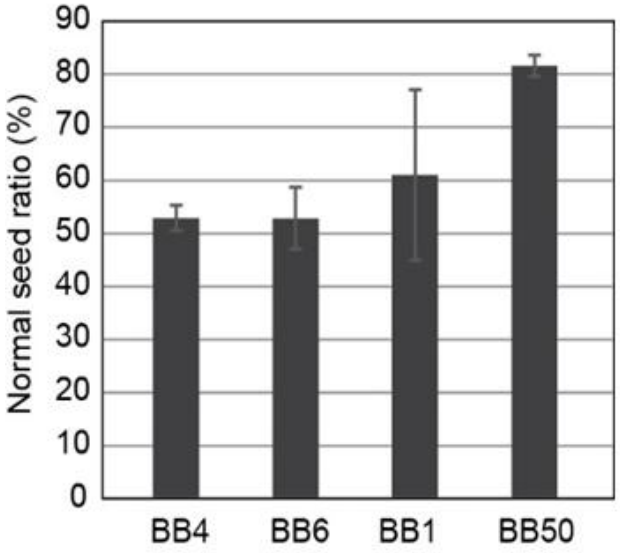

Figure II-3. Normal seed ratios in x*Brassicoraphanus* lines. Normal seed ratio following open pollination with x*Brassicoraphanus* lines.

Table II-1. Frequencies of normal and abnormal shape pollens in x*Brassicoraphanus* lines.

Lines	Pollen (%)	
	Normal	Abnormal
BB4	34.26	65.74
BB6	30.53	69.47
BB1	41.20	58.80
BB50	70.16	29.84

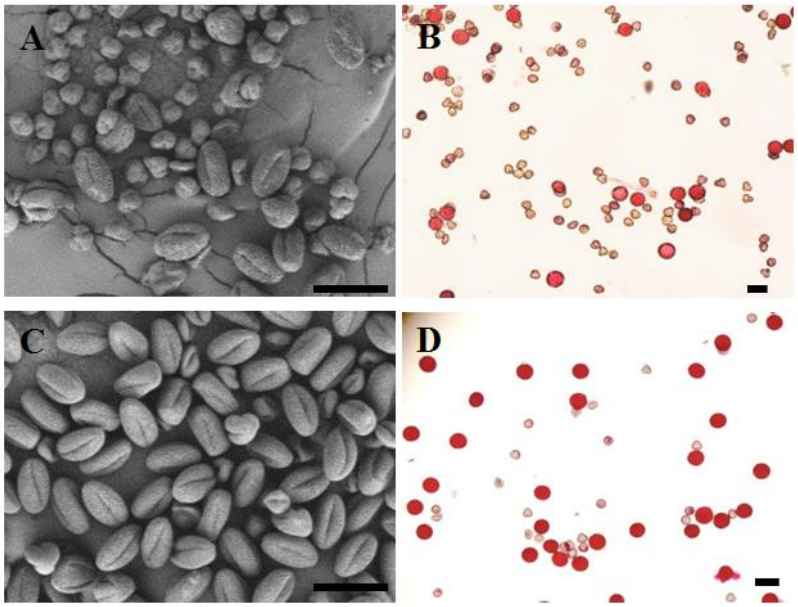

Figure II-4. Variable shapes (A and C) and viabilities (B and D) of pollen grains in x*Brassicoraphanus* lines. BB4 (A and B) and BB50 (C and D). Scale bars = 50 μm

Table II-2. Frequencies of microspore formation in x*Brassicoraphanus* lines.

Lines	Microspore frequency % (Observed cell no.)		
	Tetrad	Pentad	Polyad
BB4	93.02(240)	6.98(18)	0
BB6	95.21(338)	3.10(11)	1.69(6)
BB1	97.72(472)	2.28(11)	0
BB50	99.26(404)	0.74(3)	0

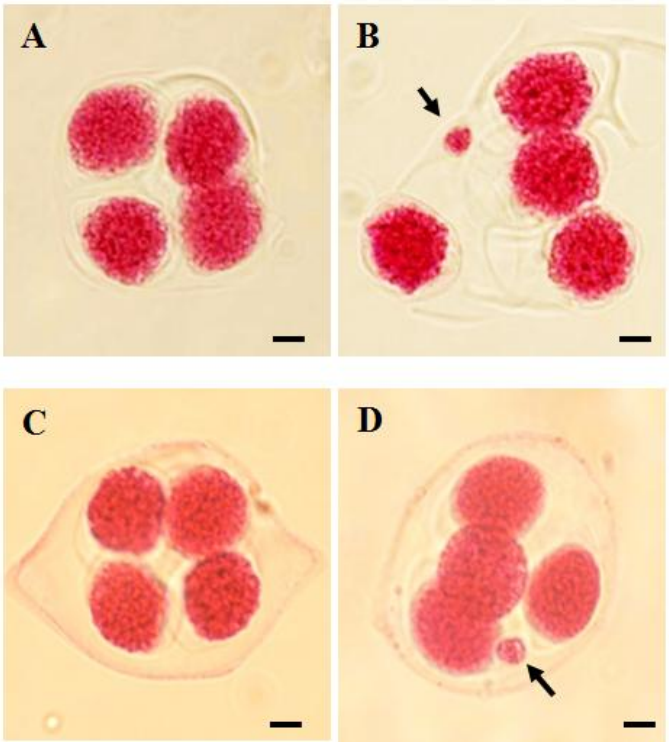

Figure II-5. Tetrad and micronuclei in two lines of x*Brassicoraphanus*. Arrows indicate micronuclei. BB4 (A and B) and BB50 (C and D). Scale bars = 10 μm.

Various meiotic chromosomal behaviors

Whole processes of meiosis were observed with DAPI staining in BB4, to determine the relationship between micronuclei and irregular meiosis. Abnormal meiotic chromosomal behavior was observed in BB4 during microsporogenesis. Homologous chromosomes were aligned with one another, however, some regions of chromosomes were not closely juxtaposed with one another (arrow) suggests that synaptonemal complex is incomplete at pachytene (Fig. II-6A). At diakinesis, chromosomes disappeared the synaptonemal complex were condensed distinctly to separate. Bivalents of homologous chromosomes then became visible. However, ring (yellow arrow), rod (white arrow), quadrivalents (red arrow) were frequently observed at diakinesis (Fig. II-6B). Frequency of abnormal meiotic behaviors including rods, rings, and multivalents in diakinesis was the highest (92.1%). Almost diakinesis pollen mother cell had ring, rod, and multivalents. Frequency of abnormal meiosis in BB4 is higher than BB50 and frequency of abnormal meiosis is gradually reduced in subsequent meiosis stage in BB4 (Table II-3). Bivalent chromosomes were aligned at metaphase plate and univalent was also observed at metaphase I. (Fig. II-6C). The homologous chromosomes were separated with bridges (red arrow) at telophase I (Fig. II-6D). Univalents (red arrow) were observed at

metaphase II (Fig. II-6E). Second meiotic division resulted in four gametes formation of different kinds of meiosis products including unbalanced tetrads (Fig. II-6F). It suggests that the abnormal meiotic behavior of BB4 was induced by micronucleus formation, pollen viability, pollen shapes, and fertility.

Genome *in situ* hybridization in BB4

Meiotic pairing pattern was investigated to distinguish chromosome derived of *B. rapa* and *R. sativus* though GISH analysis in BB4 (Fig. II-7). A univalent was detected in the A chromosome at diakinesis (Fig. II-7A) and metaphase I (Fig. II-7B) of BB4. Allosyndesis multivalents were observed at diakinesis. It suggests that 37 chromosomes are persistent in BB4, undergoing chromosome breaks, bridges, and rearrangements that lead to chromosome breaks, fusion, and deletion.

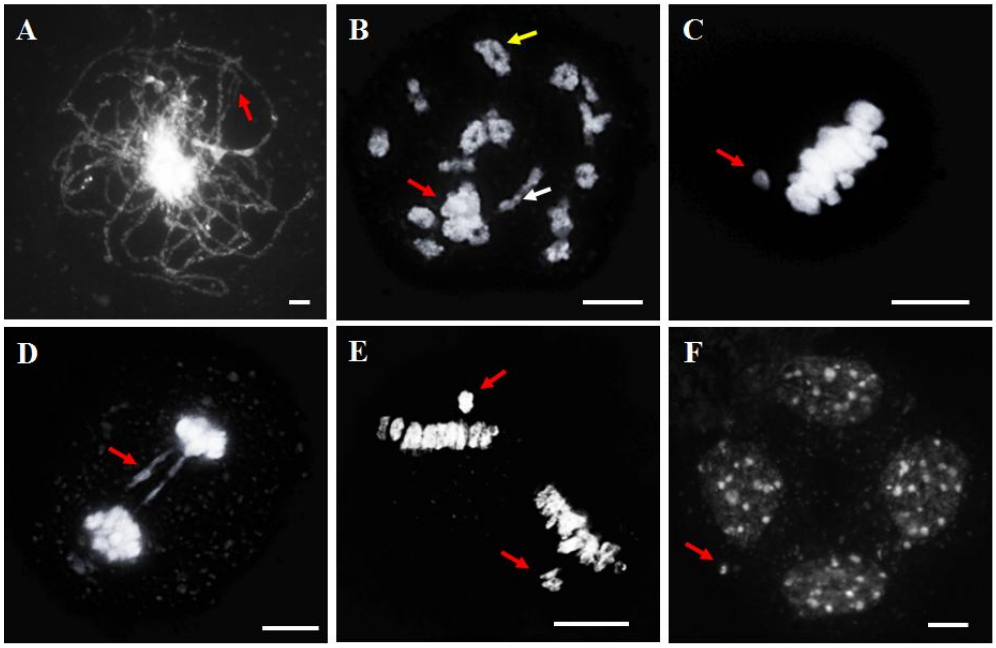

Figure II-6. Abnormal meiotic behaviors during meiosis in pollen mother cells of BB4. (A) At pachytene, some regions of chromosomes were not closely juxtaposed with one another (white arrow). (B) At diakinesis, abnormal chromosome behaviors were marked with different colored arrows; ring (yellow arrow), rod (white arrow), quadrivalents (red arrow). (C) At metaphase I, bivalents chromosomes were aligned at metaphase plate and univalent (red arrow) was also observed. (D) At telophase I, the homologous chromosomes were separated with bridges (red arrow). (E) At metaphase II, univalents (red arrow) were observed. (F) Four gametes formation including unbalanced tetrads (red arrow). Scale bars = 10 μm.

Table II- 3. Frequencies of abnormal meiosis in x*Brassicoraphanus*

Stage	BB4 (%)		BB50 (%)	
	Abnormality	Normality	Abnormality	Normality
Prophase I (diakinesis)	66.6* (20/30)	33.3 (10/30)	0**	100.0 (17/17)
Metaphase I	25.0 (12/48)	75.0 (36/48)	1.9 (1/52)	98.1 (51/52)
Anaphase I	21.7 (6/24)	78.6 (18/24)	0 (0/18)	100.0 (18/18)
Metaphase II	33.3 (2/6)	66.6 (4/6)	0 (0/4)	100.0 (4/4)
Anaphase II	0**	0**	0 (0/7)	100.0 (7/7)

* The number in each parenthesis is abnormal or normal cells / total observed cells

** No observed

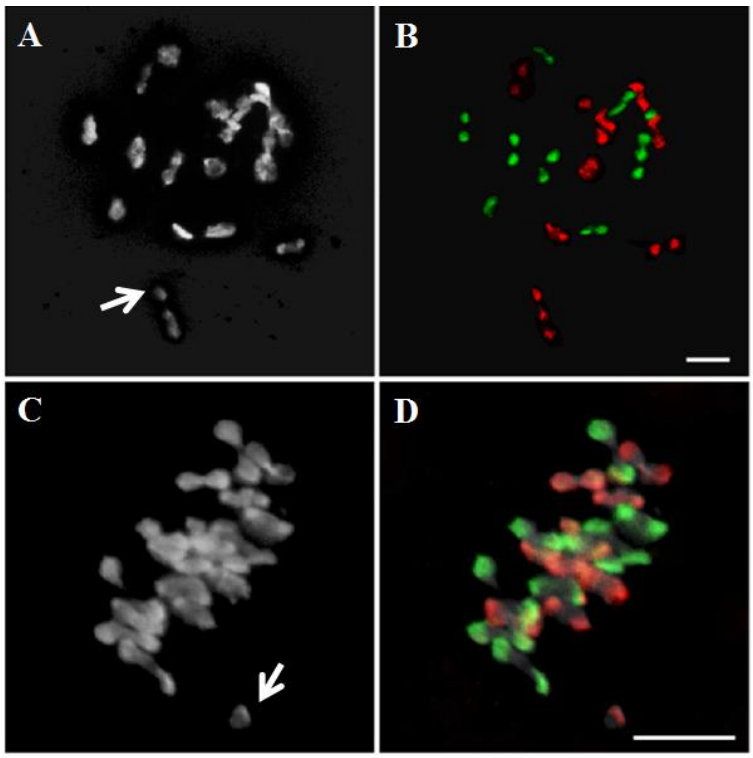

Figure II-7. Abnormal chromosome behaviors in meiosis of BB4. Diakinesis (A and B) and metaphase I (C and D). White arrow indicate isolated chromosome which have no homologous bivalent formation. The *B. rapa* and *R. sativus* chromosomes are stained in red and green, respectively Scale bars = 10 μm

DISCUSSION

Chromosome instability is persistent in the genome of allopolyploidization offsprings, presumably accompanied with the formation of micronuclei and aborted pollen. x*Brassicoraphanus* lines named BB1, BB4, BB6 and BB50 were stabilized during short periods after hybridization have low and high seed fertilities (Lee et al., 1989; 2002; 2011). Cytogenetic analysis for formation of micronucleus and aborted pollen was performed in pollen mother cells of x*Brassicoraphanus* lines. The mechanism to produce stable and fertile individuals over successive generations was investigated by observing meiosis of x*Brassicoraphanus* lines.

Irregular meiosis behaviors in BB4 (Fig. II-6, Table II-3) induced micronuclei formation at tetrad stage and resulted in low pollen viability and low seed yield. During anaphase with acentric lagging chromosome, chromosome fragmentation could be induced by nondisjunction (Fig. II-6D). Chromosome rearrangement and abnormal meiotic behavior led to loss of chromosomes and micronuclei in BB4 (Fig. II-7). Most newly synthesized allopolyploids in *Brassica* species undergo abnormal meiosis including

homoeologous pairing which confuse the proper homologous pairing from each parent (Song et al., 1995; Griffithes et al., 2006; Gaeta et al., 2007; Hollister, 2015). The two homoeologous A1 and C1 chromosomes from *B. rapa* and *B. oleracea* share synteny with each other (Cheng et al., 2014) and resulted in homoeologous recombination in allopolyploid *B. napus* (Gaeta et al., 2007; Szadkowski et al., 2010; Grandont et al., 2014). Loss and gain of chromosomes were found to be involved with homoeologous chromosomes (e.g., compensatory monosomy/ trisomy and nullisomy/tetrasomy) in *B. napus* (Szadkowski et al., 2010; Szadkowski et al., 2011; Xiong, 2011). Diploid-like meiosis in allopolyploid is controlled by a major regulator pairing gene *PrBn*, which restricts the homoeologous pairing in *B. napus* (Jenczewski et al., 2003), and *Ph1* in wheat (Griffiths et al., 2006). Likewise, meiosis behavior in BB4 was observed to have irregular meiosis with multivalents, rod, and ring chromosome formation, which led to make micronuclei by chromosome rearrangement and loss. Abnormal meiotic behavior in BB4 was observed multivalents A-R association rather than homoeologous bivalents.

Micronuclei are small nucleus that forms when chromosomes or chromosomal fragments are isolated from normal distribution into the daughter nuclei. The formation of micronuclei correlates with meiotic

failure and pollen abortion, and is possibly responsible for persistent genetic and genomic instability in successive generations. Little is known about the significance and mechanism of micronuclei formation in polyploids. Micronuclei are used as a biomarker of chromosomal damage, genome instability, and eventually of cancer risk (Bonassi et al., 2007; Iarmarcovai et al., 2008; Gibeaux et al., 2018). Also, signs of genotoxic events and chromosome instability had contributed to study of genome damage (Helt et al., 2005; Shiloh, 2006). Thus, the divergent genomes in the hybrid species still require a comprehensive stabilization process after hybridization, presumably involving gradual genome reconstruction and/or epigenetic changes to produce stable and fertile individuals over successive generations.

In this study, I found that the stable lines BB1 and BB50 still have considerable rate of disorders in meiosis and abnormalities in pollen shape and seed formation suggesting these lines are still on adaptation process. Further studies should be focused on the involvement of genes controlling homologous chromosome pairing in stability restoration of x*Brassicoraphanus* lines.

REFERENCES

Belandres, H.R., Waminal, N.E., Hwang, Y.J., Park, B.S., Lee, S.S., Huh, J.H., and Kim, H.H. (2015). FISH karyotype and GISH meiotic pairing analyses of a stable intergeneric hybrid x*Brassicoraphanus* line BB#5. Korean J. Hortic. Sci. **33,** 83-92.

Bonassi, S., Znaor, A., Ceppi, M., Lando, C., Chang, W.P., Holland, N., Kirsch-Volders, M., Zeiger, E., Ban, S., Barale, R., Bigatti, M.P., Bolognesi, C., Cebulska-Wasilewska, A., Fabianova, E., Fucic, A., Hagmar, L., Joksic, G., Martelli, A., Migliore, L., Mirkova, E., Scarfi, M.R., Zijno, A., Norppa, H., and Fenech, M. (2007). An increased micronucleus frequency in peripheral blood lymphocytes predicts the risk of cancer in humans. Carcinogenesis **28,** 625-631.

Comai, L. (2005). The advantages and disadvantages of being polyploid. Nat. Rev. Genet. **6,** 836-846.

Dolstra, O. (1982). Synthesis and fertility of x*Brassicoraphanus* and ways of transferring *Raphanus* characters to *Brassica*. Agric. Res. Rep. **917,** 1-90.

Gaeta, R.T., Pires, J.C., Iniguez-Luy, F., Leon, E., and Osborn, T.C. (2007). Genomic changes in resynthesized *Brassica napus* and their effect on gene expression and phenotype. Plant Cell **19,** 3403-3417.

Gibeaux, R., Acker, R., Kitaoka, M., Georgiou, G., van Kruijsbergen, I., Ford, B., Marcotte, E.M., Nomura, D.K., Kwon, T., Veenstra, G.J.C., and Heald, R. (2018). Paternal chromosome loss and metabolic crisis contribute to hybrid inviability in *Xenopus*. Nature

553, 337-341.

Grandont, L., Cuñado, N., Coriton, O., Huteau, V., Eber, F., Chevre, A.M., Grelon, M., Chelysheva, L., and Jenczewski, E. (2014). Homoeologous chromosome sorting and progression of meiotic recombination in *Brassica napus*: ploidy does matter! Plant Cell **26,** 1448-1463.

Griffiths, S., Sharp, R., Foote, T.N., Bertin, I., Wanous, M., Reader, S., Colas, I., and Moore, G. (2006). Molecular characterization of *Ph1* as a major chromosome pairing locus in polyploid wheat. Nature **439,** 749-752.

Helt, C.E., Cliby, W.A., Keng, P.C., Bambara, R.A., O'Reilly, M.A. (2005). Ataxia telangiectasia mutated (ATM) and ATM and Rad3-related protein exhibit selective target specificities in response to different forms of DNA damage. J. Biol. Chem. **280**, 1186–1192

Hollister, J.D. (2015). Polyploidy: adaptation to the genomic environment. New. Phytol. **205,** 1034-1039.

Iarmarcovai, G., Bonassi, S., Botta, A., Baan, R.A., and Orsiere, T. (2008). Genetic polymorphisms and micronucleus formation: a review of the literature. Mutat. Res. **658,** 215-233.

Jenczewski, E., Eber, F., Grimaud, A., Huet, S., Lucas, M.O., Monod, H., and Chevre, A.M. (2003). *PrBn*, a major gene controlling homeologous pairing in oilseed rape (*Brassica napus*) haploids. Genetics **164,** 645-653.

Kwon, J.K. and Kim, B.D. (2009). Localization of 5S and 25S rRNA genes on somatic and meiotic chromosomes in *Capsicum* species of chili pepper. Mol. Cells **27,** 205-209.

Lagercrantz, U. (1998). Comparative mapping between *Arabidopsis*

thaliana and *Brassica nigra* indicates that *Brassica* genomes have evolved through extensive genome replication accompanied by chromosome fusions and frequent rearrangements. Genetics **150,** 1217-1228.

Lee, S.S., Woo, J.G., and Shin, H.H. (1989). Obtaining intergeneric hybrid plant between *Brassica campestris* and *Raphanus sativus* through young ovule culture. Korean J. Breed. **21,** 52-57.

Lee, S.S., Choi, W.J., and Woo, J.G. (2002). Development of a new vegetable crop in x*Brassicoraphanus* by hybridization of *Brassica campestris* and *Raphanus sativus*. J. Korean Soc. Hort. Sci. **43,** 693-698.

Lee, S.S., Lee, S.A., Yang, J., and Kim, J. (2011). Developing stable progenies of x*Brassicoraphanus*, an intergeneric allopolyploid between *Brassica rapa* and *Raphanus sativus*, through induced mutation using microspore culture. Theor. Appl. Genet. **122,** 885-891.

Lee, S.S., Hwang, B.H., Kim, T.Y., Yang, J., Han, N. R., Kim, J., Kim, H. H., Belandres, H. R. (2017). Developing stable cultivar through microspore mutagenesis in ×*Brassicoraphanus koranhort*, inter-generic allopolyploid between *Brassica rapa* and *Raphanus sativus*. Am. J. Plant Sci. **8,** 1345-1356.

Lim, S.J., Lee, S.S., and Bang, J.W. (2012). Karyotype and genomic *in situ* hybridization pattern in x*Brassicoraphanus*, an intergeneric hybrid between *Brassica campestris* ssp. *pekinensis* and *Raphanus sativus*. Plant Biotechnol. Rep. **6,** 107-112.

Murashige, T. and Skoog, F. (1962). A revised medium for rapid growth and bioassays with tobacco tissue cultures. Physiol. Plant **15,** 473-

479.

Peterson, R., Slovin, J. P., and Chen, C. (2010) A simplified method for differential staining of aborted and non-aborted pollen grains. Int. J. Plant Biol. **1**, e13.

Shiloh, Y. (2006) The ATM-mediated DNA-damage response: taking shape. Trends Biochem. Sci. **31** 402-410.

Song, K., Lu, P., Tang, K., and Osborn, T.C. (1995). Rapid genome change in synthetic polyploids of *Brassica* and its implications for polyploid evolution. Proc. Natl. Acad. Sci. U. S. A. **92,** 7719-7723.

Szadkowski, E., Eber, F., Huteau, V., Lode, M., Huneau, C., Belcram, H., Coriton, O., Manzanares-Dauleux, M.J., Delourme, R., King, G.J., Chalhoub, B., Jenczewski, E., and Chevre, A.M. (2010). The first meiosis of resynthesized *Brassica napus*, a genome blender. New Phytol. **186,** 102-112.

Szadkowski, E., Eber, F., Huteau, V., Lode, M., Coriton, O., Jenczewski, E., and Chevre, A.M. (2011). Polyploid formation pathways have an impact on genetic rearrangements in resynthesized *Brassica napus*. New Phytol. **191,** 884-894.

Wendel, J.F. (2000). Genome evolution in polyploids. Plant Mol. Biol. **42,** 225-249.

Xiong, Z., Gaeta, R.T., and Pires, J.C. (2011). Homoeologous shuffling and chromosome compensation maintain genome balance in resynthesized allopolyploid *Brassica napus*. Proc. Natl. Acad. Sci. U. S. A. **108,** 7908-7913.

CHAPTER III

Genome divergence in *Brassica rapa* subspecies revealed by whole genome analysis on a doubled-haploid line of Korean Ganghwa turnip

The research described in this chapter has been published in Plant Biotechnology Reports, https://doi.org/10.1007/s11816-019-00565-w

ABSTRACT

Subspecies of *Brassica rapa* are morphologically and genetically diverse, and include a variety of fresh vegetables grown worldwide. Among them, turnip (*B. rapa* subsp. *rapa*) produces a large bulbous taproot, and thus is primarily consumed as a root vegetable in Europe and Asia. In comparison to Chinese cabbage (*B. rapa* subsp. *pekinensis*), however, genetic analysis and breeding of turnip is hampered in practice due in part to scarcity of useful genetic resources. In this study, I produced a doubled haploid (DH) line of Ganghwa turnip, an heirloom specialty crop in Korea that is usually propagated by open pollination. Microspores were isolated from young flower buds of Ganghwa turnip, and shoots and roots were sequentially regenerated *in vitro*. Chromosome doubling was induced with the colchicine treatment, and verified by flow cytometry analysis. The G14 DH line displays uniformity in overall morphology compared to heterogeneous commercial Ganghwa turnips. The whole genome of G14 was sequenced on an Illumina HiSeq 4000 platform, and the reads mapped onto the *B. rapa* reference genome identified 1,163,399 SNPs and 779,700 indels. Despite high similarity in overall genome sequence, turnips and Chinese cabbage

have different compositions of transposable elements. In particular, long terminal repeat (LTR) retrotransposons are more enriched in turnips than in Chinese cabbage genomes, in which the *gypsy* elements are classified as major LTR sequences in the turnip genome. These findings suggest that subspecies-specific TE divergence is in part responsible for huge phenotypic variations observed within the same species.

INTRODUCTION

Brassica rapa L. contains many subspecies that are cultivated as important crops worldwide. Despite their genetic similarity, many crops of the same *B. rapa* species are morphologically diverse and, in some cases, diverse enough for different parts of different subspecies to be consumed. For example, leaves of Chinese cabbage and bok choy (*B. rapa* subsp. *pekinensis*), roots of turnip, young flowering shoots of rapini (both are *B. rapa* subsp. *rapa*), and seeds of field mustard (*B. rapa* subsp. *oleifera*) are consumed as edible portions (Gómez-Campo and Prakash, 1999).

Notable among them are Chinese cabbage and turnip. The two subspecies have contrasting morphology each other - Chinese cabbage forms a large head consisting of many round rosette leaves with relatively small roots, while turnip produces lobed leaves with long petioles and a large bulbous taproot, reminiscent of radish (*Raphanus sativus* L.) that belongs to a different genus in the Brassicaceae family. Both Chinese cabbage and turnip are diploid (2n = 2x = 20) and, despite their morphological differences, they are genetically similar enough to permit the production of hybrid progeny through conventional crosses.

Turnip is an important vegetable crop, and interest in its nutritional value has recently increased. This is in part owing to its high content of glucosinolate, a group of secondary metabolites considered to have health benefits (Lee et al., 2013; Klopsch et al., 2017). However, breeding of turnip has been hindered in practice largely due to limited genetic resources and lack of pure inbred lines. In South Korea, Ganghwa turnip with an enlarged red bulbous taproot has a high commercial value, mostly consumed as one of the major ingredients of Kimchi. Ganghwa turnip is a specialty crop in Ganghwa County, grown as heirlooms with substantial heterogeneity due to open pollination.

Genome information on the line of interest and its comparison to the reference sequence should facilitate the understanding of genetic variation within a population, and provide valuable resources for endeavors such as genome-wide association studies (Lin et al., 2014; Cheng et al., 2016; Pang et al., 2015; Zhang et al., 2018). Thus, establishment of homozygous lines, either from inbreeding or doubling of haploid individuals, is a logical first step in genetic study and systematic breeding. *In vitro* culture techniques with isolated anthers, ovaries, or microspores are generally used to produce homozygous doubled-haploid (DH) plants that are useful for crop breeding programs (Gil-Humanes and Barro, 2009; Ferrie and Caswell, 2011).

However, anther or ovary culture is often problematic, as heterozygous progenies can be regenerated from diploid somatic cells. Haploid gametic cells from isolated microspores in culture are more promising to generate homozygous progenies after chromosome doubling (Yuan et al., 2015).

In the Brassicaceae family, induction of DH plants from isolated microspore was first accomplished in *B. napus* (Lichter, 1982), and has since been successfully carried out in *B. rapa* (Ferrie et al., 1995), *B. carinata* (Barro and Marti, 1999), *B. oleracea* (Na et al., 2011; Yuan et al., 2011), and x*Brassicoraphanus*, an intergeneric hybrid of *B. rapa* and *R. sativus* (Lee et al. 2011). Protocols to produce haploid and DH plants from microspore in *Brassica* vary with respect to species and genotype (Ferrie, 2003). The efficiency of microspore-derived embryo formation was highly variable in different turnip varieties, depending on their sites of origin whether from Taiwan, Japan, India, or Uzbekistan (Seo et al., 2014).

In this study, I analyze genetic diversity among *Brassica rapa* species, with Ganghwa turnip being a primary subspecies in comparison to the others. Although several studies have reported genetic diversity in turnip germplasm collected from different geographical locations (Padilla et al., 2005; Zhang et al., 2014), relatively few studies have assessed turnip germplasm to Chinese cabbage at the genome level. Here, I report a

procedure for the production of DH lines of Korean Ganghwa turnip by microspore culture. The homozygosity of the microspore-derived plants was confirmed with simple sequence repeat (SSR) markers and cleaved amplified polymorphic sequence (CAPS) marker. I also sequenced one of the Ganghwa turnip DH lines, and examined the abundance of transposable elements in comparison to those of Chinese cabbage. Genomic resources obtained from this study such as a whole genome sequence, SNPs and molecular markers will further facilitate in-depth genetic analysis and systematic breeding of turnips.

MATERIALS AND METHODS

Plant materials

Commercial Ganghwa turnip landrace seeds were purchased from a local seed market (Dong Won Nong San Seed Co., Ltd., Republic of Korea). This landrace is simply referred to as Ganghwa turnip in this study unless otherwise indicated. The Ganghwa turnip and its DH line seeds were initially sown on Murashige and Skoog (MS) medium (Murashige and Skoog, 1962) in petri dishes in a growth chamber with a 16-h day length and vernalized at 4°C. After vernalization, the plants were transferred to a greenhouse and grown at 25°C under the same light condition. The plants were also grown in the field of Seoul National University in Suwon, South Korea, from September to November in 2016 and 2018, and from April to June in 2018.

Microspore isolation

For microspore culture, the methods of Hong and Lee (1995), Na et al., (2011), and Seo et al., (2014) were adopted with modifications. Briefly, approximately 80 flower buds of the size of 1–2 mm in length, with the

petals being shorter than the pistil, were harvested for microspore isolation. The buds were surface-sterilized in 70% ethanol for 30 sec, transferred to sterile distilled water and rinsed for 40 sec, transferred to 50% of bleach solution with shaking at 70 rpm for 12 min, and rinsed three times for 3 min each in sterile water. The buds were gently macerated in 4 mL of B5 medium (Gamborg et al., 1968) with 13% sucrose (B5-13, w/v), ground using a mortar and pestle, filtered through a 45-μm metal mesh and collected in a 50 mL conical tube. The microspore suspension was washed three times with 10 mL of B5-13 medium and centrifuged at 1,000 rpm for 3 min. The supernatant was removed, and the microspore pellets were resuspended in Nitsch and Nitsch medium (Lichter, 1982) with 13% sucrose (NLN-13, w/v) and 0.1 $mg \cdot L^{-1}$ 6-benzylaminopurine (BA) at a density of 33,000 microspores per mL. The number of microspore was estimated using a hemocytometer under a light microscope. The microspore suspension (3.0 mL) was dispensed into a 60 × 15-mm sterile petri dish and sealed with Parafilm. All culture media were adjusted to pH 5.7 using either KOH or HCl. After 24–48 h of heat treatment at 32.5°C and 14 days of incubation at 25°C in darkness (Seo et al., 2014), all microspores were placed on a shaker at 60 rpm at 25°C under a 16-h day length for 2 weeks.

Induction of plantlets from microspore-derived embryos

Regenerated plantlets from microspore-derived embryos were placed into MS medium containing 1.0 $mg \cdot L^{-1}$ 6-benzyladenine (BA) and 0.2 $mg \cdot L^{-1}$ naphthaleneacetic acid (NAA). For shooting, the plantlets were cut into pieces and placed into an MS medium with different concentrations of BA (0.5, 1.0, 2.0, and 4.0 $mg \cdot L^{-1}$). For root induction, a shoot of each plantlet was placed into MS medium with different concentrations of indole-3-butyric acid (IBA; 0.5 and 1.0 $mg \cdot L^{-1}$) and NAA (0.5 and 1.0 $mg \cdot L^{-1}$). Rooted plantlets were washed with sterile distilled water and transferred to soil to continue growing. Acclimated plantlets from microspore-derived embryos in pots received colchicine treatment, in which the shoot apical meristems were submerged in the solution of 0.3% colchicine for 24 h in the greenhouse (Smykalova et al., 2006).

Flow cytometric analysis

Leaves of the plants regenerated from microspore culture were subjected to ploidy analysis. Chinese cabbage, *B. rapa* cv. Chiifu (2n = 2x =20), was used as a diploid control. Approximately 20 mg of leaves were used for each sample, which were finely chopped with a clean razor blade in 1 mL of ice-cold Tris-$MgCl_2$ buffer (0.2 M Tris, 4 mM $MgCl_2$, 0.5% Triton

X-100, pH 7.5) in a glass petri dish on ice (Pfosser et al., 1995). DNA from the cells was stained in 50 $\mu g \cdot L^{-1}$ of propidium iodide with 50 $\mu g \cdot L^{-1}$ of RNase, filtered through a 40-μm cell strainer, and kept on ice. Flow cytometry was performed with a medium flow rate in a FACS Canto II flow cytometer (BD Biosciences, CA, USA), and data were analyzed with BD FACSDiva software (BD Biosciences, CA, USA). An FL2 detector was used to measure fluorescence, and phycoerythrin (PE), peridin chlorophyll protein (PerCP), forward Scatter (FSC), and side scatter (SSC) parameters were used for analysis according to the manufacturer's protocol.

Cytological analysis

The floral buds were fixed in aceto-ethanol (1:3 v/v) for 24 h and stored at -20°C in 70% ethanol. Anthers were digested in an enzyme mixture including 2% Cellulase R-10 (Duchefa Biochemie, Haarlem, The Netherlands), 1% Macerozyme R-10 (Duchefa Biochemie, Haarlem, The Netherlands), 1% Pectinase (Sigma-Aldrich Ltd, MO, USA), and 0.5% Pectolyase Y23 (Sigma-Aldrich Ltd, MO, USA) in 150 mM citrate buffer (pH 4.5) to degrade the cell walls at 37°C for 90 min (Kwon and Kim, 2009; Belandres et al., 2015). Treated anthers were squashed in 60% acetic acid on a slide warmer and air dried. The slides were stained and mounted with 4',

6-diamidino-2-phenylindole (DAPI) in Vectashield antifade Mounting Medium (Vector Laboratories, CA, USA). The images were processed using an Axioskop2 microscope (Zeiss Germany). DAPI fluorescent images were captured using Axiocam 506 color CCD camera (Zeiss Germany).

Extraction of genomic DNA

Young leaves were collected from each individual and stored at -80°C until use. DNA was extracted with the cetyl trimethylammonium bromide (CTAB) method, and RNase was added to obtain genomic DNA for PCR amplification. The quality and quantity of DNA was measured with a NanoDrop spectrophotometer (Thermo Fisher Scientific, USA).

Genotyping with SSR markers

Thirty-eight simple sequence repeats (SSR) markers were adopted from Suwabe et al. (2002). These markers were expected to amplify repeats of approximately 100–250 bp long. The SSR markers were applied to the microspore donor plants (Ganghwa turnip) and DH lines to test homozygosity. The following conditions were used to perform PCR amplification: initial denaturation at 94°C for 4 min, and 30 cycles of denaturation at 94°C for 30 sec, annealing at 54°C for 30 sec, extension at

72°C for 30 sec, then the final extension at 72°C for 4 min. PCR products were separated on a 2.5% agarose gel, stained with ethidium bromide (EtBr), and visualized under the UV light.

SNP calling

Thirty-eight DNA of Ganghwa turnip and a selected DH line obtained through microspore culture was extracted from three 14-day-old seedlings. Sequencings were performed on a Illumina Hi-seq 4000 flatform. Approximately 27 Gb for Ganghwa turnip and 17 Gb for line G14 of raw reads were obtained. Low-quality reads were filtered with manual code ($Q < 20$, $P < 70$) and trimmed out using Trimmomatic v0.38 (Bolger et al., 2014). The filtered reads were aligned to the *B. rapa* reference genome v3.0 (release in BRAD, Zhang et al., 2018) with BWA-MEM (Li, 2013) V.0.7.17 with default parameters. Genome Analysis Toolkit (McKenna et al., 2010) HaplotypeCaller V.3.6-0 was followed to identify single nucleotide polymorphisms (SNPs) and indels with default parameters. The filtering settings for SNPs were QD < 2.0, FS > 60.0, MQ < 40.0, MQRankSum < -12.5, ReadPosRankSum < -8.0, and SOR > 4.0. The SNP calling was performed twice for Base Quality Score Recalibration. Variant filtration was performed with manual script based on quality score, read depth, and

haplotype of Ganghwa turnip and DH lines. Only homozygous sites of the DH lines were selected, and SNP sites were filtered out if the haplotype the DH line was not within the haplotype of Ganghwa turnip.

Phylogenetic tree construction

For phylogenetic tree constructions, the SNP and Indel datasets of 199 *B. rapa* accessions (Cheng et al., 2016) were downloaded from Database BRAD (http://brassicadb.org/brad/datasets/pub/ReseqPars/genotypes/). SNPs of G14 were extracted with *B. rapa* genome (relese version 1.5 in BRAD) according to datasets of 199 *B. rapa* accessions. A total of 16,166 variant positions in the gene body region were collected, and 201 accessions, including the DH line 14 and *B. rapa* cv. Chiifu, were used for analysis. The phylogenetic tree was drawn with MEGA X software (Kumar et al., 2018) using the Neighbor-joining method.

Genotyping by CAPS markers

Among the filtered SNP sites of Ganghwa turnip that had a depth greater than five, the flanking 11-bp sequences (extending 5 bp from SNP on both sides) of both alleles from heterozygous sites were compared. If one allele included the target site of the restriction enzyme (*Bam*HI or *Hind*III),

the flanking 2-kb sequences of both alleles were examined to determine if another restriction enzyme target site was included. Primers (Table III-1) were designed in this region with Primer3 (Untergasser et al., 2012) and evaluated with BLAST (Boratyn et al., 2012) and bowtie (Langmead et al., 2009) to assess target specificity. PCR amplification was conducted in a 20-μL reaction mix, containing about 20 ng of genomic DNA, 1 unit of Taq polymerase (Takara), 0.2 mM dNTPs, and 0.2 mM primers with 1 × PCR reaction buffer (Takara) under the following conditions: denaturation at 95℃ for 5 min followed by 30 cycles of amplification (95℃ for 30 sec, 60℃ for 30 sec, and 72℃ for 1 min) and a final extension at 72℃ for 10 min. Restriction enzyme treatment was performed in a 20-μL reaction mix containing 5 units of restriction enzymes (*Bam*HI-HF, Takara, or *Hind*III-HF, Takara), 3–5 μL of PCR product with 1× cutsmart buffer (Takara) at 37℃ for 3 h. The PCR amplicons and restriction fragments were visualized with EtBr by 2% agarose gel electrophoresis.

Repeat sequence analysis

Repetitive sequences of G14 were analyzed with dnaPipeTE (Goubert et al., 2015) using five million raw reads. To compare repeat sequence abundance between turnip and Chinese cabbage, whole genome sequencing

was performed on two Chinese cabbage lines CR291 and Hwi on an Illumina Hi-seq 4000 as described above. Approximately 36 Gb and 32 Gb of raw reads were obtained from CR291 and Hwi, and five million each of raw reads were subjected to repeat sequence analysis with dnaPipeTE.

Table III-1. CAPS primers used in this study.

Primer	Sequence (5' to 3')	Tm
DG3429 - A02_1638170_2_BamHI_F	TCGTTAAGACCAGCCACCAC	59.0
DG3430 - A02_1638170_2_BamHI_R	CCAAGCATCCTCTATCCGGG	58.7
DG3467 - A09_15411850_0_HindIII_F	CACATCGGCCAAGAGGAGAG	59.2
DG3468 - A09_15411850_0_HindIII_R	TAGGGGTGGGCATTTTTCCC	59.0
DG3443 - A09_13456734_2_BamHI_F	ACAAGGTAGATGGGGCGTTG	59.1
DG3444 - A09_13456734_2_BamHI_R	AACTCAGCCGTCTCATGTCC	58.8
DG3457 - A04_11498102_0_HindIII_F	ACCCGCAAACACACAAATGG	58.9
DG3458 - A04_11498102_0_HindIII_R	TCCAGATGATCGTTGAGCCG	58.9

RESULTS

Establishment of microspore culture conditions in *Brassica rapa* subsp. *rapa* cv. Ganghwa

Microspores were isolated from 1–2 mm long flower buds from Ganghwa turnip, prepared in B5-13 medium, and cultured in NLN-13 medium with 0.1 mg·L-1 BA. Four weeks after microspore isolation, 32 microspores developed embryos (5.2 ± 1.1 mm tall) large enough to be visible under the light microscope (Fig. III-1A). Initially, simultaneous regeneration of both shoots and roots was tried. However, in case of Ganghwa turnip, it was proven that induction of shoot in the BA containing medium (Fig. III-1B) followed by induction of root in the IBA containing medium (Fig. III-1C) was more efficient. Detailed procedure is provided below.

Heat shock treatment was given at 32.5℃ for 24 or 48 h. Efficiency of embryogenesis in the 24 h heat-shocked microspores was 0.73 embryos per bud, which was twice that in the 48 h treatment (Fig. III-3A). However, unlike the previous report (Na et al., 2011), the addition of activated charcoal to the culture had no effect on the frequency of embryogenesis.

After heat shock for 24 h, embryos with well-developed cotyledons and radicles were transferred to solid MS media with variable amounts of BA and NAA. Abnormal plantlets were produced in the regeneration MS medium containing both 1.0 mg·L^{-1} BA and 0.2 mg·L-1 NAA. Procedures of simultaneous shoot and root induction by others for Brassicaceae plants were unsuccessful in microspore culture of Ganghwa turnip (Hong and Lee, 1995; Chun et al., 2011; Na et al., 2011; Seo et al., 2014), as most of the embryos transferred to the regeneration medium failed to form callus or shoots. However, regeneration of shoots only in the MS medium supplemented with varying concentrations of BA (0.5, 1.0, 2.0, and 4.0 mg·L^{-1}) in the absence of NAA was more efficient, while achieving a high rate of shoot regeneration at 1.0 mg·L^{-1}BA within four weeks. Under this condition, 52.2% of the embryos produced multiple shoots from a single apical meristem (Fig. III-3B), while greater concentrations of BA (2.0 and 4.0 mg·L^{-1}) caused hyperhydricity or vitrification of shoots-abnormal shoots without an apical meristem. The regenerated shoots were excised and then transferred to the root-inducing medium containing NAA (0.5 or 1.0 mg·L^{-1}) or IBA (0.25, 0.5, or 1.0 mg·L^{-1}). The highest root induction rate approximately 68%, was achieved with 0.5 mg·L^{-1} IBA (Fig. III-3C). Most of the plantlets that received NAA treatment were transformed to callus-like

structures with few roots, indicating that IBA was more efficient in inducing roots in Ganghwa turnip.

Induction of doubled-haploid Ganghwa turnip with colchicine treatment

The plantlets derived from the *in vitro* microspore culture were acclimatized in the greenhouse. In order to double the chromosome number, 0.3% colchicine was treated to the shoot apical meristem of the regenerated plants two days after transfer to soil. Although 15.5% of plants spontaneously doubled their chromosome numbers without colchicine treatment, 39.3% of the plants treated with colchicine were found to have doubled chromosome numbers (Fig. III-3D). These observations indicate that DH individuals may spontaneously appear in the absence of colchicine treatment, but the efficiency is significantly improved by colchicine-mediated chromosome doubling in Ganghwa turnip.

Characterization of doubled-haploid line G14 Ganghwa turnip

Among several DH lines obtained from the microspore culture, a representative line G14 was chosen for further genome analysis. All DH lines (G14, G16, G22, G26, G30, and G56) were grown in the field, along

with commercial Ganghwa turnips, at the Experimental Farm of Seoul National University in Suwon during the spring and fall of 2018 (Fig. III-1E). Despite some variations in morphology among the individuals, commercial Ganghwa turnips typically have long petioles, lobed leaves, and a large bulbous taproot with white and purple skin colors (left panel on Fig. III-1E; also see Fig. III-2). Mature Ganghwa turnips (approximately 45 days after transfer to soil) were 75.9 ± 9.8 cm tall, weighed 1,461 ± 224 g (entire plant), and had roots with a weight of 748.6 ± 71.6 g (fresh weight; mean ± SE). However, self-pollinated progenies of representative DH Ganghwa turnip line G14 were morphologically more uniform than the commercial ones (right panel on Fig. III-1E). G14 DH lines were 65.0 ± 3.9 cm tall, had a total fresh weight of 788 ± 126 g, and root fresh weight of 460 ± 80.9 g; slightly smaller than Ganghwa plants. The bulbous taproots of line G14 were white-skinned while developing a purple color on the shoulder when exposed to sunlight.

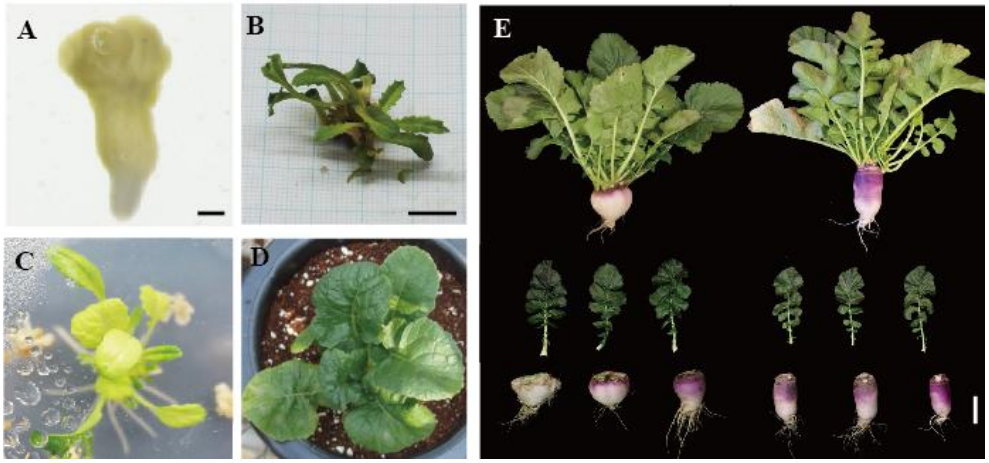

Figure III-1. Ganghwa turnip regenerated from the microspore culture. (A) The embryo developed after four weeks of microspore culture (Bar = 1 mm); (B) Multiple shoots after four weeks from embryo grown in Murashige and Skoog (MS) medium with 1.0 mg·L^{-1} BA (Bar = 1 cm); (C) Plantlet grown for four weeks in MS medium with 0.5 mg·L^{-1} IBA (Bar = 1 cm); (D) An acclimatized plant from in vitro culture after transfer to the greenhouse (Bar = 5 cm); (E) Ganghwa turnip (left) and mature doubled-haploid line G14 (right) (Bar = 10 cm). BA, benzylaminopurine; IBA, indole-3-butyric acid..

Figure III-2. Photographs of commercial Ganghwa turnip plants. Commercial Ganghwa turnips exhibited morphological variations among the individuals typically having long petioles, lobed leaves, and a large bulbous taproot with white and purple skin colors. Bar = 10 cm.

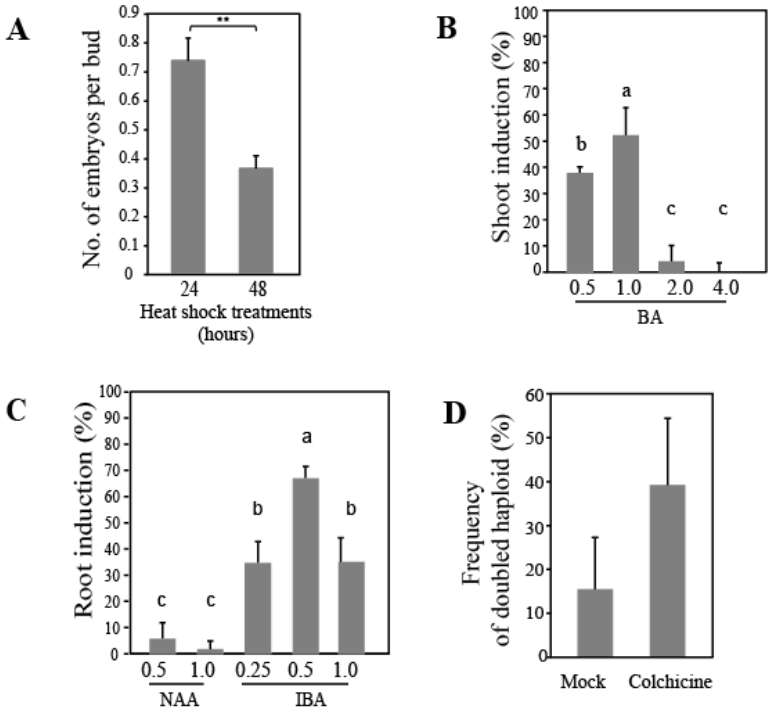

Figure III-3. The effects of various treatments on the microspore culture of Ganghwa turnip. (A) Efficiency of embryogenesis by heat shock treatments; ** $p < 0.01$ (B) Shoot induction in response to BA concentrations. Percentage of shoot induction represents the number of embryos with shoots. Values represent the mean ± SD from three batches with three plates containing about eight embryos. The differences among treatments were confirmed with one-way ANOVA ($p = 1.52e^{-5}$) as indicated with letters by Duncan test ($p < 0.05$). (C) Root induction in response to NAA or IBA concentrations. Percentage of root induction represents the number of rooted shoots. Values are the mean ± SD from four batches with five plates containing about 10 shoots. One-way ANOVA showed differences among treatments ($p = 5.46e^{-8}$) and letters indicate the differences according to Duncan test ($p < 0.05$). (D) The frequency of doubled haploids formation by colchicine treatment. Data were collected four weeks after the treatment. BA, benzylaminopurine; NAA, naphthaleneacetic acid; IBA, indole-3-butyric acid. radicles were transferred to solid MS media with variable amounts of BA radicles were transferred radicles were transferred to solid MS media

Validation of doubled-haploid Ganghwa turnips

In order to confirm chromosome doubling of DH Ganghwa turnip lines, observation of chromosomes in metaphase I and flow cytometry analysis were performed. The pollen mother cells of G14 DH line had 20 chromosomes in metaphase I (Fig. III-4A), the same as those of Chinese cabbage cv. Chiifu used as a diploid control (Fig. III-4C). Flow cytometry analysis also confirmed that both G14 DH line and Chinese cabbage cv. Chiifu had similar DNA contents (Fig. III-4B and III-4D).

In order to confirm the homozygosity of G14 DH line, several molecular markers such as simple sequence repeats (SSRs) developed in Chinese cabbage (Suwabe et al., 2002) were applied to the DH lines. The BRSM-007 locus was found to be heterozygous for commercial GH individual, but homozygous for either G14 or G36 line, both of which were generated from microspore culture (Fig. III-5A). The PCR products of BRSM-007 alleles from GH, G14, and G36 were analyzed by sequencing, in which the larger fragment (~180 bp) was found to have a longer stretch of CT dinucleotides than the small fragment (~120 bp) (Fig. III-5B). In addition, whole genome sequencing of G14 allowed to identify numerous single nucleotide polymorphisms (SNPs) between G14 and Chinese cabbage *B. rapa* cv. Chiifu. Some cleaved amplified polymorphic sequence (CAPS)

markers were developed according to the SNPs, and both BC02 and HC09 CAPS markers revealed the loci heterozygous in a commercial GH individual but homozygous in both G16 and G36 DH lines (Fig. III-5C and III-5D). These findings indicate that the progenitor GH plant was heterozygous for many loci, but its DH progenies G14 and G36 became homozygous for every locus in the genome after microspore culture and chromosome doubling.

Genomic variations and genetic relationship of Ganghwa turnip

Both commercial Ganghwa turnip GH plant and G14 DH line were sequenced on an Illumina HiSeq 4000 platform to approximately 60× and 30× coverages, respectively. High-quality reads of 27 Gb and 17 Gb were obtained and filtered reads were mapped onto the *B. rapa* reference genome (Zhang et al., 2018) for extracting SNPs and Indels. In comparison to *B. rapa* reference genome, a total of 1,720,740 heterozygous SNPs, 990,659 homozygous SNPs, 524,950 heterozygous indels, and 254,750 homozygous indels were detected in the commercial heterozygous Ganghwa turnip GH plant, indicating that commercial Ganghwa turnips are highly heterogeneous due mainly to open pollination in the field. Such sequence variations were evenly distributed on every chromosome (Fig. III-6A), with relatively few

SNPs and indels detected in the centromere regions due probably to a high density of repeats therein. Among 2,245,690 heterozygous SNP and indel sites in GH, approximately a half of them (48.68%, 1,093,312 sites) were inherited to the G14 DH line, revealing a 1:1 segregation in the progeny. To assess the genetic relationship of Ganghwa turnip within the *B. rapa* species, phylogenetic trees were constructed in comparison to various *B. rapa* accessions, including the G14 DH line and *B. rapa* cv. Chiifu. SNP datasets of 199 *B. rapa* accessions were obtained from the *Brassica* genome database BRAD, and 16,166 SNP sites in gene body regions were comparatively analyzed for the construction of a phylogenetic tree. Consistent with the previous study (Cheng et al., 2016), the tree of *B. rapa* accessions was divided into six groups: (i) Chinese cabbage, (ii) European turnip, (iii) Chinese turnip, (iv) sarsons and rapid cycling, (v) Japanese turnip, and (vi) turnip rape including Taicai, Pak choi, Wutacai, Zicaitai, and Caixin (Fig. III-6B). The G14 DH line was assigned to the Chinese turnip clade, suggesting that Ganghwa turnips may have originated from China.

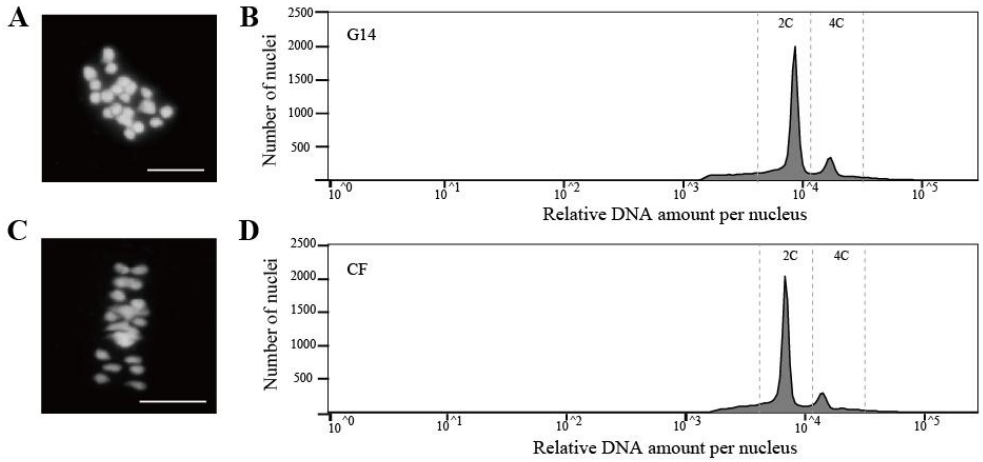

Figure III-4. Chromosome observation and flow cytometry analysis of DH line G14 and Chinese cabbage cultivar Chiifu. (A) Image of 20 chromosomes in a pollen mother cell of G14. (B) Flow cytometry analysis to determine the ploidy level of leaf tissues of G14. (C) Image of 20 chromosomes in a pollen mother cell of CF. (D) Flow cytometry analysis to determine the ploidy level of leaf tissues of CF. Bar = 5 μm.

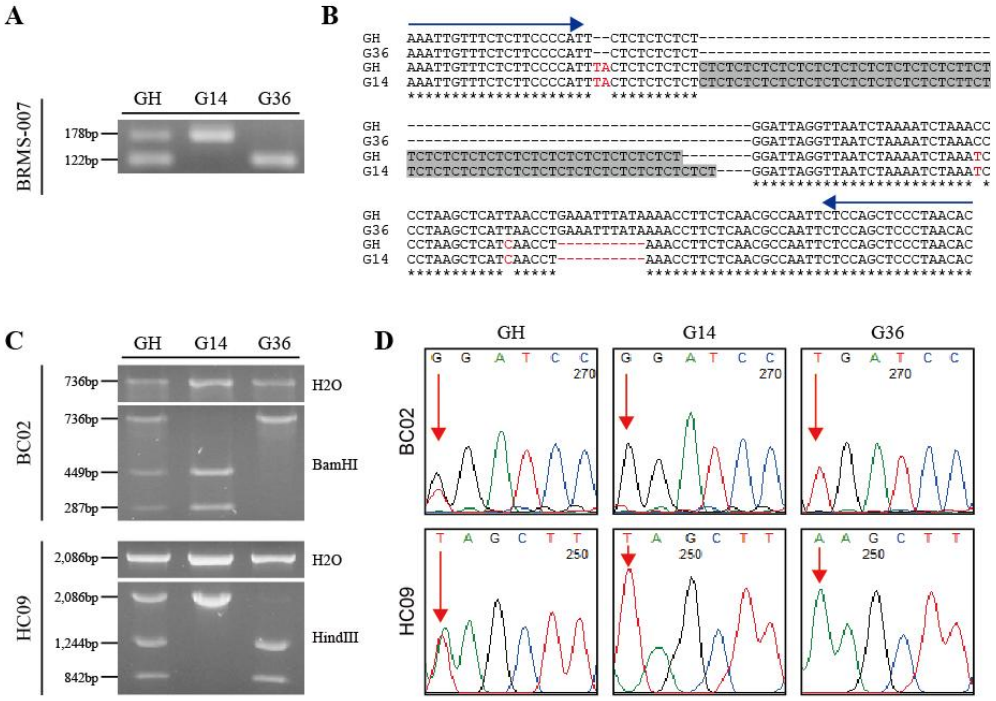

Figure III-5. Assessment of homozygosity in turnip DH lines with SSR and CAPS markers and sequence analysis. (A) PCR amplicons with the SSR marker BRMS-007 in GH, G14 and G36 turnips. (B) Sequence analysis of 122-bp and 178-bp PCR products with the BRMS-007 marker. The blue arrows indicate the pair of forward and reverse primer sequences and the shaded boxes show the simple sequence repeats. SNPs and indels are shown in red. (C) Products of CAPS markers BC02 and HC09 digested with *Bam HI* and *Hind III*, respectively, for GH, G14 and G36 turnips. (D) DNA sequence chromatograms of the PCR products for BC02 and HC09 CAPS markers. SNPs at *Bam HI* and *Hind III* restriction enzyme sites are denoted with red arrowheads. Heterozygosity was detected at polymorphic nucleotides in a commercial GH individual.

A

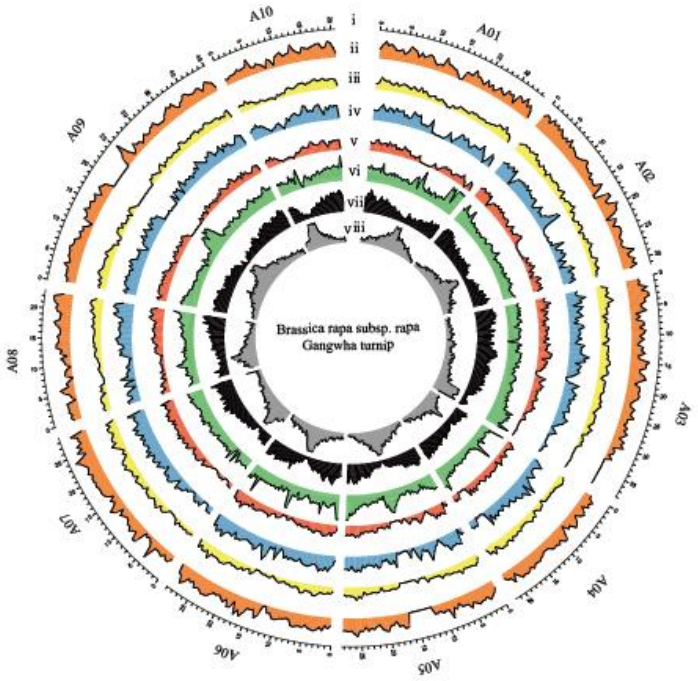
A01
A02
A03
A04
A05
A06
A07
A08
A09
A10
i
ii
iii
iv
v
vi
vii
viii
Brassica rapa subsp. rapa
Gangwha turnip

B

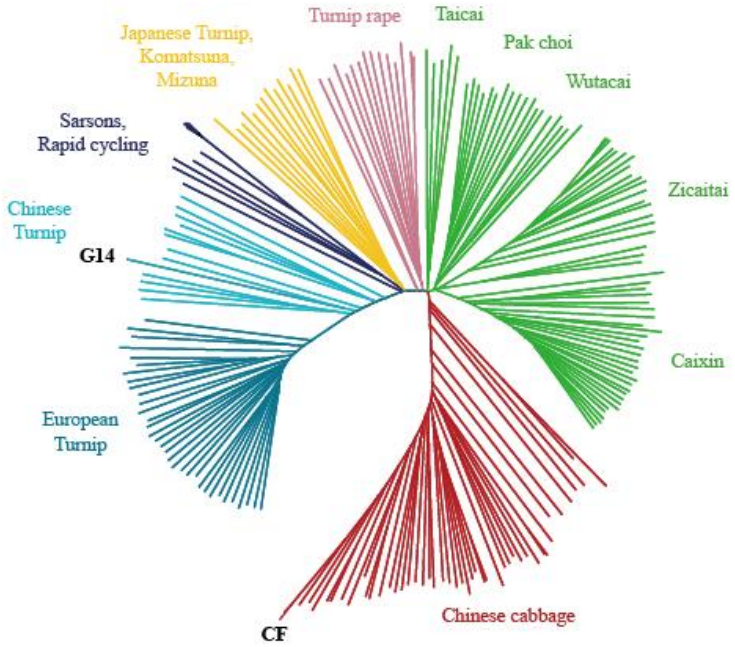
Turnip rape
Taicai
Japanese Turnip,
Komatsuna,
Mizuna
Pak choi
Wutacai
Sarsons,
Rapid cycling
Zicaitai
Chinese
Turnip
G14
Caixin
European
Turnip
Chinese cabbage
CF

Figure III-6. Genome structure of Ganghwa turnip DH line G14 and phylogenetic relationship within *Brassica rapa* subspecies. (A) Distribution of genomic variations in Ganghwa turnip (GH) and its doubled haploid line. G14. i: The chromosome of *B. rapa* genome with 1 Mb scale. ii: SNPs of G14 (orange). iii: INDELs of G14 (yellow). iv: heterozygous SNP sites in GH (blue). v: heterozygous INDEL sites in GH (red). vi: mapped read counts of G14 (green). vii: gene density (black). viii: Transposable elements (TE) density (grey). Each circle was represented with 1-Mb windows. (B) Phylogenetic tree of 199 *B. rapa* accessions and Chinese cabbage cultivar Chiifu (CF) and G14. The tree was constructed with 16,166 SNP information obtained from 201 *B. rapa* accessions using the neighbor-joining method.

Repeat sequence analysis of doubled-haploid line G14 and Chinese cabbage cultivars

Turnip exhibits similar overall morphology to radish (*Raphanus sativus*), although they belongs to different genera. The genomic sequences of coding region were compared among the DH line G14, *B. rapa* cv. Chiifu-401, and *R. sativus* cv. Wonkyo10039 (Jeong et al., 2016) to assess their sequence similarities. The sequence similarity between turnip and Chinese cabbage was 99.37%, whereas that of turnip between radish was 90.88%. Thus, different phenotypes of turnip and Chinese cabbage are presumably the consequence of other genomic or epigenomic factors such as structural variation, DNA methylation, or enhancer element distributions. Since transposable elements (TE) such as LINE (long interspersed element) or *Alu* are one of the most well-known driving factor of genomic structural variation (Payer et al., 2017; Xing et al., 2009), I examined the composition of repetitive sequences of turnip and Chinese cabbages. The abundance of repeat elements of DH turnip G14 and two Chinese cabbage lines CR291 and Hwi was analyzed (Table III-2). Despite high similarity in overall genome sequence, turnips and Chinese cabbage have different compositions of transposable elements. In particular, long terminal repeat (LTR) retrotransposons are more enriched in G14 (20.16%) than in CR291

(15.95%) and Hwi (15.14%) genomes (Table III-2, Figure III-7A). Moreover, the *gypsy* elements are classified as major LTR sequences in the turnip genome (12.82%) compared to those of Chinse cabbage (9.09% in CR291 and 9.24% in Hwi) (Table III-3, Figure III-7B). These findings suggest that subspecies-specific TE divergence, abundance of LTR, is responsible for huge phenotypic variations observed within the same species.

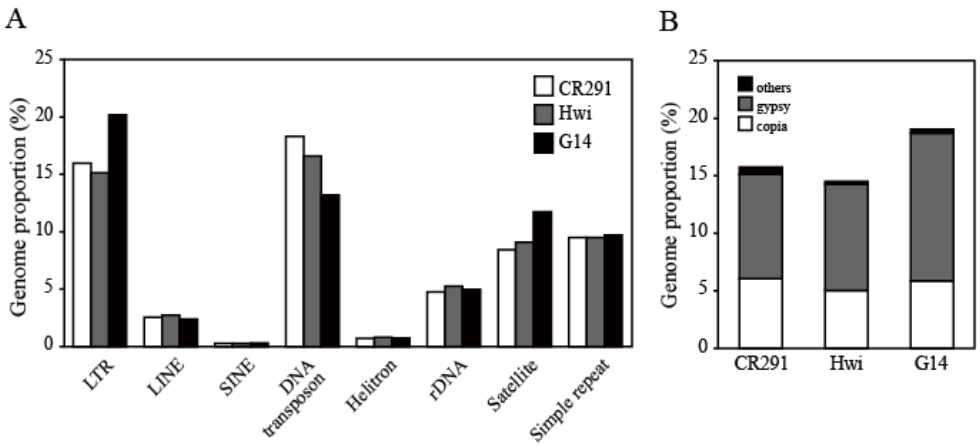

Figure III-7. Abundance of repeat elements in Chinese cabbage and Ganghwa turnip DH line G14. (A) Genome abundance of LTR, LINE, SINE, DNA transposon, Hellitron, rDNA, satellite, and simple repeat in Chinese cabbage CR291 and Hwi, and turnip DH line G14. (B) Genome abundance of LTR subfamilies in CR291, Hwi, and G14. Others: *Cassandra*, *DIRS*, *ERV*, *Ngaro*, *Pao*, *viper* and unclassified LTRs.

Table III-2. Abundance of repeat elements in DH turnip and Chinese cabbage.

	Proportion (%)		
	CR291	Hwi	G14
LTR	15.95	15.14	20.16
LINE	2.53	2.73	2.4
SINE	0.27	0.27	0.3
DNA transposon	18.31	16.61	13.21
Helitron	0.69	0.79	0.74
rDNA	4.74	5.25	4.98
Satellite	8.44	9.09	11.72
Simple_repeat	9.47	9.47	9.7

Table III-3. Abundance of LTR subfamilies in DH turnip and Chinese cabbage.

	Proportion (%)		
	CR291	Hwi	G14
Cassandra	0.062	0.063	0.059
DIRS	0.017	0.009	0.005
ERV	0.139	0.066	0.172
copia	6.046	5.027	5.88
gypsy	9.091	9.241	12.817
Ngaro	0.003	0.003	0.001
Pao	0.147	0.065	0.057
viper	0	0	0
unclassified LTR	0.245	0.044	0.058
Total	15.948	15.144	20.161

DISCUSSION

In this study, I generated DH Ganghwa turnip lines from microspore culture, with several modifications from previous procedures (Na et al., 2011; Chun et al., 2011; Seo et al., 2014). It was found that successive induction of shoots and roots in the medium supplemented only with BA and IBA, respectively, was more efficient for organ regeneration of Ganghwa turnip (Fig. III-2). Colchicine treatment was proven efficient to double the haploid chromosomes. Chromosome doubling of DH line was assessed by counting the chromosome number and flow cytometry (Fig. III-3). Homozygosity of DH line was also verified with molecular markers (Fig. III-4), and further supported by whole-genome sequencing. In fact, it is important for breeding to select true DH lines with reliable methods. All these evaluation processes not only allowed us to confirm diploidy and homozygous allelic configuration of DH lines throughout the genome, but also to help eliminate unexpected heterozygous plants that can be regenerated from somatic tissues during in vitro culture.

Commercial Ganghwa turnips are diverse in morphology, owing to open pollination in the field grown as heirlooms, indicating that a high level of heterogeneity persists in the population. It is noteworthy that

heterogeneous commercial Ganghwa turnips are superior to the homozygous DH lines in many traits (Fig. III-1). The fresh weight of commercial Ganghwa turnip (1,461 ± 224 g) is almost as twice as that of DH line G14 (748.6 ± 71.6 g). The root of open pollinated turnips also weighs more than that of G14 (788 ± 126 g vs. 460 ± 80.9 g). Commercial Ganghwa turnips are also slightly taller than G14 DH lines (75.9 ± 9.8 cm vs. 65.0 ± 3.9 cm). These observations strongly suggest that a substantial level of heterozygosity in open pollinated Ganghwa turnip is in part responsible for the superior phenotype, which is destabilized once the plants become doubled-haploid and lose heterozygosity by the acquisition of homozygous allele configuration in the entire genome. One possible explanation is that deleterious recessive alleles become homozygous in DH lines and no longer complemented by superior dominant alleles as in hybrids, which is epitomized as a dominance model (Hochholdinger and Baldauf, 2018).

Comparison of whole genome sequences between G14 DH line and Chinese cabbage revealed high levels of SNPs and indels, indicating that Korean Ganghwa turnips are quite distinct from Chinese cabbage for genome composition. Moreover, the turnip genome is more enriched with LTR family transposons, with less DNA transposons, than Chinese cabbage.

It is widely regarded that TEs may cause a wide range of changes in gene expression and genome configuration (Lisch, 2013; Xing et al., 2009). Thus, expansion and contraction of TEs are likely responsible not only for changes in expression of the genes nearby TEs, but also for speciation and evolution of many plant species (Feulner and De-Kayne, 2017; Kim et al., 2017). For instance, rapid evolution of LTR family transposons such as *gypsy* elements was found in *Oryza* species, suggesting that different repertoires of TEs significantly contribute to phenotypic variations and speciation (Zhang and Gao, 2017). Similarly, subspecies-specific TE divergence in *B. rapa* is also likely responsible for highly contrasting phenotypes in the same species.

REFERENCES

Barro, F., and Martin, A. (1999). Response of different genotypes of *Brassica carinata* to microspore culture. Plant Breeding **118,** 79-81.

Belandres, H.R., Waminal, N.E., Hwang, Y.J., Park, B.S., Lee, S.S., Huh, J.H., and Kim, H.H. (2015). FISH karyotype and GISH meiotic pairing analyses of a stable intergeneric hybrid x*Brassicoraphanus* line BB#5. Korean J. Hortic. Sci. **33,** 83-92.

Bolger, A.M., Lohse, M., and Usadel, B. (2014). Trimmomatic: a flexible trimmer for Illumina sequence data. Bioinformatics **30,** 2114-2120.

Boratyn, G.M., Schaffer, A.A., Agarwala, R., Altschul, S.F., Lipman, D.J., and Madden, T.L. (2012). Domain enhanced lookup time accelerated BLAST. Biology Direct. **7,** 12.

Cheng, F., Sun, R., Hou, X., Zheng, H., Zhang, F., Zhang, Y., Liu, B., Liang, J., Zhuang, M., Liu, Y., Liu, D., Wang, X., Li, P., Liu, Y., Lin, K., Bucher, J., Zhang, N., Wang, Y., Wang, H., Deng, J., Liao, Y., Wei, K., Zhang, X., Fu, L., Hu, Y., Liu, J., Cai, C., Zhang, S., Zhang, S., Li, F., Zhang, H., Zhang, J., Guo, N., Liu, Z., Liu, J., Sun, C., Ma, Y., Zhang, H., Cui, Y., Freeling, M.R., Borm, T., Bonnema, G., Wu, J., and Wang, X. (2016). Subgenome parallel selection is associated with morphotype diversification and convergent crop domestication in *Brassica rapa* and *Brassica oleracea*. Nat. Genet. **48,** 1218-1224.

Chun, C., Park, H., and Na, H. (2011). Microspore-derived embryo formation in radish (*Raphanus sativus* L.) according to nutritional

and environmental conditions. Hortic. Environ. Biote. **52,** 530-535.

Ferrie, A.M.R., Epp, D.J., and Keller, W.A. (1995). Evaluation of *Brassica rapa* L. genotypes for microspore culture response and identification of a highly embryogenic line. Plant Cell Rep. **14,** 580-584.

Ferrie, A.M.R. (2003). Microspore culture of *Brassica* species. In Doubled haploid production in crop plants (Springer), pp. 205-215.

Ferrie, A.M.R., and Caswell, K.L. (2011). Isolated microspore culture techniques and recent progress for haploid and doubled haploid plant production. Plant Cell. Tiss. Org. **104,** 301-309.

Feulner, P.G.D., and De-Kayne, R. (2017). Genome evolution, structural rearrangements and speciation. J. Evol. Biol. **30,** 1488-1490.

Gamborg, O.L., Miller, R.A., and Ojima, K. (1968). Nutrient requirements of suspension cultures of soybean root cells. Exp. Cell. Res. **50,** 151-158.

Gil-Humanes, J., and Barro, F. (2009). Production of doubled haploids in *Brassica*. In Advances in haploid production in higher plants (Springer), pp. 65-73.

Gómez-Campo, C., and Prakash, S. (1999). Origin and domestication. In Developments in plant genetics and breeding (Elsevier), pp. 33-58.

Goubert, C., Modolo, L., Vieira, C., ValienteMoro, C., Mavingui, P., and Boulesteix, M. (2015). *De novo* assembly and annotation of the asian tiger mosquito (*Aedes albopictus*) repeatome with dnaPipeTE from raw genomic reads and comparative analysis with the yellow fever mosquito (*Aedes aegypti*). Genome Biol. Evol. **7,** 1192-1205.

Hochholdinger, F., and Baldauf, J.A. (2018). Heterosis in plants. Curr. Biol. **28,** R1089-R1092.

Hong, S.Y., and Lee, S.S. (1995). Microspore culture of x*Brassicoraphanus*. J. Korean Soc. Hortic. **36,** 453-459.

Jeong, Y.M., Kim , N., Ahn, B.O., Oh, M., Chung, W.H., Chung, H., Jeong, S., Lim, K.B., Hwang, Y.J., Ki, G.B., Baek, S., Choi, S.B., Hyung, D.J., Lee, S.W., Sohn, S.H., Kwon, S.J., Jin, M., Seol, Y.J., Chae, W.B., Choi, K.J., Park, B.S., and Yu, H.J. (2016). Elucidating the triplicated ancestral genome structure of radish based on chromosome-level comparison with the *Brassica* genomes. Theor. Appl. Genet. **129,** 1357-1372.

Kim, S., Park, J., Yeom, S.I., Kim, Y.M., Seo, E., Kim, K.T., Kim, M.S., Lee, J.M., Cheong, K., Shin, H.S., Kim, S.B., Han, K., Lee, J., Park, M., Lee, H.A., Lee, H.Y., Lee, Y., Oh, S., Lee, J.H., Choi, E., Choi, E., Lee, S.E., Jeon, J., Kim, H., Choi, G., Song, H., Lee, J., Lee, S.C., Kwon, J.K., Lee, H.Y., Koo, N., Hong, Y., Kim, R.W., Kang, W.H., Huh, J.H., Kang, B.C., Yang, T.J., Lee, Y.H., Bennetzen, J.L., and Choi, D. (2017). New reference genome sequences of hot pepper reveal the massive evolution of plant disease-resistance genes by retroduplication. Genome Biol. **18,** 210.

Klopsch, R., Witzel, K., Borner, A., Schreiner, M., and Hanschen, F.S. (2017). Metabolic profiling of glucosinolates and their hydrolysis products in a germplasm collection of *Brassica rapa* turnips. Food. Res. Int. **100,** 392-403.

Kumar, S., Stecher, G., Li, M., Knyaz, C., and Tamura, K. (2018). MEGA X: molecular evolutionary genetics analysis across computing platforms. Mol. Biol. Evol. **35,** 1547-1549.

Kwon, J.K., and Kim, B.D. (2009). Localization of 5S and 25S rRNA genes on Somatic and meiotic chromosomes in *Capsicum* species of

chili pepper. Mol. Cells **27,** 205-209.

Langmead, B., Trapnell, C., Pop, M., and Salzberg, S.L. (2009). Ultrafast and memory-efficient alignment of short DNA sequences to the human genome. Genome Biol. **10,** R25.

Lee, J.G., Bonnema, G., Zhang, N.W., Kwak, J.H., de Vos, R.C.H., and Beekwilder, J. (2013). Evaluation of glucosinolate variation in a collection of turnip (*Brassica rapa*) germplasm by the analysis of intact and desulfo glucosinolates. J. Agr. Food Chem. **61,** 3984-3993.

Lee, S.S., Lee, S.A., Yang, J., and Kim, J. (2011). Developing stable progenies of x*Brassicoraphanus*, an intergeneric allopolyploid between *Brassica rapa* and *Raphanus sativus*, through induced mutation using microspore culture. Theor. Appl. Genet. **122,** 885-891.

Li, H. (2013). Aligning sequence reads, clone sequences and assembly contigs with BWA-MEM. arXiv preprint arXiv**,** 1303.3997.

Lichter, R. (1982). Induction of haploid plants from isolated pollen of *Brassica napus*. Z. Pflanzenphysiol **105,** 427-434.

Lin, K., Zhang, N.W., Severing, E.I., Nijveen, H., Cheng, F., Visser, R.G.F., Wang, X.W., de Ridder, D., and Bonnema, G. (2014). Beyond genomic variation - comparison and functional annotation of three *Brassica rapa* genomes: a turnip, a rapid cycling and a Chinese cabbage. BMC Genomics **15,** 250.

Lisch, D. (2013). How important are transposons for plant evolution? Nat. Rev. Genet. **14,** 49.

McKenna, A., Hanna, M., Banks, E., Sivachenko, A., Cibulskis, K., Kernytsky, A., Garimella, K., Altshuler, D., Gabriel, S., Daly, M., and DePristo, M.A. (2010). The genome analysis toolkit: a

MapReduce framework for analyzing next-generation DNA sequencing data. Genome Res. **20,** 1297-1303.

Murashige, T., and Skoog, F. (1962). A revised medium for rapid growth and bio assays with tobacco tissue cultures. Physiol. Plantarum **15,** 473-497.

Na, H., Kwak, J.H., and Chun, C. (2011). The effects of plant growth regulators, activated charcoal, and $AgNO_3$ on microspore derived embryo formation in broccoli (*Brassica oleracea* L. var. *italica*). Hortic. Environ. Biote. **52,** 524-529.

Padilla, G., Cartea, M.E., Rodriguez, V.M., and Ordas, A. (2005). Genetic diversity in a germplasm collection of *Brassica rapa* subsp *rapa* L. from northwestern Spain. Euphytica **145,** 171-180.

Pang, W., Li, X., Choi, S.R., Dhandapani, V., Im, S., Park, M.Y., Jang, C.S., Yang, M.S., Ham, I.K., Lee, E.M., Kim, W., Lee, S.S., Bonnema, G., Park, S., Piao, Z.Y., and Lim, Y.P. (2015). Development of a leafy *Brassica rapa* fixed line collection for genetic diversity and population structure analysis. Mol. Breeding **35,** 54.

Payer, L.M., Steranka, J.P., Yang, W.R., Kryatova, M., Medabalimi, S., Ardeljan, D., Liu, C., Boeke, J.D., Avramopoulos, D., and Burns, K.H. (2017). Structural variants caused by *Alu* insertions are associated with risks for many human diseases. Proc. Nat. Acad. Sci. U. S. A. **114,** E3984-E3992.

Pfosser, M., Amon, A., Lelley, T., and Heberlebors, E. (1995). Evaluation of sensitivity of flow-cytometry in detecting aneuploidy in wheat using disomic and ditelosomic wheat-rye addition lines. Cytometry **21,** 387-393.

Seo, M.S., Sohn, S.H., Park, B.S., Ko, H.C., and Jin, M. (2014). Efficiency of microspore embryogenesis in *Brassica rapa* using different genotypes and culture conditions. J. Plant Biotechnol. **41,** 116-122.

Smykalova, I., Vetrovcova, M., Klima, M., Machackova, I., and Griga, M. (2006). Efficiency of microspore culture for doubled haploid production in the breeding project "Czech Winter Rape". Czech J. Genet. Plant Breed. **42,** 58.

Suwabe, K., Iketani, H., Nunome, T., Kage, T., and Hirai, M. (2002). Isolation and characterization of microsatellites in *Brassica rapa* L. Theor. Appl. Genet. **104,** 1092-1098.

Untergasser, A., Cutcutache, I., Koressaar, T., Ye, J., Faircloth, B.C., Remm, M., and Rozen, S.G. (2012). Primer3-new capabilities and interfaces. Nucleic Acids Res. **40,** e115.

Xing, J., Zhang, Y., Han, K., Salem, A.H., Sen, S.K., Huff, C.D., Zhou, Q., Kirkness, E.F., Levy, S., Batzer, M.A., and Jorde, L.B. (2009). Mobile elements create structural variation: analysis of a complete human genome. Genome Res. **19,** 1516-1526.

Yuan, S.X., Liu, Y.M., Fang, Z.Y., Yang, L.M., Zhuang, M., Zhang, Y.Y., and Sun, P.T. (2011). Effect of combined cold pretreatment and heat shock on microspore cultures in broccoli. Plant Breeding **130,** 80-85.

Yuan, S.X., Su, Y.B., Liu, Y.M., Li, Z.S., Fang, Z.Y., Yang, L.M., Zhuang, M., Zhang, Y.Y., Lv, H.H., and Sun, P.T. (2015). Chromosome doubling of microspore-derived plants from cabbage (*Brassica oleracea* var. *capitata* L.) and broccoli (*Brassica oleracea* var. *Italica* L.). Front Plant Sci. **6,** 1118.

Zhang, N., Zhao, J., Lens, F., De Visser, J., Menamo, T., Fang, W., Xiao,

D., Bucher, J., Basnet, R.K., and Lin, K. (2014). Morphology, carbohydrate composition and vernalization response in a genetically diverse collection of Asian and European turnips (*Brassica rapa* subsp. *rapa*). PLoS One **9,** e114241.

Zhang, Q.J., and Gao, L.Z. (2017). Rapid and recent evolution of LTR retrotransposons drives rice genome evolution during the speciation of AA-genome *Oryza* species. G3-Genes Genom. Genet. **7,** 1875-1885.

Zhang, L., Cai, X., Wu, J., Liu, M., Grob, S., Cheng, F., Liang, J.L., Cai, C.C., Liu, Z.Y., Liu, B., Wang, F., Li, S., Liu, F.Y., Li, X.M., Cheng, L., Yang, W.C., Li, M.H., Grossniklaus, U., Zheng, H.K., and Wang, X.W. (2018). Improved *Brassica rapa* reference genome by single-molecule sequencing and chromosome conformation capture technologies. Hortic. Res. England **5,** 50.

ABSTRACT IN KOREAN

배추와 무를 비롯한 배추과 식물들은 전세계에서 유지, 조미, 채소작물로 이용되는 중요한 작물들이다. 배추과 작물은 진화적으로 배수화 과정을 거쳐 다양한 종으로 분화되었고, 이로 인해 여러 표현형을 가지게 되었다. 배수화는 유전적 다양성에 기여하지만, 배수화 과정을 거친 식물에서 유전체 불안정성과 불임성이 자주 나타난다. 또한 합성된 유전체간의 유전적 거리가 가까울수록 유전체 친화성에 의한 염색체 결함이 발생되기 쉽다. 서로 다른 유전체가 합성되었을 때 일어나는 염색체 안정화 과정을 이해하기 위해 속간교배체인 배무채에서 세포유전학적 연구를 수행하였다. 배무채는 배추와 무의 교잡으로 합성된 속간이질사배체로 자연계에서는 극히 드문 경우이다. 1 장에서는 새로 합성된 속간이질이배체와 속간이질사배체의 배무채에서 초기 감수분열 과정을 비교 연구하였다. 종간교잡체인 유채와 비교하였을 때 속간교배체인 배무채에서 비상동염색체의 접합 빈도가 적음을 확인할 수 있었다. 이는 배무채가 합성초기에 유전적 안정성을 얻게 되었음을 의미한다. 또한 배수화 과정을 거친 속간이질사배체 배무채에서 정상적인 상동염색체의 접합을 관찰함으로써 염색체의 행동측면에서 안정화를 확인할 수 있었다. 2 장에서는 임성의 차이를 보이는 배무채의 다양한 계통에서 화분과 종자 형성을 관찰하였다. 그 중 화분의 활력이 낮은 계통인 BB4 에서는 높은 빈도로 다가염색체가 관찰되었다. 또한

비정상적인 감수분열과 그로 인한 미소핵의 발생을 지속적으로 관찰할 수 있었다. 3 장에서는 배추와 순무의 유전체 분석을 통해 아종 간의 표현형의 다양성에 영향을 미치는 유전적 요인에 대해 연구하였다. 순무는 지하부 직근이 발달한 배추의 아종으로 배추와는 형질적으로 큰 차이를 보인다. 본 연구에서 제작한 강화순무 배가 반수체와 배추의 유전체를 비교 분석하였다. 이를 통해 long terminal repeat (LTR) retrotransposons 이 배추보다 순무에서 더 축적되어 있음을 확인하였고, 이는 transposable elements (TEs) 가 아종 간의 표현형의 차이에 영향을 줄 수 있다는 것을 보여준다. 본 연구를 통해 배수화 작물의 합성 시 염색체의 친화성에 따른 안정화 기작을 세포유전학적으로 이해하고 이는 새로운 종분화에 있어 유전체 다양성을 연구하는데 실마리를 제공할 것으로 기대된다.